UNIVERSITÀ DELLA CALABRIA

UNIVERSITA' DELLA CALABRIA

Dipartimento di Chimica e Tecnologie Chimiche

Dottorato di Ricerca in

Scienze e Tecnologie Fisiche, Chimiche e dei Materiali

CICLO

XXXI

TITOLO TESI

Description of Potentially Ordered Liquid Phases through Statistical Thermodynamics Tools. Molecular Field and Computer Simulation Approaches: Comparing two Techniques.

Settore Scientifico Disciplinare CHIM/02

Coordinatore: Ch.mo Prof. Vincenzo Carbone

Firma Vincenzo Carbone

Supervisore: Ch.mo Prof. Giorgio Celebre

Firma Giorgio Celebre

Dottorando: Dott. Christian D'Urso

Firma Christian D'Urso

Contents

List of Figures

Abstract

Il campo di ricerca in cui il Progetto si colloca è quello dello studio termodinamico statistico di sistemi fluidi complessi, potenzialmente ordinati. Esso ha preso spunto dalle precedenti ricerche svolte presso il laboratorio LX-NMR S.C.An. del Dipartimento di Chimica e Tecnologie Chimiche dell'Università della Calabria dove, da lungo tempo, ci si occupa di problematiche connesse ai Cristalli Liquidi, conducendo studi che potrebbero essere definiti di 'base', miranti cioè alla comprensione delle interessantissime proprietà molecolari di cui godono questi sistemi. La finalità del Progetto implica, come appena detto, uno studio della materia a livello molecolare. Spesso, sulla base dei dati sperimentali raccolti (ad esempio, mediante le competenze NMR del Laboratorio presso il quale ha avuto luogo lo svolgimento del presente Progetto di Dottorato) si rende necessaria una 'interpretazione' dei risultati sperimentali, allo scopo di fornire una chiave di lettura dei fenomeni che avvengono su scala molecolare, in modo da coniugare, possibilmente, aspetti microscopici e macroscopici (provando cioè a fornire una giustificazione e 'razionalizzazione' microscopica dei comportamenti macroscopici della materia stessa). Gli approcci adottati nel perseguire tale scopo devono necessariamente far riferimento alla Termodinamica Statistica. Storicamente, presso il Gruppo di Ricerca del Laboratorio presso il quale è stato sviluppato Progetto di Dottorato, l'approccio utilizzato è stato di tipo *Molecular Field* (MF); tuttavia, nell'ultima decade, grazie alla collaborazione con altri gruppi di Ricerca (in particolare, in collaborazione col prof. Giorgio Cinacchi*) ci si è avvicinati allo studio delle problematiche riguardanti le fasi parzialmente ordinate anche per mezzo di simulazioni numeriche (tipicamente Monte Carlo, ma non solo...). Pertanto, nell'ottica di valorizzare sinergicamente quelle che possono essere considerate due importanti chiavi di lettura dei fenomeni a livello molecolare (ai quali, come Chimico-Fisici, siamo interessati), si è pensato di coniugare sinergicamente i due approcci (MF e MC) cui si è appena accennato. Entrambe le metodologie presentano ovviamente pregi e difetti, spesso (fortunatamente...) complementari. Ad esempio, il MF ha il pregio di partire, tipicamente, da una certa

* Departamento de Fisica Teorica de la Materia Condensada, Instituto de Fisica de la Materia Condensada (IFIMAC) and Instituto de Ciencias de Materiales 'Nicolas Cabrera', Universidad Autonoma de Madrid, Campus de Cantoblanco, 28049 Madrid, Spain

'semplicità' descrittiva, che spesso si origina su basi intuitive (a volte, anche 'elementari'), al fine di cogliere quelle che sono le caratteristiche *essenziali* dei fenomeni che si stanno investigando. Di contro, come pecca, esso risulta spesso troppo 'a grana grossa'; alle volte anche troppo essenziale nelle linee, tanto da non permettere di cogliere pienamente i dettagli e/o gli aspetti peculiari cui si aspirerebbe. D'altro canto, l'approccio stesso può presentare un aspetto matematico impegnativo, a causa di calcoli di un certo rilievo che richiedono l'utilizzo di software opportuni (spesso originali e/o commerciali), sebbene non sia strettamente necessario disporre di una imponente potenza di calcolo. Nelle simulazioni numeriche, al contrario, l'obiettivo è quello di costruire, partendo dalla modellizzazione delle interazioni molecolari, una 'realtà molecolare virtuale', ovviamente anch'essa influenzata dalla metodologia utilizzata (Monte Carlo, Molecular Dynamics, ecc...) che getti luce su aspetti magari meno intuitivi del comportamento dei sistemi fluidi studiati. Per sperare di ottenere dei dati affidabili e realistici, però, occorre mettere in gioco una quantità di particelle significativa che può essere anche imponente (a seconda del fenomeno che si sta investigando), con la possibile conseguente dilatazione dei tempi di calcolo, a volte tali da rendere inattuabili i calcoli stessi. In tale ottica, per cogliere il meglio di entrambe le metodologie, è necessario a nostro avviso, metterle a confronto. Ciò che ci siamo dunque proposti per lo svolgimento del lavoro di Dottorato è stato di provare entrambi gli approcci il più possibile 'in parallelo'. Questa prospettiva risultava alquanto 'intrigante' e ci siamo riproposti di applicarla a quell'Universo ancora nebuloso rappresentato delle affascinanti fasi *termotropiche nematiche biassiali* (ma non solo...vide infra). L'esistenza di tale mesofase è ancora oggi oggetto di dibattito, in quanto la prova ultima ed inequivocabile dell'osservazione di tali fasi non è stata fornita al di là d'ogni ragionevole dubbio; infatti, negli anni, questa fase ha pienamente meritato l'appellativo di fase 'elusiva e sfuggente', tale da essere definita da alcuni ricercatori del campo, come il 'Sacro Graal' dei Cristalli Liquidi. Facendo riferimento più in dettaglio al lavoro di Tesi, abbiamo pensato di organizzare il materiale con una Introduzione complessiva, in cui si focalizzano quelle che saranno le finalità del lavoro. Il Capitolo 1, invece, è dedicato ad un'impostazione teorica generale della materia trattata, che farà da supporto anche per i successivi capitoli (senza però dilungarci nell'ennesima e ridondante descrizione dettagliata delle fasi liquido-cristalline, che risulta essere praticamente ubiquitaria, al fine di non appesantire eccessivamente la lettura). Nel Capitolo 2, ci si occupa di una parte consistente dell'attività del Progetto (parte del quale è stato svolto presso l'Università Autonoma di Madrid sotto la supervisione del prof. Giorgio Cinacchi. In tale periodo ci si è dedicati prevalentemente all'apprendimento delle metodologie (con particolare attenzione ai metodi MC), non solo teoricamente. ma anche e soprattutto dal punto di vista pratico. In particolare, abbiamo studiato come le caratteristiche di simme-

tria delle singole particelle componenti il sistema studiato (dunque, l'appartenenza delle molecole a particolari point groups, quali il D_{2h}, C_{2h}, C_{2v}, ecc...) possano, in linea di principio, originare regioni ove i sistemi acquisiscano, ad es., la caratteristica di essere orientazionalmente biassiali. Procedendo in questa disamina, nel Capitolo 3 è illustrata una particolare applicazione di una metodologia MF (elaborata precedentemente dal prof. Celebre), in scenari molecolari nel cui contesto altri approcci dello stesso tipo denotavano limiti e difficoltà. In particolare, sono state investigate le interazioni orientazionali cosiddette 'parzialmente repulsive' tra le molecole, consentendo di 'correlare' direttamente i parametri di biassialità γ e λ che compaiono all'interno dell'espressione del potenziale orientazionale, alle proprietà di forma delle particelle (nel caso in questione, schematizzate come mattoncini a simmetria D_{2h}). Ciò può consentire, in linea di principio, di esplorare le conseguenze dell'alterazione dei parametri geometrici molecolari su caratteristiche peculiari del sistema, come le Temperature di transizioni di fase, l'eventuale biassialità delle fasi ecc. Nel corso dello svolgimento del Progetto di Dottorato, è sorta (anche in sinergia con le diverse attività di ricerca all'interno del Laboratorio LX-NMR S.C.An.) una problematica in cui l'apporto delle simulazioni numeriche poteva risultare particolarmente utile. L'interesse era quello di cogliere come sistemi ordinati, composti da particelle elicoidali, potessero impartire un determinato ordine orientazionale a dei piccoli soluti, a loro volta elicoidali, a seconda del senso di avvolgimento delle particelle di solvente. Vista la peculiarità oggettiva (morfologica) delle particelle, i risultati ottenuti potrebbero fungere da banco di prova per un processo di 'enantioriconoscimento' assoluto. Dalle simulazioni abbiamo osservato che talune volte (non sempre...) è possibile discriminare senza ambiguità i due enantiomeri (trattandosi di particelle elicoidali, essi vengono tipicamente individuati mediante i descrittori P ed M), È stato accertato che il verificarsi delle possibilità di enantiodiscriminazione dipende da determinate condizioni (che vengono dettagliatamente discusse nel Capitolo 4). L'idea e le simulazioni numeriche hanno altresì costituito prezioso materiale per un modello MF del fenomeno, in grado di consentire appunto, in linea di principio, la distinzione assoluta dei due enantiomeri (assunta nota l'elicità del solvente). Ciò è reso possibile dalla formulazione di un potenziale orientazionale sensibile alla chiralità, capace di tenere conto del senso di avvolgimento delle particelle elicoidali che si stanno considerando. Il modello elaborato viene presentato e discusso nel Capitolo 5: esso sembra essere particolarmente interessante, avendo anche, a nostro avviso, i requisiti necessari per essere, successivamente, ulteriormente migliorato e 'affinato' per la trattazione di sistemi reali. Per concludere, l'aspetto che maggiormente ci preme sottolineare quale 'filosofia' che permea l'intero lavoro di Tesi, è quello di concepire le due metodologie, *Molecular Field* e *Simulazioni Numeriche*, come sinergiche (e pertanto non mutuamente esclusive, bensì complementari) una

loro corretta applicazione potrebbe condurre il Ricercatore ad amplificarne l'efficacia ed allo stesso tempo aumentare la possibilità di 'innescare' nuove idee sulla base dei dati ottenuti.

Introduction

For a Chemist, the creation of new materials often starts with the study of the building blocks of the material itself: the molecules. What we hope to understand in this work is the role of the shape of the particles of a fluid to obtain a certain macroscopic behaviour. To pursue this goal, one of the most used theoretical tools is, of course, the *Statistical Thermodynamics*, by which it is possible, for example, to predict phase behaviours and, in particular, phase transitions starting from the formulation of the molecular interactions. This kind of study is difficult because there are a lot of variety of phases and behaviours and the complexity of their molecular interactions represents a hard challenge for theoreticians. The basic idea behind this Thesis work derives from previous studies carried out in the LXNMR_S.C.An. Lab at the University of Calabria, initially in the field of thermotropic nematic Liquid Crystals (LCs), and, subsequently, in general about various kinds of partially ordered anisotropic phases, both from the experimental point of view (LX-NMR) as well as from the theoretical point of view (with the purpose of explaining/interpreting the data acquired experimentally) [1–10]. The necessity of this work starts from the attempt to reconcile/combine synergistically two powerful statistical thermodynamics tools constituted by (1) the Mean Field approach (we strictly speak about Molecular Field (MF) approaches) [11] and (2) the Computer Simulations (CS) [12, 13], which are gradually gaining ground in the study of this type of phases, also to make up for the lack of experimental data, as well as to suggest to the experimentalists possible hypotheses of work. Even though the field of research on statistically ordered liquids is not new (their discovery date back to about 120 years ago [14, 15]), in the last decades the amount of studies has been large and varied, so that we decided to choose topics regarding specific contents never treated before.

For this purpose, our attention has been turned toward the study of systems potentially suitable to generate the elusive thermotropic nematic biaxial phase (N_b) [16]. Regarding this mesophase, its existence was hypothesized by Freiser [2] and Straley [3]; the latter in particular, formulated a mean field theory for a system made up of anisometric particles as board-like particle with D_{2h} symmetry. Unfortunately, the N_b has never been observed in real systems; nevertheless, it seems that another kind of particles (bent-core shaped, boomerang-like) that possess the C_{2v} symme-

try [5, 6] are able to give rise to the formation of the biaxial phase. There are, anyway, many other possible particle symmetries that are in principle able to form N_b phases [21–23] and among these symmetries also the C_{2h} one. A significant part of the PhD Research project has been spent to the study of systems composed of C_{2h} particles, marginally or not at all treated in literature; therefore, we believed that it was appropriate to employ CS tools for the investigation of this type of systems. To better understand the spirit that has pushed us towards this type of research it is good to spend a few words of premise on the various approaches that over time have succeeded. In this regard, it is clear that to understand or, at least, to realize which are the intermolecular forces that are responsible for the behaviour of the system under investigation is of fundamental importance. It is possible to distinguish two main currents of thought where a different weight to short- and long- range interactions has been attributed. The founder of theories based exclusively on the (short-range) repulsive interactions is Onsager [24]: in his formulation the excluded volumes play a fundamental role in inducing a nematic order. On the contrary, in 1959 Maier and Saupe [25], suggested that the (long-range) dispersion forces are responsible of the emergence of the nematic phase. The main divergence between the two approaches is due to the temperature dependence (T); in fact, in Onsager's theory, it does not play any direct role (the theory is sensitive to density variations) while, in Maier-Saupe's theory, the T has an important direct role. This, in the field of thermotropic liquid crystals, is reflected on how much the two theories can reproduce the experimental data. Considering the Nematic (N)→Isotropic (I) transition, using the Onsager approach the value of the uniaxial order parameter, S (a measure of the orientation degree of the molecules) has a value of about 0.85, about twice with respect to that observed in real systems of typical nematics (nonetheless, this approach continues to play a very important role in the theory of liquid crystals); on the contrary, while using the mean-field approach of Maier-Saupe (MS), a value of about $S = 0.43$ is obtained, which is quite close to that observed experimentally. This description (certainly not exhaustive, but which will be resumed in more detail in Chapter 1) leads one to notice that both the mentioned theories have strengths and weakness points, but they share a common goal, that is to create a link between the microscopic and macroscopic properties of the system that is under investigation. The possibility to predict the behaviour of a system could, among other things, contribute to support the experimentalists in elaborating and designing the synthesis of particular compounds with predetermined characteristics, so avoiding what could be the waste of both material and human resources due to a 'trial and error' processes.

As said above, we have studied a system composed of C_{2h} symmetry particles [26], using Monte Carlo Simulation technique (up to now there are no similar issues in

the literature). In parallel, we have also investigated the behaviour of a D_{2h} particle system, using a Molecular Field method, in a region of molecular partially repulsive interactions, not addressed and explored so widely as done in [27]. Moreover, we also decided to address the problem of chirality [28], ubiquitous in many fields of natural sciences and phenomena (biological, chemical, etc ...) by using the peculiar properties of oriented systems. Our choice fell on a problem, such as chiral recognition, by exploiting the potential of the ordered phases in inducing different ordering between the two enantiomers. The best suited situation to achieve this goal was to consider systems made up of helical particles. Also for these systems there are various studies of various kind (DNA, proteins, etc ...); anyway, we have focused our attention on phases composed of helical chiral solutes dissolved/dispersed in (enantiopure) chiral solvents, in their turn formed by (concordant) helical particles [29]. For the investigation of this system, CS have been carried out and they have highlighted interesting aspects related to the orientational order and the use of order parameters as recognition tools. The pseudo-experimental data acquired by the CS were spent to validate a MF approach to the problem, through the formulation/proposition of a mean-torque potential sensitive to the handedness of the helical particles (i.e. P and M) and, therefore, potentially useful for the assignment of the absolute configuration.

This Thesis is organized 5 chapters: The first chapter gives the theoretical principles as a general support for the following chapters. In the second chapter, the operational details of the CS will be provided on systems of C_{2h} symmetry particles modelled as dimers of shifted spherocylinders. In the third chapter, a Molecular Field study carried out on D_{2h} symmetry particles will be illustrated, where an almost unexplored region of intermolecular interactions has been investigated, that can allow an important link between the microscopic and macroscopic properties of the system. In chapters 4 and 5, the problem of chirality referred to helical particle systems will be investigated, using CS for the prediction of virtual experimental data, that can be used to validate a Molecular Field approach as a model of interpretation of data in the cases where orientational differences between the two enantiomers emerge.

Bibliography

[1] G. Celebre, G. De Luca, M. Longeri, Internal Rotation Potential Function for Anisole in Solution: A Liquid Crystal NMR Study, *J. Phys. Chem.*, **96**, 2466-2470 (1992).

[2] G. Celebre, G. Cinacchi, The prediction of ordering of parallelepipedal solute particles in nematic solvents. A comparison among different methodologies, *Chem. Phys. Lett.*, **384**, 344-349 (2004).

[3] G. Celebre, G. Cinacchi, Orientational Ordering of Solutes in Confined Nematic Solvents: a Possible Way to Probe Director Distributions, *Phys. Rev. E*, **73**, 020702(R) (2006).

[4] C. Aroulanda, G. Celebre, G. De Luca, M. Longeri, Molecular Ordering and Structure of Quasi-spherical Solutes by Liquid Crystal NMR and Monte Carlo Simulations: The Case of Norbornadiene, *J. Phys. Chem. B*, **110**, 10485-10496 (2006).

[5] G. Celebre, G. Cinacchi, On the Analysis of LX-NMR dipolar coupling data via mixed *a priori*-maximum entropy methods, *J. Chem. Phys.*, **124**, 176101 (2006).

[6] G. Celebre, G. Cinacchi, G. De Luca, Solvent Smectic Order Parameters from Solute Nematic Order Parameters, *J. Chem. Phys.*, **129**, 094509 (2008).

[7] M.E. Di Pietro, G. Celebre, G. De Luca, G. Cinacchi, Rigid Probe Solutes in a Smectic-A Liquid Crystal: an Unconventional Route to the Latter's Positional Order Parameters, *Phys. Rev. E*, **84**, 061703 (2011).

[8] M.E. Di Pietro, G. Celebre, G. De Luca, H. Zimmermann, G. Cinacchi, Smectic Order Parameters via Liquid Crystal NMR Spectroscopy: Application to a Partial Bilayer Smectic A Phase, *Eur. Phys. J. E*, **35**, 112 (2012).

[9] A. Pizzirusso, M.E. Di Pietro, G. De Luca, G. Celebre, M. Longeri, L. Muccioli, C. Zannoni, Order and Conformation of Biphenyl in Cyanobiphenyl Liquid Crystals: A Combined Atomistic Molecular Dynamics and ^{1}H NMR Study, *ChemPhysChem*, **15**, 1356 (2014).

[10] G. Celebre, G. De Luca, M.E. Di Pietro, B.M. Giuliano, S. Melandri, G. Cinacchi, Detection of Significant Aprotic Solvent Effects on the Conformational Distribution of Methyl 4-Nitrophenyl Sulfoxide: from Gas-Phase Rotational to Liquid-Crystal NMR Spectroscopy, *ChemPhysChem*, **16**, 2327-2337 (2015).

[11] F. Bisi, G.R. Luckhurst, E. Virga, Dominant biaxial quadrupolar contribution to the nematic potential of mean torque, *Phys. Rev. E*, **78**, 021710 (2008).

[12] M.P. Allen, D.J. Tildesley, Computer Simulation of liquids, (Clarendon Press, Oxford, Second Edition, 2017).

[13] D. Frenkel, B. Smit, Understanding Molecular Simulation, (Academic Press, Cambridge, 2002)

[14] F. Reinitzer, *Monatsch. Chem.*, **9**, 421-441 (1888).

[15] O. Lehmann, *Z. Physkal. Chem.*, **4**, 462-472 (1889).

[16] G. R. Luckhurst, T.J. Sluckin, Biaxial Nematic Liquid Crystals (John Wiley & Sons, Ltd, Chichester, 2015)

[17] M.J. Freiser, Ordered phases of a nematic liquid, *Phys. Rev. Lett.*, **24**, 1041-1043 (1970).

[18] J.P. Straley, Ordered phases of a liquid of biaxial particles, *Phys. Rev. A*, **10**, 1881-1887 (1974).

[19] B.R. Acharya, A. Primak, S. Kumar, Biaxial Nematic Phase in Bent-Core Thermotropic Mesogens, *Phys. Rev. Lett.*, **92**, 145506 (2004).

[20] L.A. Madsen, T.J. Dingemans, M. Nakata, E.T. Samulski, Thermotropic Biaxial Liquid Crystals, *Phys. Rev. Lett.*, **92**, 145505 (2004).

[21] N. Boccara, Violation of rotational invariance and mesomorphic phase transitions characterized by an order parameter, *Ann. Phys.*, **76**, 72-79 (1973).

[22] B. Mettout, Theory of uniaxial and biaxial nematic phases in bent-core systems, *Phys. Rev. E*, **72**, 031706 (2005).

[23] B. Mettout, Macroscopic and molecular symmetries of unconventional nematic phases, *Phys. Rev. E*, **74**, 041701 (2006).

[24] L. Onsager, The effects of shape on the interaction of colloidal particles, *Ann.N. Y. Acad. Sci.*, **51**, 627-659 (1949).

[25] W. Maier, A. Saupe, A simple molecular statistical theory of the nematic crystalline-liquid phase, *Z. Naturforsch. A*, **14**, 882 (1959).

[26] C. D'Urso, G. Celebre, G. Cinacchi, Phase behaviour of hard-C_{2h} symmetric-particle systems, xxx, xxx, xxx, in preparation.

[27] G. Celebre, C. D'Urso, M. Porto, Extensive molecular field theoretical investigation of thermotropic biaxial nematics composed of board-like (D_{2h}) molecules in the partially repulsive regime of orientational interactions, *J. Mol. Liq.*, **248**, 847-853 (2017).

[28] G.H. Wagnière, Chirality and the Universal Asymmetry: Reflections on Image and Mirror Image (Wiley-VCH, Weinheim, 2007).

[29] J. Gutierrez Bojart, C. D'Urso, G. Celebre, G. Cinacchi, Probing the sensitivity of orientational ordering as a way towards absolute enantiorecognition: helical-particle solutes in helical-particle nematic solvents, *Phys. Rev. E*, **98**, 042704 (2018).

CHAPTER 1

Theoretical Background

1.1 Introduction

As said in the introduction, the creation of new materials often starts with the study of the building blocks of the material itself: the molecules. What we hope to understand in this work is the role of the shape of the particles of a fluid to obtain a certain macroscopic behaviour. One way to proceed is to suggest, starting from the molecular structure, a simplified molecular model, trying to keep only those aspects which are thought to be relevant for the macroscopic behaviour.
The simplest model that can allow to obtain a nematic phase is that where the particles are rigid rods (cylindrical symmetry, $D_{\infty h}$), as shown in Figure 1.1. If we choose a reference frame in which the **Z**-axis is parallel to the principal director of the phase $\boldsymbol{n}$ (that identifies the direction along which the particles are, on average, aligned [1]), the orientation of every particle can be given in terms of the polar angle ϑ that the molecular long axis (C_∞), identified with **z**) forms with the **Z** axis, and of the azimuthal angle φ (the angle that the projection of **z** in the **XY** plane makes with the **X** axis.

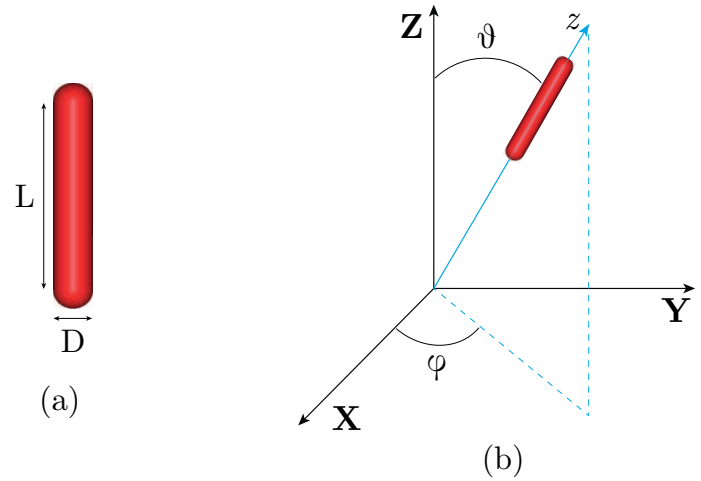

Figure 1.1: (a) Geometrical features of a spherocylinder particle: D is the diameter of the particle and L is the length of the cylinder part whose value is $L = 5D$ (b) Description of the orientation of a single $D_{\infty h}$ particle (in this case, a spherocylinder) with respect to the Laboratory system (**X, Y, Z**) through the polar (ϑ) and azimuthal (φ) angles.

It is appropriate, in this scenario, to introduce the distribution function $f(\vartheta, \varphi)$ corresponding to the probability density of finding the rod in a particular orientational state (then, the infinitesimal probability dP of finding the orientation of the particle within a small solid angle $d\Omega = sin\vartheta d\vartheta d\varphi$ will be $dP = f(\vartheta, \varphi)\ d\Omega$). For a uniaxial apolar phase, as the conventional nematics, this function has two important properties:

1. $f(\vartheta, \varphi) = f(\vartheta)/2\pi$, is indipendent of φ (this property is strictly attribuited to the cylindricl symmetry of the phase about the director);

2. $f(\vartheta) = f(\pi - \vartheta)$, due to the lack of polarity of the director **n** (see Chapter 1)

Due to the angular dependence of the orientational distribution function, it is possible to perform a multipole expansion (in terms of Cartesian tensors [2] or, alternatively, in terms of spherical tensors as Wigner rotation matrices [3], a generalization of Spherical Harmonics), to define mathematical quantities, called *order parameters*, that describe the nature and the degree of orientational order of the mesophase. The number of non-vanishing parameters strictly depend on both the symmetry of the particles and the phase. Just to describe with an example the general meaning of the term 'order parameter' (an exhaustive discussion on the order parameters will be successively presented in this work), for a uniaxial phase there is just one non-null order parameter (called S), that corresponds to the average of the first non-trivial term of the expansion (the quadrupolar one). It is defined in eq. (1.1):

$$S = \langle P_2(cos\vartheta) \rangle = \int_0^{\pi} P_2(cos\vartheta) f(\vartheta) sin\vartheta d\vartheta = \left\langle \frac{3}{2} cos^2\vartheta - \frac{1}{2} \right\rangle \tag{1.1}$$

where $P_2(cos\vartheta)$ is the second order Legendre polynomial [3]. In practice, when the molecules are, on average, perfectly aligned with the director, $S = 1$ (this happens for $\vartheta = 0$ and $\vartheta = \pi$). On the contrary, when $S = 0$, the particles are, on average, completely randomly oriented $\left(\left\langle cos^2\vartheta \right\rangle = \frac{1}{3}\right)$, see Figure 1.2. Of course, these definitions correspond to realistic physical situations that can be supported and confirmed by experimental results carried out by many techniques (LX-NMR, SAXS, etc. . .).

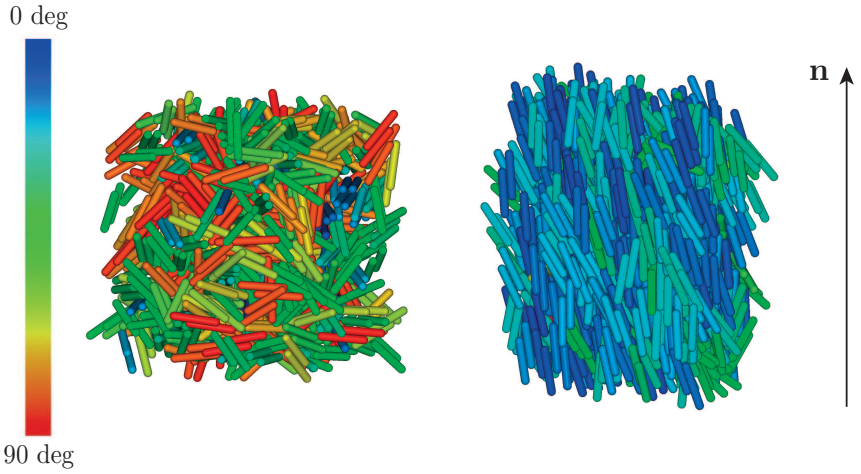

Figure 1.2: The colour of the particles is related with their orientation with respect to the director of the phase. Isotropic phase (left); Nematic phase $\vartheta \simeq 0°$ (right).

In general, from a thermodynamic point of view one possible aim of the work is to build a 'phase diagram' of the particular system under examination, in order to predict its behaviour. The use of the order parameters, together with other quantities (that will be discussed later), allows one not only to quantify the ordering present in the phase, but also to locate the temperature of the phase transitions and the physical nature of the phases present in the diagram. The challenge is to understand which is the effect of changing physical and chemical properties of the constituent molecules on the macroscopic behaviour of the system. The theoretical approaches that allow us to achieve these results are (basically) two: (1) Mean/Molecular Field Theories (MF) and (2) Computer Simulations (CS).

1.2 Molecular/Mean Field Theories

This kind of theories are founded on the mean field approximation in which, with the aim to simplify the calculations (often, strictly speaking, 'impossible' to do), we move from a many-body to a one-body problem. The heart of a Mean Field Theory [4] is indeed the formulation of a potential $U(\Omega)$, also called effective/pseudo/mean torque potential, from which the behaviour of the system under examination depends. In practice, instead of taking into account all the particle - particle interactions, we

consider the interaction of the single particle with the mean field generated by the other $N-1$ molecules: this is the trick. A fine but important difference must be necessarily done between *Mean and Molecular* Field: the former, following the Landau theory [5], utilises *phenomenological* parameters that it is not trivial to link with specific molecular properties; in other words, the parameters have to be phenomenologically adjusted in order to obtain an effective form of the potential, able to reproduce the physics of the studied system. On the contrary, in *Molecular Field* approach, these parameters can be, in principle, linked in some way with molecular properties. The two most important (pioneering) MFs theories in the field of LCs, are those due to the studies of Onsager [6] and Maier-Saupe [7], for the theoretical study of the transition from isotropic to nematic phase. In the Onsager Theory, the effects of the anisometry of the particles (assumed to be spherocylinders) were explored by using the so-called '*excluded volume*' approximation (Figure 1.3), where the interaction of particles is regulated by the use of a hard-core potential. In the Onsager's approach, there is not a direct dependence on Temperature (diathermic approach), but particular attention is paid, as said above, to the excluded volume (i.e., the region of space of each particle that is inaccessible to the other molecules). The free energy [6] is parametrized in terms of shape and orientations of the particles (described as spherocylinders) composing the phase themselves. Onsager was the first to predict entropy-driven phase transitions in liquid crystals. The system moves from an isotropic state, in which the orientations and positions of the particles are randomly distributed, to a nematic one, in which the molecules are, statistically, aligned along one preferred direction. There are two different contributions to the entropy, the translational (packing entropy) and the orientational one. When the rods are aligned, they lose orientational entropy but, at the same time, there is a decrease in the excluded volume, as shown in Figure 1.3, and therefore there is a *gain* in translational entropy.

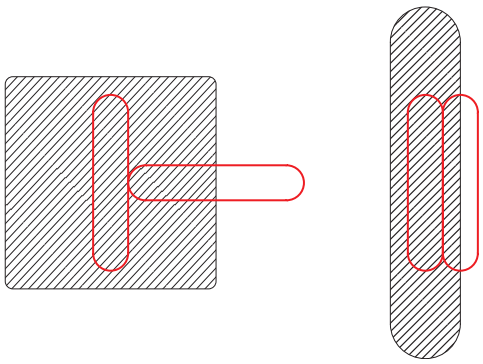

Figure 1.3: Excluded volumes (shaded area) for two spherocylinders in: (left) T configuration and (right) Parallel configuration.

The driving force, as stated above, is then the competition between rotational (orientational) and translational entropy: it is the balance between these two contribu-

tions to the total entropy of the system that determines the phase transitions. When the density increases, the space in which the particles can freely moves, decreases; therefore, the molecules prefer to align each other in order to minimize the excluded volumes, so minimizing the Helmholtz free energy: this is the reason why, in this approach, the order of the phase increases with the density. The Maier-Saupe Theory [7, 8] (MS), on the contrary, has an alternative approach: it is founded on the contribution of the dispersion forces (long-range interactions), to the orientational potential. According to this model every molecule experiences an effective potential of the following type:

$$U(\vartheta, S) = -A_0 S\left(\frac{3}{2}cos^2\vartheta - \frac{1}{2}\right) \tag{1.2}$$

where A_0 is a constant that depends on the sixth power of the inverse of interparticle distance (r_{ij}^{-6}). This theory predicts that, at the clearing temperature T_c, the value of the uniaxial order parameter is 0.43 and the transition will be classifiable like a weak first order transition. In spite of a better accordance with experimental data, with respect to the Onsager theory, this model is not free from limitations because, as the experiments show [9] , it is important to consider orientational short-range effects too.

The models discussed above allowed to study and build the basics of the phenomena that control and determine the fascinating properties of this particular condensed phase. The purpose of the present work is to go beyond the 'conventional' LCs; in particular, we have turned our attention to the *Thermotropic Biaxial Nematic Phase*. The existence of the biaxial phase, as stated in the Introduction Section, was first postulated by Freiser [10], in 1970, then by Straley [11] , in 1974. The latter presents a formal generalization of the Maier-Saupe theory, in which, instead of using a cylindrical symmetry, the particles are modelled as platelets possessing D_{2h} symmetry. The form of the potential of Maier-Saupe can be generalised to the biaxial D_{2h} nematic phases by using the following expression:

$$U = -u_0\{\mathbf{q}\cdot\mathbf{Q} + \gamma(\mathbf{q}\cdot\mathbf{B} + \mathbf{b}\cdot\mathbf{Q}) + \lambda(\mathbf{b}\cdot\mathbf{B})\} \tag{1.3}$$

where

$$\mathbf{q} = \mathbf{e}_z \otimes \mathbf{e}_z - \frac{1}{3}\mathbf{I} \tag{1.4}$$

$$\mathbf{b} = \mathbf{e}_x \otimes \mathbf{e}_x - \mathbf{e}_y \otimes \mathbf{e}_y \tag{1.5}$$

$$\mathbf{Q} = S\left(\mathbf{e}_Z \otimes \mathbf{e}_Z - \frac{1}{3}\mathbf{I}\right) + \frac{1}{3}P\big(\mathbf{e}_X \otimes \mathbf{e}_X - \mathbf{e}_Y \otimes \mathbf{e}_Y\big) \tag{1.6}$$

$$\mathbf{B} = D\left(\mathbf{e}_Z \otimes \mathbf{e}_Z - \frac{1}{3}\mathbf{I}\right) + \frac{1}{3}C\left(\mathbf{e}_X \otimes \mathbf{e}_X - \mathbf{e}_Y \otimes \mathbf{e}_Y\right) \tag{1.7}$$

The molecular orientation is expressed by the $\mathbf{q}$ and $\mathbf{b}$ tensors, with $\{\mathbf{e}_x, \mathbf{e}_y, \mathbf{e}_z\}$ the molecular unit vectors of the PAS. The tensors $\mathbf{Q} \equiv \langle \mathbf{q} \rangle$ and $\mathbf{B} \equiv \langle \mathbf{b} \rangle$ (where $\{\mathbf{e}_X, \mathbf{e}_Y, \mathbf{e}_Z\}$ indicates the Laboratory PAS) are functions of the S, P, D, C orientational order parameters. The latter can be obtained by the general expression of the Cartesian supermatrix given in eq. (1.8), in particular, their specific expressions are reported in eqs. (1.9-1.12). In order to mathematically describe these order parameters for a phase made up by platelets (see Figure 1.4) several different, but equivalent, definitions of the order parameters have been used in the past by many authors (table of correspondences can be found elsewhere [12]).

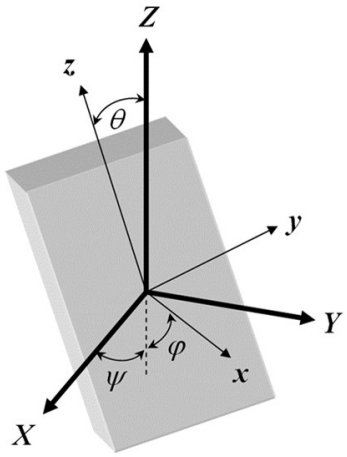

Figure 1.4: Molecular reference system (small letters) and Laboratory reference (capital letters) with the definition of the Eulerian angles φ, ϑ, ψ.

$$S_{ab}^{AB} = \langle (3 l_{ab} l_{AB} - \delta_{ab}\delta_{AB}) \rangle / 2 \tag{1.8}$$

$$S = S_{zz}^{ZZ} = \frac{1}{2}\langle 3 l_{zZ}^2 - 1 \rangle = \frac{1}{2}\langle 3 cos^2\vartheta - 1 \rangle \tag{1.9}$$

$$D = S_{xx}^{ZZ} - S_{yy}^{ZZ} = \frac{3}{2}\langle l_{xZ}^2 - l_{yZ}^2 \rangle = \frac{3}{2}\langle sin^2\vartheta - cos2\psi \rangle \tag{1.10}$$

$$P = S_{zz}^{XX} - S_{zz}^{YY} = \frac{3}{2}\langle l_{zX}^2 - l_{zY}^2 \rangle = \frac{3}{2}\langle sin^2\vartheta - cos2\varphi \rangle \tag{1.11}$$

$$\begin{aligned} C = (S_{xx}^{XX} - S_{yy}^{XX}) - (S_{xx}^{YY} - S_{yy}^{YY}) = \frac{3}{2}\langle (l_{xX}^2 - l_{yX}^2) - (l_{xY}^2 - l_{yY}^2) \rangle = \\ \frac{3}{2}\langle (1 + cos^2\vartheta)\, cos2\varphi\, cos2\psi \; - 2 cos\vartheta\, sin2\varphi\, sin2\psi \rangle \end{aligned} \tag{1.12}$$

where l_{aB} represents the direction cosines, the capital letters denote the Lab reference frame (PAS) and the small ones the molecular frame, finally, the angular brackets represent the statistical average. In an isotropic phase, all the order parameters are zero ($S = D = C = P = 0$); in a uniaxial phase, only the first two order parameters (S and D) will be non-zero, whereas in the biaxial phase all four order parameters are non-zero. Following the Freiser's work, it is possible to write the Helmholtz free energy as reported in eq. (3.4):

$$F = \frac{u_0}{3}\left\{S^2 + \frac{1}{3}P^2 + 2\gamma\left(SD + \frac{1}{3}PC\right) + \lambda\left(D^2 + \frac{1}{3}C^2\right) - \frac{3}{\beta}ln\left(\frac{Z}{8\pi^2}\right)\right\} \quad (1.13)$$

$$Z = \int_{\psi}^{2\pi}\int_{\varphi}^{2\pi}\int_{\vartheta}^{\pi} e^{-\beta(U/u_0)} sin\vartheta \, d\vartheta d\varphi d\psi \quad (1.14)$$

where Z is the partition function, u_0 a positive parameter and $\beta = u_0/kT$ [4]. If we were able to minimize the F free energy as a function of the orientational order parameters, it would be possible to obtain the stable states, compatible to the molecular field, for the system. To do this the expression of Z-function should be in principle known: by this way, it would be possible, in principle, to calculate all the thermodynamic properties of the system, by using the usual formulas provided by the statistical thermodynamics. The problem is that Z cannot be obtained by an exactly analytical integration of eq. (1.14). Then, one possibility is to use numerical techniques of approximated integration of eq. (1.14) or try to obtain a closed analytical (even though approximated) form of the partition function [13].
The choice of the study of this particular symmetry of the particles is surely due to the fact that it represents the simplest case to deal with. However, the biaxial phase can, in principle, exist for a widely range of symmetries other then D_{2h} and, from the seminal work of Boccara [14], many progress in the field have been done [15, 16]. In recent years, for example, many scientists used V-shaped (bent-core) molecules [17–19] a promising morphology to obtain the elusive researched phase. In our Project, on the contrary, we focused our attention on C_{2h} symmetry of the particles, that should be able, in principle, to give a thermotropic nematic biaxial phase one [20]. The complexity of the intermolecular interaction potential requires the use of a more extensive and convenient basis set instead of the cartesian one: the Wigner matrices [3], a generalization of the Spherical Harmonics functions, and the formalism of the irreducible spherical tensors. Then the orientational potential can be then conveniently expressed as:

$$U(\Omega) = U_u(\Omega) + U_{D_{2h}}(\Omega) + U_{C_{2h}}(\Omega) \quad (1.15)$$

where each single term of the sum is given in the eqs. (1.16-1.18)

$$\begin{aligned} U_u(\Omega) = -[&(\langle R_{00}\rangle + 2\gamma_s\langle R_{02}\rangle - 2\gamma_a\langle I_{02}\rangle)R_{00}(\Omega)+ \\ &+ (2\gamma_s\langle R_{00}\rangle + 4\lambda_s\langle R_{02}\rangle - 2\lambda_0\langle I_{02}\rangle)R_{02}(\Omega)+ \\ &+ (-2\gamma_a\langle R_{00}\rangle - 2\lambda_0\langle R_{02}\rangle - 4\lambda_a\langle I_{02}\rangle)I_{02}(\Omega)] \end{aligned} \tag{1.16}$$

$$\begin{aligned} U_{D_{2h}}(\Omega) = -2\{[&(\langle R_{20}\rangle + \gamma_s\langle R^s_{22}\rangle - \gamma_a\langle I^s_{22}\rangle)R_{20}(\Omega)+ \\ &+ (\gamma_s\langle R_{20}\rangle + \lambda_s\langle R^s_{22}\rangle - \frac{1}{2}\lambda_0\langle I^s_{22}\rangle)R^s_{22}(\Omega)+ \\ &+ (-\gamma_a\langle R_{20}\rangle - \frac{1}{2}\lambda_0\langle R^s_{22}\rangle - \lambda_a\langle I^s_{22}\rangle)I^s_{22}(\Omega)]\} \end{aligned} \tag{1.17}$$

$$\begin{aligned} U_{C_{2h}}(\Omega) = -2\{[&(\langle I_{20}\rangle + \gamma_s\langle I^a_{22}\rangle + \gamma_a\langle R^a_{22}\rangle)I_{20}(\Omega)+ \\ &+ (\gamma_a\langle I_{20}\rangle + \frac{1}{2}\lambda_0\langle I^a_{22}\rangle - \lambda_a\langle R^a_{22}\rangle)R^a_{22}(\Omega)+ \\ &+ (\gamma_s\langle I_{20}\rangle + \lambda_s\langle I^a_{22}\rangle + \frac{1}{2}\lambda_0\langle R^a_{22}\rangle)I^a_{22}(\Omega)]\} \end{aligned} \tag{1.18}$$

where the term $U_u(\Omega)$ (eq. (1.16)) is responsible of the formation of the uniaxial nematic phase, the $U_{D_{2h}}(\Omega)$ (eq. (1.17)) accounts for the possible existence of biaxial nematic regions with D_{2h} symmetry and the $U_{C_{2h}}(\Omega)$ (eq. (1.18)) describes the biaxial nematic phase with C_{2h} symmetry (it should be noticed as, in this case, it is possible to obtain a D_{2h} biaxial mesophase starting from C_{2h} particles [20, 21]). Furthermore Ω denotes the set of angular variables $(\varphi, \vartheta, \psi)$, with $R^{s,a}_{l,m}$ and $I^{s,a}_{l,m}$ the appropriate real and imaginary parts of the Wigner matrices (symmetrical and antisymmetric). The order parameters required to properly describe the statistical ordering of the mesophase should amount to 25. However, for symmetry reasons [20], their number can reduced to 9, whose expressions are reported in the eqs. (1.19-1.27):

$$\langle R_{00}\rangle = S^{ZZ}_{zz} \tag{1.19}$$

$$\langle R_{02}\rangle = \frac{1}{\sqrt{6}}(S^{ZZ}_{xx} - S^{ZZ}_{yy}) \tag{1.20}$$

$$\langle I_{02}\rangle = \sqrt{\frac{2}{3}}S^{ZZ}_{xy} \tag{1.21}$$

$$\langle R_{20}\rangle = \frac{1}{\sqrt{6}}(S^{XX}_{zz} - S^{YY}_{zz}) \tag{1.22}$$

$$\langle R^s_{22}\rangle = \frac{1}{3}[(S^{XX}_{xx} - S^{YY}_{xx}) - (S^{XX}_{yy} - S^{YY}_{yy})] \tag{1.23}$$

$$\langle I^s_{22}\rangle = \frac{2}{3}(S^{XX}_{xy} - S^{YY}_{xy}) \tag{1.24}$$

$$\langle R^a_{22} \rangle = \frac{2}{3}[(S^{XY}_{xy} - S^{YX}_{xy})] \tag{1.25}$$

$$\langle I_{20} \rangle = -\sqrt{\frac{2}{3}} S^{XY}_{zz} \tag{1.26}$$

$$\langle I^a_{22} \rangle = -\frac{2}{3}(S^{XY}_{xx} - S^{XY}_{yy}) \tag{1.27}$$

It is interesting to note that, if the D_{2h} phase exists then $\langle R_{00} \rangle \to 1$,$\langle R_{20} \rangle$, $\langle R_{02} \rangle \to 0$ and $\langle R^s_{22} \rangle \to 1$. On the contrary, if nematogenic molecules have C_{2h} symmetry and the phase has the same symmetry then $\langle R_{00} \rangle$,$\langle R^s_{22} \rangle$,$\langle R^a_{22} \rangle$ are expected to be large whereas the other parameters are expected to be small.

1.3 Computer Simulations (CS)

Computer Simulations [22] play an important role in the prediction of phase behaviours and, at the same time, the simulated results can be compared with those obtained from real experiment. The double role of CS, as a bridge between models and experimental results, is very important, because often can allow to perform useful *virtual* experiments, very difficult to carry out in practice. Today, the role of Computer Simulations is well defined and they find applications in almost all fields of science; of course, they become even more attractive and useful thanks to the increase in computing power, as the Moore's law* suggests. It should be emphasized that our interest is not that of investigating the detailed properties of specific molecules; on the contrary, we often have the problem of designing molecules of which, probably, the detailed structure is not known; therefore the ultimate goal of CS is that of sketching molecules that have not yet been synthesised and that are, in principle, able to yield mesophases with specific properties of interest. This turns possible when the characteristic of the molecules is responsible of a certain collective behaviour is well understood. The most useful techniques for studying and to achieve this result from a simulation point of view are: Molecular Dynamics (MD) and Monte Carlo (MC) [22]. With the first method it is possible to solve step by step classical equation of motions for all the N particles in the system: this allows us to calculate some properties (observables) from the trajectories obtained. The choice between MC and MD is largely determined by the phenomena under investigation: since, in this work, the aim is to study only the effect of the shape of the particles on the macroscopic behaviour of the system, we choose to use MC which will be described more accurately.

* It is a famous informatic law: it establishes that every 18/24 months the number of transistors on a chip doubles, while at the same time increasing the computing power

MC methods allow us to calculate the properties of interest, the observables, from equilibrium configurations, where a configuration stands for a set of positions and orientations of the molecules, generated from an appropriate algorithm. Suppose that, in a Canonical ensemble (NVT) [23] (where the number of particles, N, the volume of the system,V, and the Temperature T are fixed) we want to calculate the observable $\langle A \rangle$, depending on positions and orientation of all the N particles. If we indicate the six variables ($\boldsymbol{r}_i$, Ω_i) of each particle as $\boldsymbol{X}$, then:

$$Z_N = \int d\boldsymbol{X}^N \, e^{(-\beta U_N)} \tag{1.28}$$

$$\langle A \rangle = \frac{1}{Z_N} \int d\boldsymbol{X}^N \, A e^{(-\beta U_N)} \tag{1.29}$$

where Z_N is the canonical partition function, $d\boldsymbol{X}^N = \prod_{i=1}^{N} d\boldsymbol{X}_i$ and the volume element in the phase space is $d\boldsymbol{X}_i{=}d\boldsymbol{r}_i d\Omega_i$ with $d\boldsymbol{r}_i = dx_i, dy_i, dz_i$ and $\mathrm{d}\Omega_i{=}\sin\theta_i \mathrm{d}\theta_i \mathrm{d}\varphi_i \mathrm{d}\psi_i$. Imagine now that it is possible to take some snapshots of the system and store them to calculate the observable of interest, replacing the previous formula for A with the form of eq. (1.30), thanks to the *ergodic hypothesis* (the long-time average of any mechanical property is equal to the average value of that property over all the M microscopic states, M configurations in this case, of the system):

$$\langle A \rangle = \frac{1}{M} \sum_{j=1}^{M} A^j \tag{1.30}$$

The 'trick' is to calculate A in every configuration, A^j; then, to average over the configurations themselves. Obviously, it is necessary a high number of configurations is required to minimize statistical errors and fluctuations. The crucial point is the generation of these configurations, which represents the role of MC technique, paying attention to the fact that this must be done respecting the physical and thermodynamic conditions of the chosen ensemble. In this Project, the Metropolis [24, 25] technique has been used, where every configuration appears with a frequency proportional to the Boltzmann factor. This is made possible thanks to the utilization of the so-called Markov chain: the probability of occurrence of each event, k, at time t depends only by the state of the system immediately preceding k. The basic simulation procedure of MC method goes as follows: first of all, the energy of the initial configuration (U^{old}) will be calculated; then, one particle is randomly chosen and a trial move (rotation, translation) is attempted; finally the new energy of the system (U^{new}) will be evaluated. If ($U^{new} - U^{old} < 0$) the new configuration is accepted; on the contrary, if this does not happen, the new configuration will not be

rejected immediately, but it will be accepted or not in accord with the probability $e^{-\beta(U^{new}-U^{old})}$, where $\beta = 1/kT$. In practice, when a random number α, randomly generated between 0 and 1, is less then $e^{-\beta(U^{new}-U^{old})}$ the configuration (and thus the trial move) is accepted (rejected otherwise and the old configuration restored). This procedure will be carried out several times in the simulations until the equilibrium is reached. The working flow of the MC method is reported in Figure 1.5:

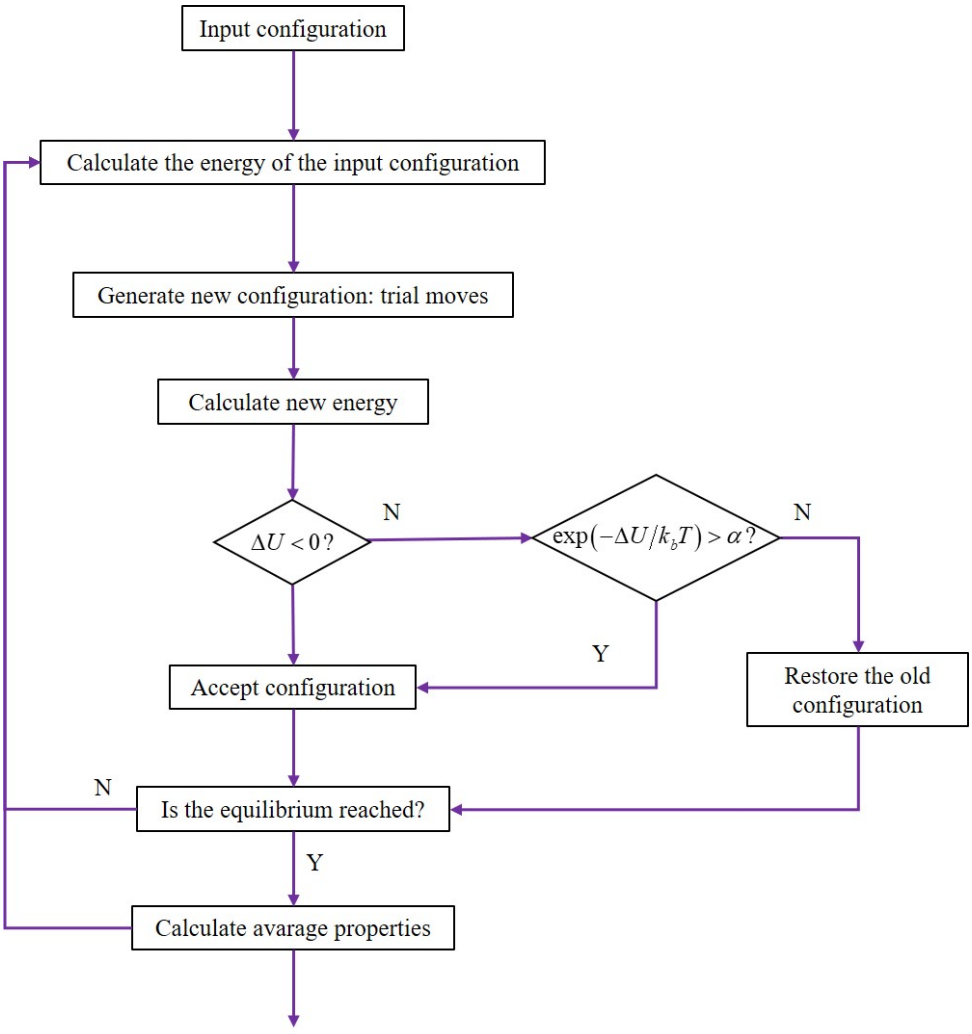

Figure 1.5: Flow chart of a Metropolis Monte Carlo Simulations.

With the aim to apply CS to the study liquid crystal systems, two kinds of approach are possible. The first is the *on-lattice model*, where the particles have fixed positions at the lattice sites. One of the most famous application of this type is Lebwohl-Lasher one [27]. Rod-like molecules can freely rotating and they are subjected to an exclusively orientational intermolecular potential of the form reported in eq. (1.31).

For this type of simulations, only the interactions between nearest neighbours are taken into account:

$$U_{ij} = -\epsilon_{ij} P_2(cos\beta_{ij}) \tag{1.31}$$

where ϵ_{ij} is a positive constant, $P_2(...)$ represents the second-order Legendre polynomial and β_{ij} is the angle between the orientation of the particle i and j. Despite its simplicity, by this model it is possible to obtain quite 'good' information about the orientational states of the system under examination. Using this approach, it is, of course, not possible to acquire information about the positional order possibly present in the phase; then in the years, a second approach to CS of LCs became more important, the *off-lattice model*, where translational freedom is present besides the rotational one.

The earliest work on liquid crystals using an off-lattice model was conducted by Viellard-Baron [28], by studying the behaviour of a system made up of hard ellipsoid particles (Figure 1.6), while the first attempt to construct a phase diagram for a three-dimensional system of the same particles is amenable to Frenkel et al [29] (however, in his work a MD technique has been used):

Calamitic LCs can be modelized also as hard spherocylinders (as in the Onsager

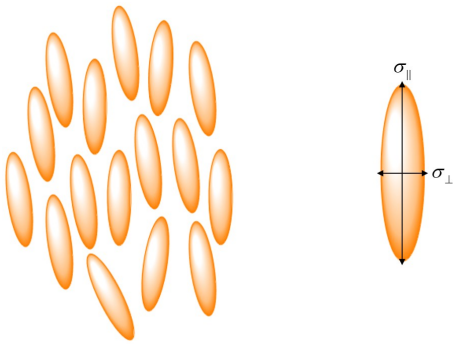

Figure 1.6: (left): System composed of ellipsoidal particles; (right); shape parameters for ellipsoidal particle.

theory), similar to the shape of various mesogenic colloids, as, for example, the tobacco mosaic virus. If we assume a hard-core potential in the MC simulations the interaction energy can assumes only the values ∞ or 0, based on whether or not there is an overlap between the particles, as reported in Figure 1.7:

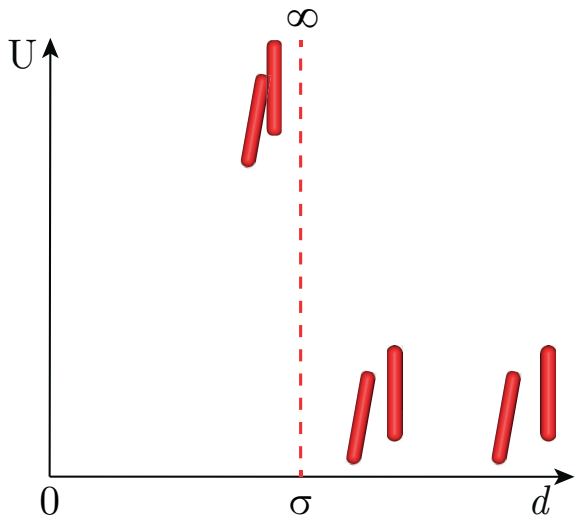

Figure 1.7: Potential (U) of interaction between hard-core particles, d is the distance between them and σ is the distance at which the overlap occurs.

where d is the distance between the particles and the red dashed line represents the distance σ at which the overlap occurs. It must be emphasised that, due to the anisometry of the particles (non-spherical particles), the interaction potential depends not only on the distance between the centres of the molecules but also on their orientation $d(r_{ij}, \Omega)$. By using a hard-core particle model, only the repulsive interactions between particles are taken into account; however, in the years, others theories have been developed that consider the attractive interactions too, labelled as soft-core models. The most famous and useful of these models is the Gay-Berne (GB) potential [30] one. It can be seen as a generalised anisotropic and shifted version of the Lennard-Jones interaction, with attractive and repulsive parts that decrease as inverse powers of distances. Here the pair-interaction energy is:

$$U_{ij}(u_i, u_j, r_{ij}) = 4\epsilon_{ij}(u_i, u_j, r_{ij}) \left[\frac{\sigma_0}{r - \sigma(u_i, u_j, r_{ij}) + \sigma_0} \right]^{12} + - \left[\frac{\sigma_0}{r - \sigma(u_i, u_j, r_{ij}) + \sigma_0} \right]^{6} \tag{1.32}$$

In the GB model the strength ϵ_{ij}, and the σ parameters depend on the orientation vectors $\mathbf{u_i}$ and $\mathbf{u_j}$ of the two particles and on their separation vector $\mathbf{r_{ij}}$. Generally, this potential is characterized by parameters (correlated to the shape of the model particles, that determine the overall form of the potential), that take into account different ways to in which the particles can interact, as for example: end to end interaction, side by side interaction and face to face interaction.

Bibliography

[1] P.G. de Gennes, J. Prost, The Physics of Liquid Crystals (University Press, Oxford, 1993).

[2] M.E. Rose, Elementary Theory of Angular Momentum, (John Wiley and Sons Inc., New York, 1967).

[3] D.M. Brink, G.R. Satchler, Angular Momentum, ed.2, (Oxford University Press, Oxford, 1962).

[4] F. Bisi, G. R. Luckhurst, E. Virga, Dominant biaxial quadrupolar contribution to the nematic potential mean torque, *Phys. Rev. E*, **78**, 021710 (2008).

[5] L.D. Landau, Toward a theory of phase transitions. Zh.E.T.F., 7, 19 (1937). English translation in Collected Works of L.D. Landau (Pergamon Press, Oxford, 193–216, 1965).

[6] L. Onsager, The effects of shape on the interaction of colloidal particles, *Ann.N. Y. Acad. Sci.*, **51**, 627-659 (1949).

[7] W. Maier, A. Saupe, A simple molecular statistical theory of the nematic crystalline-liquid phase, *Z. Naturforsch. A*, **14**, 882 (1959)

[8] W. Maier, A. Saupe, Eine einfache molekulare Theorie des nematischen kristallinflüssigen Zustandes , *Z. Naturforsch. A*, **13**, 564 (1958).

[9] J. R. McColl C. S. Shih, Temperature dependence of orientational order in a nematic liquid crystal at constant molar volume, *Phys. Rev. Lett.*, **29**, 85-87 (1972).

[10] M.J. Freiser, Ordered phases of a nematic liquid, *Phys. Rev. Lett.*, **24**, 1041-1043 (1970).

[11] J.P. Straley, Ordered phases of a liquid of biaxial particles, *Phys. Rev. A*, **10**, 1881-1887 (1974).

[12] R. Rosso, Orientational order parameters in biaxial nematics: Polymorphic notation, *Liq. Cryst.*, **34**, 737-748 (2007).

[13] G. Celebre, Statistical thermodynamics of thermotropic biaxial nematic liquid crystals: An effective, molecular-field based theoretical description by means of a closed approximate form of the orientational partition function, *J. Mol. Liq.*, **209**, 104-114 (2015).

[14] N. Boccara, Violation of rotational invariance and mesomorphic phase transitions characterized by an order parameter, *Ann. Phys.*, **76**, 72-79 (1973).

[15] M. Liu, Hydrodynamic theory of biaxial nematics, *Phys. Rev. A*, **24**, 2720-2726 (1981).

[16] B. Mettout, P. Toledano, H. Takezoe, J. Watanabe, Theory of polar biaxial nematic phases, *Phys. Rev. E*, **66**, 031701 (2002).

[17] B. Mettout, Theory of uniaxial and biaxial nematic phases in bent-core systems, *Phys. Rev. E*, **72**, 031706 (2005).

[18] B.R. Acharya, A. Primak, S. Kumar, Biaxial Nematic Phase in Bent-Core Thermotropic Mesogens, *Phys. Rev. Lett.*, **92**, 145506 (2004).

[19] L.A. Madsen, T.J. Dingemans, M. Nakata, E.T. Samulski, Thermotropic Biaxial Liquid Crystals, *Phys. Rev. Lett.*, **92**, 145505 (2004).

[20] G.R. Luckhurst, S. Naemura, T.J. Sluckin, T.B.T. To, S. Turzi, Molecular field theory for biaxial nematic liquid crystals composed of molecules with C_{2h} point group symmetry, *Phys. Rev. E*, **84**, 011704 (2011).

[21] T.C. Lubensky, L. Radzihovsky, A Classification of the Possible Symmetry Groups of Liquid Crystals, *Phys. Rev. E*, **66**, 031704 (2002).

[22] M.P. Allen, D.J. Tildesley, Computer Simulation of liquids, (Clarendon Press, Oxford, 2017).

[23] T.L. Hill, An Introduction to Statistical Thermodynamics, (Dover Publications Inc., New York, 1986).

[24] N. Metropolis, A.W. Rosenbluth, M.N. Rosenbluth, A.H. Teller, E. Teller, Equation of State Calculations by Fast Computing Machines, *J. Chem. Phys.*, **21**, 1087-1092 (1953).

[25] W. Feller, An Introduction to Probability Theory and its Applications, (Wiley, 1950).

[26] W.Krauth, Algorithms and Computations, (Oxford University Press, 2006).

[27] P.A. Lebwohl, G. Lasher, Nematic-Liquid-Crystal Order-A Monte Carlo Calculation, *Phys. Rev. A*, **6**, 426-429 (1972).

[28] J. Viellard-Baron, Phase Transitions of the Classical Hard-Ellipse System, *J. Chem. Phys.*, **56**, 4729-4744 (1972).

[29] D. Frenkel, J.F. Maguire, Molecular Dynamics Study of Infinitely Thin Hard Rods: Scaling Behavior of Transport Properties, *Phys. Rev. Lett.*, **47**, 1025-1028 (1981).

[30] J.G. Gay, B.J. Berne, Modification of the overlap potential to mimic a linear site–site potential, *J. Chem. Phys.*, **74**, 3316-3319 (1981).

CHAPTER 2

Computer Simulations of Biaxial Particles with C_{2h} Symmetry

2.1 Introduction

The quest for a truly *Thermotropic Biaxial Nematic Phase*, N_b, has been aptly named *the holy grail* [1] of Liquid Crystals, since it has fuelled experimental and theoretical research for more than 45 years, starting from the theoretical paper of Freiser [2] and Straley [3]. There are scientists who claim to have found this phase experimentally [4–6], but there are others who question these results and the debat [7, 8] is still open. This elusiveness may be due to the fact that some features (morphology of molecules, molecular interactions, etc..) favouring the formation of the biaxial nematic phase also favour their packing in the competing smectic (Sm) or crystalline (K) biaxial phases; moreover, also we need to keep in mind that the original predictions of the existence of this mesophase are based on a 'simple' mean field theory that sometimes makes mistakes in determining phase boundaries. The use of Computer Simulations can help us to draw direct relations between specific molecular properties (in particular, the molecular shape and its symmetry) and macroscopic behaviour; in other words, we are speaking about *Molecular Design of Biaxial Liquid Crystals*.
The fundamental questions that should be, in principle, answered are the following:

1. What are the molecular interactions able to promote the formation of the N_b and how much is the molecular shape (and its symmetry) important/decisive?

2. How much good are the Mean/Molecular field models in predicting the phase transitions?

3. What are the features that can destabilize the competing phases of the N_b one?

The task of answering is mainly entrusted to the theoreticians, with the aim of collaborating, after the engineering step, in synergy with the experimentalists by proposing, for example, some structures (morphologies) that a molecule must have to be a good candidate in order to obtain a stable N_b phase. The most 'natural' computational technique to make this study could seem to be the atomistic one, where each atom (or small group of atoms) is represented by a suitable attractive-repulsive centre, with the construction (or the use of a already existing) suitable force field, by means of which the particle interactions can be modelized. Many scientists assert that the shape [9, 10] of the particles plays a decisive role in the formation of this particular phase. Since we share this opinion, we decided to use a hard particle model. In our work we modelized the particles as dimers of shifted spherocylinders with C_{2h} symmetry, see Figure 2.1:

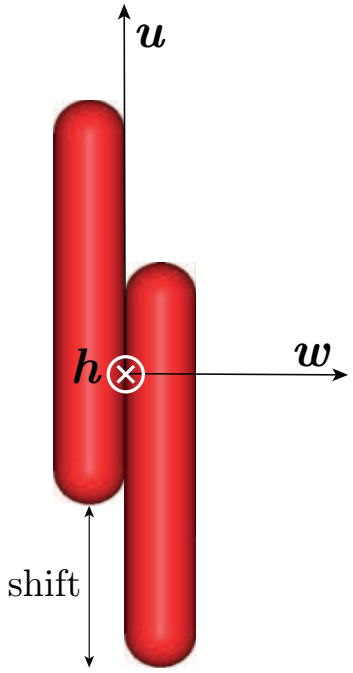

Figure 2.1: Image of the dimer of shifted spherocylinders with indicated: (I) the molecular reference frame represented by the triad of unit vectors $\{\boldsymbol{u}, \boldsymbol{w}, \boldsymbol{h}\}$ and (II) the shift between the two spherocylinders.

The most important reasons about this choice are the following:

- This kind of particle symmetry has been scarcely explored, until now, by CS;
- Phases made by spherocylinders present stable positional and orientational ordered states; then, it should be possible, in principle, to study if some features exist that can disfavour the formation of competing phases.

2.2 Computational Details

It is known from thermodynamics that the Equation of State (EoS), for a particular system, is determined experimentally. For most of the real systems, the expression of EoS is not known analytically; then, the description of the phase diagram and, therefore, the prediction of the stable states of the system is quite difficult. This is even more true for the phase we are dealing with, not having ever, so far, been found experimentally. Given the necessity to have at one's disposal this kind of thermodynamic data, both to test theoretical models (e.g. Mean/Molecular theories) and/or to understand to which extent the purely shape/symmetry molecular features are able to promote the formation of the searched phase, we have turned our attention to the use of CS (mainly thanks to the collaboration with Prof. Giorgio Cinacchi*). The study of phase behaviour has been performed by using MC simulations (in NPT ensemble) over system size ranges from N=576 to N=2400 dimers; it should be emphasized that, in the simulations, 'reduced dimensionless units' have been used, labelled with an asterisk. Every system has been simulated at different reduced pressures P^* ($P^* = PD_3/kT$ where D is the diameter of the spherocylinders) and, during the simulation, the density ρ^* ($\rho^* = \rho D^3$) has been equilibrated , where ρ is the number density N/V (V being the volume of simulation box of sides L_x, L_y, L_z); in practice, Pressure (Temperature) scans have been done. Actually, a useful dimensionless quantity to be used, instead of ρ^*, is the packed fraction $\phi = \rho^* \cdot (V_{dim}/D^3) = \rho \cdot V_{dim}$ where $V_{dim} = 2\pi[\frac{LD^2}{4} + \frac{D^3}{6}]$ is the volume of the dimer. The potential chosen is the 'hard-core potential', whose form is given in Chapter 1 (see Figure 1.7). To obtain equilibrated configurations, several MC steps (typically of the order of 10^6 steps) were performed, each step consisting of N+2 attempts to: (a) translate/rotate a random chosen particle or (b) change the volume of the simulation box, changing randomly the length of one edge at time; moreover, simulations were performed using fixed (cubic) and variable (triclinic) boxes.
The most expensive computational part is to evaluate, move after move, if overlaps occur between particles. An effective technique to reduce the computational times of this procedure is to use the Verlet list algorithm [11], where only the interactions of the moved particle with its nearest neighbours are taken into account. The final purpose of our work is to obtain a complete phase diagram [12] for hard dimers of shifted spherocylinders.

* Department of Theoretical Physics of Condensed Matter, Institute of Condensed Matter Physics (IFIMAC) and Institute of Materials Sciences 'Nicolas Cabrera', Universidad Autonoma de Madrid, Campus de Cantoblanco, 28049 Madrid, Spain.

The flow chart of the entire 'mechanism' of the simulations is reported in Figure 2.2:

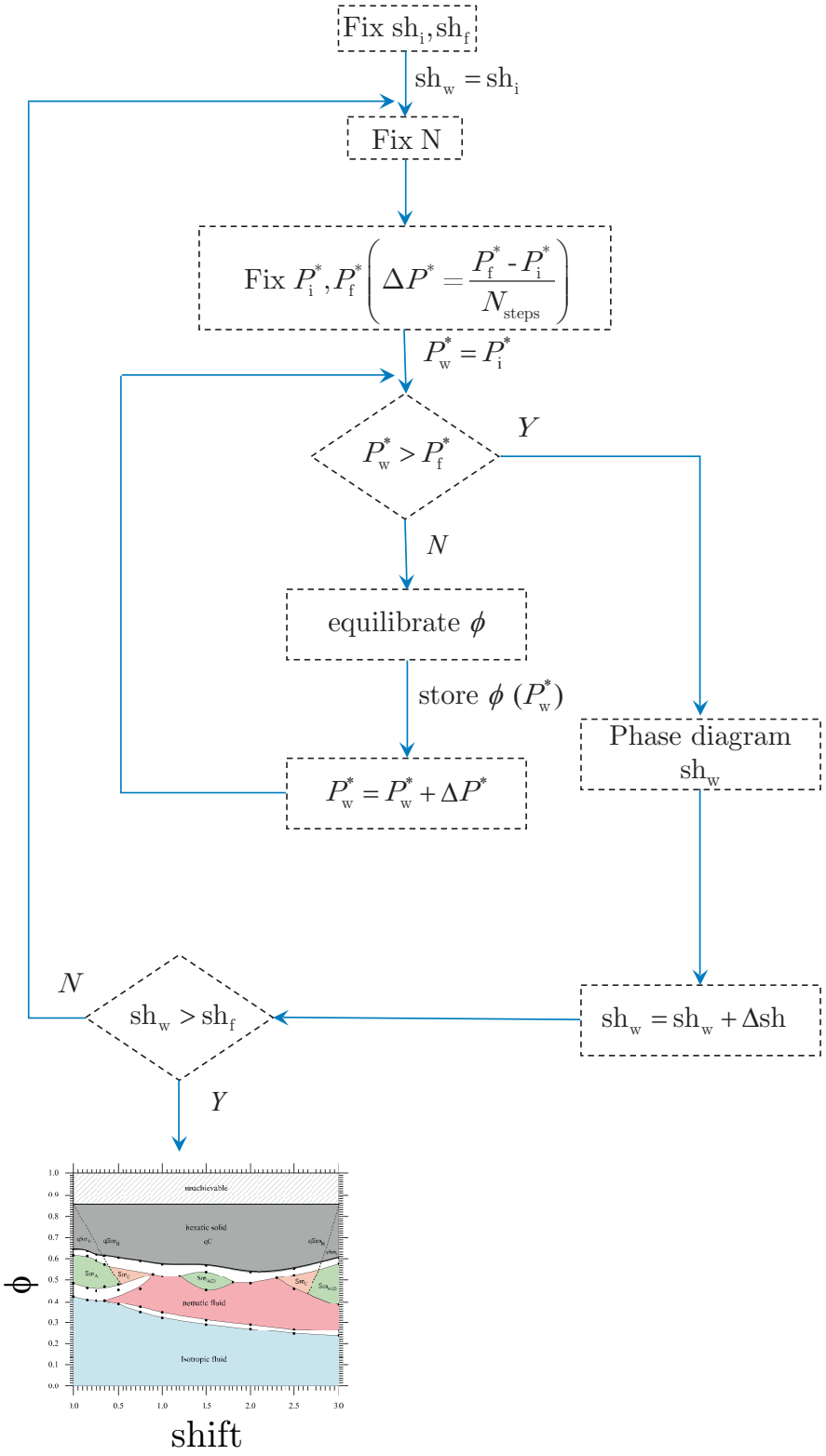

Figure 2.2: Flow chart of the simulation process, where sh=shift, ϕ=volume (or packed) fraction, N=number of particles, P=pressure, Δ sh=incremental value of shift, the subscripts i, w, f stay for initial, working, final.

In order to obtain a correct and reliable sampling of the configurational space (but also to limit calculation times) the percentage of acceptance of the random moves must be kept in a range that varies from 10 and 30 percent; this is obtained by adjusting the magnitude of the random moves, the maximum translation/rotation of the particle (the software does not adjust automatically these parameters because, doing this, could introduce 'bias' so that the results could be significantly affected and very wrong (as reported in the literature [13]). The automatic adjustment of the magnitude of the moves makes the probability of attempting a new trial move dependent on the previous configuration history (not only dependent on the last one) thus violating the Markovian process. In addition, the correlation between the configurations has, as a consequence that it is not respected the balance condition [14, 15]. As a last part of this introduction to the computational work, it should be emphasized that the whole MC code (routines and subroutines of analysis) is an entirely in-house software (written in Fortran77). It represented a significant part of the Project.
Exactly as after a chemical synthesis, it needs to characterize what has been obtained in order to verify whether or not the desired compound has been obtained, in the same way, after a 'virtual' CS experiment, it needs to recognize the phases virtually emerging from the simulations; in particular, the aim is to quantify the orientational and positional statistical order present in the obtained phases. The tools used for this purpose were:

- Visualization (by the QMGA [16] software) of the output configurations;
- Evaluation of the:
  a) Order parameters;
  b) Correlation and distribution functions;
  c) Mean square displacements (msd);

2.3 Simulated Order Parameters

For a uniaxial phase composed of N uniaxial particles, the order parameter is calculated as reported in eqs. (2.1) [17], where:

$$Q^{uu}_{\alpha,\beta} = \frac{1}{N}\sum_{i=1}^{N}\frac{3}{2}u_{i\alpha}u_{i\beta} - \frac{1}{2}\delta_{\alpha\beta} \tag{2.1}$$

with $\alpha, \beta = \boldsymbol{X}, \boldsymbol{Y}, \boldsymbol{Z}$ the axes of the LAB reference frame, the $u_{i\alpha}$ the α component of the unit vector $\boldsymbol{u}$ (i.e. the direction) of the long molecular axis with respect to the **Z** axis of the box (of the Lab) of the i-th molecule and $\delta_{\alpha\beta}$ the Kronecker symbol.

The order parameter, denoted as S, is defined as the largest (in magnitude) eigenvalue of the $\boldsymbol{Q^{uu}}$ tensor, and the corresponding eigenvector identifies the nematic director $\boldsymbol{n}$. In the definitions of the biaxial order parameters, instead, the symmetry of the particles (and, of course, of the phase) is of fundamental importance. Remembering that our aim is to study a phase composed of C_{2h} particles, as suggested in literature [18], it could be possible, in principle, to think different *idealised shapes* [18] (in the case of board-like particles for example) possessing the desired C_{2h} symmetry. The first possible shape (see Figure 2.3, model 1) is that in which the long molecular axis $\boldsymbol{u}$ coincide with the C_2 symmetry axis of the particle [19], anyway, other two possible choices exist: (I) a particle shape in which the two-fold axis of the molecule coincides with the short $\boldsymbol{w}$ molecular axis, (Figure 2.3, model 2) and (II) a shape in which the two-fold axis coincide with the shortest molecular axis $\boldsymbol{h}$ (Figure 2.3, model 3). The idealised shapes just described are shown in the following figure:

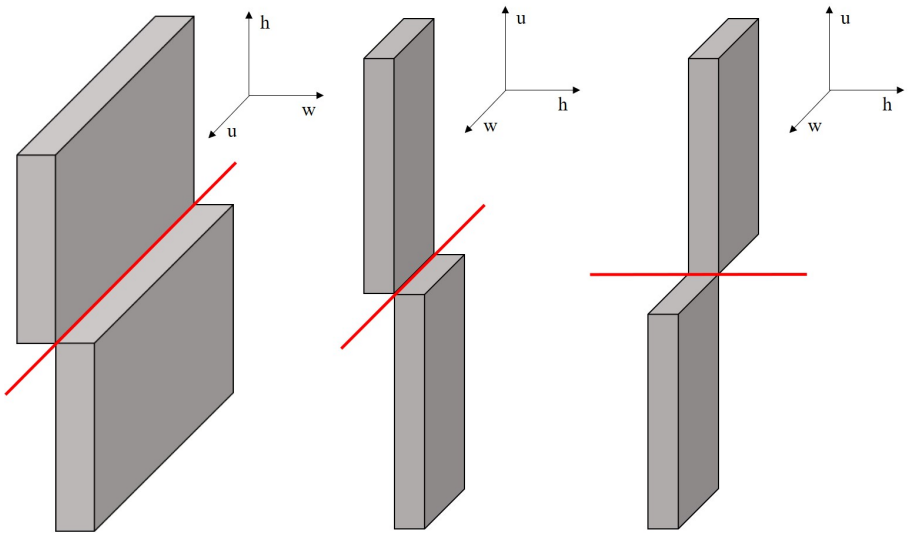

Figure 2.3: Idealised shapes for a C_{2h} particle: model 1, 2 and 3 (from left to right); the red line represents the C_2 symmetry axis and $\boldsymbol{w}, \boldsymbol{h}, \boldsymbol{u}$ represent the molecular reference frame.

The choice among the models 1, 2 or 3 suggests the use of different forms of the effective orientational potential and, as a consequence, the use of different order parameters for each case. The model 3 is that consistent and comparable with our scenario made of dimers of spherocylinders. In this scenario, for a phase made up of dimers, the peculiar order parameters [18] are reported, in the form in which they are implemented into the code, in eqs. (2.2-2.4). It should be emphasized that, in principle, for this kind of phase one can have 25 order parameters, but for symmetry reasons [18, 19] and for sake of simplicity this number is approxiamted to just 3 'fundamental' order parameters:

$$R_{00} = \frac{1}{N}\sum_{i=1}^{N}\frac{3}{2}(\boldsymbol{u_i}\cdot\boldsymbol{Z})^2 - \frac{1}{2} \tag{2.2}$$

$$R_{22} = \frac{1}{N}\sum_{i=1}^{N}\frac{1}{3}\left[(\boldsymbol{w_i}\cdot\boldsymbol{X})^2 + (\boldsymbol{h_i}\cdot\boldsymbol{Y})^2 - (\boldsymbol{w_i}\cdot\boldsymbol{Y})^2 - (\boldsymbol{h_i}\cdot\boldsymbol{X})^2\right] \tag{2.3}$$

$$R^a_{11} = \frac{1}{N}\sum_{i=1}^{N}\frac{2}{3}\left[(\boldsymbol{w_i}\cdot\boldsymbol{X})\cdot(\boldsymbol{u_i}\cdot\boldsymbol{Z}) - (\boldsymbol{w_i}\cdot\boldsymbol{Z}) - (\boldsymbol{u_i}\cdot\boldsymbol{X})\right] \tag{2.4}$$

where, $\boldsymbol{w_i}$, $\boldsymbol{h_i}$, $\boldsymbol{z_i}$ are the unit vectors (i.e. the direction) of the molecular axes with respect to the **X**, **Y**, **Z** axis of the box (of the Lab) of the i-th molecule. In order to be able to calculate these quantities it is necessary to define the **X**, **Y** and **Z** of the Lab reference frame. This step can results often quite 'ambiguous'; so, in order to avoid confusion, we decided to introduce new *molecular order parameters* defined as follows:

$$Q^{ww}_{\alpha,\beta} = \frac{1}{N}\sum_{i=1}^{N}\frac{3}{2}w_{i\alpha}w_{i\beta} - \frac{1}{2}\delta_{\alpha\beta} \tag{2.5}$$

$$Q^{w_\perp w_\perp}_{\alpha,\beta} = \frac{1}{N}\sum_{i=1}^{N}2w_{\perp i\alpha}w_{\perp i\beta} - \delta_{\alpha\beta} \tag{2.6}$$

with $w_{\perp i\alpha}$ the α component of the unit vector $\boldsymbol{w_{\perp i\alpha}}$, being $\boldsymbol{w_{\perp\alpha}} = (\boldsymbol{w}\times\boldsymbol{n})/|\boldsymbol{w}\times\boldsymbol{n}|$. The two mathematical quantities just reported are very useful in quantifying the biaxial order with D_{2h} symmetry; the procedure of calculation is the same as that of the calculation of S, where rather than taking into account the orientation of the long molecular the orientation of the short molecular axis $\boldsymbol{w}$ is taken into account. From the diagonalization of the two tensors given in eqs. (2.5-2.6), we have defined two new orientational order parameters for a biaxial phase (possessing D_{2h}) that will be denoted as S_w and $S_{w_\perp}$.

As repeatedly reported, since for our simulations we are using particles with C_{2h} symmetry (Figure 2.1), it could be possible that the biaxial phase with C_{2h} symmetry appears; so, we decided to define another order parameter sensitive to the formation of this kind of symmetry of the mesophase, whose expression is reported in eq. 2.7:

$$P_{C_{2h}} = \left\langle \frac{1}{N}\left|\sum_{i=1}^{N}(\boldsymbol{u_i}\cdot\boldsymbol{n})(\boldsymbol{w_{\perp i}}\cdot\boldsymbol{m})\right|\right\rangle \tag{2.7}$$

where $\boldsymbol{n}$ and $\boldsymbol{m}$ are the principal and secondary director, both available from the calculation of S first and $S_{w_\perp}$ after; $\langle ...\rangle$ indicating an arithmetic mean over configurations. The order parameters just introduced are independent of external reference

frame, since they are obtained by using exclusively the molecular reference system; this is possible thanks to the use of CS, because, with this technique, it is possible to know the orientation of each single particle in each single instant. As said in Chapter 1 (in the section regarding the Molecular Field), when C_{2h} symmetry particles are considered, it is necessary to take into account the possibility of formation of a biaxial phase possessing D_{2h} symmetry; in our case, this could be possible when configurations (schematized in Figure 2.4) occurs; if it happens: $S_{w_\perp} \to 1$ and $P_{C_{2h}} \to 0$.

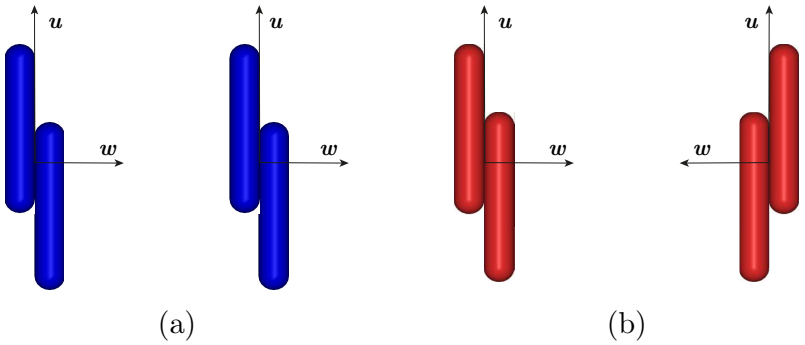

Figure 2.4: Possible configurations of (a) C_{2h} and (b) D_{2h} phase.

Until now, it has been taken into account only the orientational order of the particles but LCs can exhibit also a statistical positional order; this is peculiar for smectic phase, for example. To identify and quantify this kind of order in our simulations, we used the well-know positional (or translational) smectic order parameter τ [20], whose expression is reported in eqs.(2.8-2.9):

$$\lambda_k(d) = \sum_{j=1}^{N} \left| \exp\left(i2\pi k \frac{\boldsymbol{r_j} \cdot \boldsymbol{n}}{d} \right) \right| \tag{2.8}$$

$$\tau = max\, \lambda_k(d) \tag{2.9}$$

where k is the order of the parameter, $\boldsymbol{r_j}$ are the positions of the centres of mass with respect to a fixed origin of the particles, $\mathbf{n}$ is the principal director and d is the 'guess' parameter: the value of d that maximize the function represent the spacing of the smectic layers. In general, for a Sm_A phase ones can have a situation as shown in Figure 2.5 where the characteristic trend of the function of eq. (2.8) for a layered phase is shown. This parameter quantify the extent of layering of the particles: when $\tau \to 0$ there is an absence of a layered structure and, on the contrary, $\tau \to 1$ indicates the presence of a high degree of stratification of the particles.

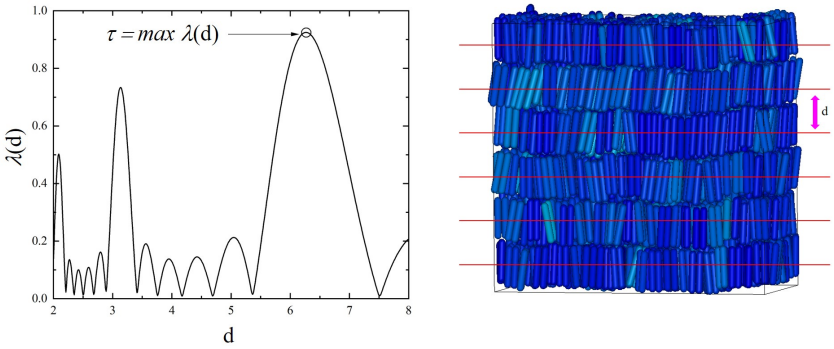

Figure 2.5: Behaviour of smectic function of eq. (2.8), assuming k=1, for the case at P*=0.90 where the shift between the spherocylinders is set to 0.

The procedure reported above can be applied when the normal to the layers is aligned along $\boldsymbol{n}$ is known, but unfortunately, this direction is not a priori detectable. We have faced the problem when it was necessary to have a positional order parameter able to detect the presence of a Sm_C phase. It is possible to realise that, searching for the maximum of eq. (2.8) is nothing else than searching for the maximum of the structure factor among the reciprocal-lattice vectors of the form $\boldsymbol{k} = \frac{2\pi}{d}\boldsymbol{n}$; due to that, the layer normal can be obtained by determining the $\boldsymbol{k_{max}}$ at which the structure factor $S(k)$ shows the most prominent Bragg peak. In practice, $\boldsymbol{k_{max}}$ identifies the direction of the layer normal that allows to calculate the τ_C using the same procedure adopted for the calculation of τ_A. In addition, the tilting angle between the director and the layer normal is: $\theta = arccos[(\boldsymbol{k_{max}} \cdot \boldsymbol{n})/|\boldsymbol{k_{max}}|]$ and it is also possible to note that the Sm_A phase can be simply considered as a particular case of Sm_C phase with $\theta = 0$ and $\boldsymbol{k_{max}} = \boldsymbol{n}$.
It is known from literature [21] that a phase composed of calamitic particles can give rise to the hexatic phase, therefore to take into account this, we have also calculated the hexatic order parameter [22, 23], whose expression is reported in eq. 2.10:

$$\psi_6 = \left\langle \frac{1}{N}\sum_{i=1}^{N}\left|\frac{1}{n_i}\sum_{j=1}^{n_i}\exp(6i\theta_{ij})\right|\right\rangle \tag{2.10}$$

Here the inner sum runs over the nearest neighbours of particle i within a single layer, and θ_{ij} is the angle between the orientation of the line connecting the centroids of nearby molecules, finally $\langle ... \rangle$ means an average over the configurations. The value of ψ_6 equals 1 in case of perfect hexatic ordering.

2.4 Correlation Functions

In order to study in detail the microstructure (short and long range order) of the phase we calculate the correlation functions, giving a series of statistical averages

that allow us to describe the orientation and organization of the particles within the phase under examination, in order to be able to rationalize and link together: (1) the display of the simulation output, (2) the value of the order parameters and, of course, (3) the trend of the functions themselves. The expressions of the calculated quantities and their descriptions are reported into eqs. (2.11-2.19):

$$g(r) = \frac{1}{N}\left\langle \frac{1}{\rho}\sum_{i=1}^{N}\sum_{j\neq i}^{N}\delta(r - r_{ij})\right\rangle \tag{2.11}$$

where $\rho = N/V$ is the number density , $r_{ij} = |\boldsymbol{r_{ij}}| = |\boldsymbol{r_j} - \boldsymbol{r_i}|$, $\delta()$ is the δ-function and $\langle ...\rangle$ means an arithmetic mean over configurations. This is the most basic positional pair correlation function, proportional to the conditional probability density of finding the centroid of a particle j at a distance r from the centroid of a particle i.

Another important information is that related to the structure of the fluid along the director and perpendicularly to it. In order to 'resolve' the structure along these two directions, the so-called parallel, eq. (2.12), and perpendicular, eq. (2.13), correlation function have been calculated:

$$g(r_{\parallel}) = \frac{1}{N}\left\langle \frac{1}{\rho}\sum_{i=1}^{N}\sum_{j\neq i}^{N}\delta(r_{\parallel} - \boldsymbol{r_{ij}}\cdot\boldsymbol{n})\right\rangle \tag{2.12}$$

$$g(r_{\perp}) = \frac{1}{N}\left\langle \frac{1}{\rho}\sum_{i=1}^{N}\sum_{j\neq i}^{N}\delta(r_{\perp} - |\boldsymbol{r_{ij}}\times\boldsymbol{n}|)\right\rangle \tag{2.13}$$

They represent the probability of finding a particle j, whose distance from a central particle i, projected along (perpendicular to) the director is $r_{\parallel}$ ($r_{\perp}$). The functions reported until now can be called 'positional' correlation functions, due to the fact that the orientation of the particles has been neglected; however, as can be expected, it is of fundamental importance equip ourselves with other functions that consider the orientation too, for this purpose we have calculated the quantities $g_{2u}(r)$, $g_{2ur}(r)$, $g_{2w}(r)$ and $g_{2w_{\perp}}(r)$:

$$g_{2u}(r) = \left\langle \frac{\sum_{i=1}^{N}\sum_{j\neq i}^{N}P_2(\boldsymbol{u_i}\cdot\boldsymbol{u_j})\delta(r - r_{ij})}{\sum_{i=1}^{N}\sum_{j\neq i}^{N}\delta(r - r_{ij})}\right\rangle \tag{2.14}$$

the function gives the degree of correlation in the orientations of two particles whose centroids are separated by a distance r;

The function:

$$g_{2ur}(r) = \left\langle \frac{\sum_{i=1}^{N}\sum_{j\neq i}^{N} P_2(\boldsymbol{u_i}\cdot\hat{\boldsymbol{r}}_{\boldsymbol{ij}})\delta(r-r_{ij})}{\sum_{i=1}^{N}\sum_{j\neq i}^{N}\delta(r-r_{ij})} \right\rangle \tag{2.15}$$

where $\hat{\boldsymbol{r}}_{\boldsymbol{ij}} = \boldsymbol{r_{ij}}/r_{ij}$, measures the degree of orientational ordering of the fictious bond $\boldsymbol{r_{ij}}$, established between the centroids of two particles i and j, with respect to $\boldsymbol{u_i}$;
The functions:

$$g_{2w}(r) = \left\langle \frac{\sum_{i=1}^{N}\sum_{j\neq i}^{N} P_2(\boldsymbol{w_i}\cdot\boldsymbol{w_j})\delta(r-r_{ij})}{\sum_{i=1}^{N}\sum_{j\neq i}^{N}\delta(r-r_{ij})} \right\rangle \tag{2.16}$$

and

$$g_{2w_\perp}(r) = \left\langle \frac{\sum_{i=1}^{N}\sum_{j\neq i}^{N} \left[2\left(\boldsymbol{w}_{\perp\boldsymbol{i}}\cdot\boldsymbol{w}_{\perp\boldsymbol{j}}\right)^2-1\right]\delta(r-r_{ij})}{\sum_{i=1}^{N}\sum_{j\neq i}^{N}\delta(r-r_{ij})} \right\rangle \tag{2.17}$$

indicate the degree of correlation in the orientations of the $\boldsymbol{w}$ and $\boldsymbol{w}_\perp$, of two particles, whose centroids are separated by a distance r. They are particularly useful in obtaining information about the distribution of the short molecular axis, that is be very useful for the recognition of an hypothetical appearance of the biaxial or hexagonal phase; for example, for a 'perfect' hexatic phase, the particles are 'organised' so that their cross-sections form hexagons, as shown in Figure 2.6:

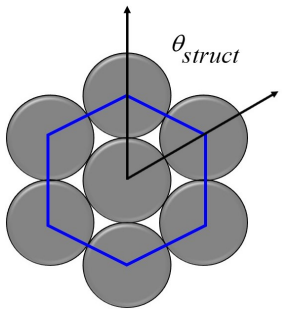

Figure 2.6: Schematization of a hexagonal configuration formed by spherocilinder particles.

It should be noticed that, in eqs. (2.16- 2.17), there is a squared dependence on the unit vector of the particles; then, it is impossible to distinguish between D_{2h} and C_{2h} phases. For this reason, we implemented another correlation function given in eq. 2.18:

$$g_{uw}(r) = \left\langle \frac{\sum_{i=1}^{N}\sum_{j\neq i}^{N}(\boldsymbol{u_i}\cdot\boldsymbol{u_j})(\boldsymbol{w}_{\perp\boldsymbol{i}}\cdot\boldsymbol{w}_{\perp\boldsymbol{j}})\delta(r-r_{ij})}{\sum_{i=1}^{N}\sum_{j\neq i}^{N}\delta(r-r_{ij})} \right\rangle \tag{2.18}$$

This function, can be called *biaxial correlation function*, because it measures the degree of correlation (at the same time) of the orientations $\boldsymbol{u_i}$ and $\boldsymbol{w}_{\perp\boldsymbol{i}}$ of two parti-

cles separated by a distance r. Due to the linear dependence on the unit vectors $\boldsymbol{u_i}$ and $\boldsymbol{u_i}$, the information about the alignment of the particles is not lost; this could be particularly useful in detecting the presence of long-range orientational (biaxial) order.

It is also known that phases made up of simple spherocylinders can possess a columnar structure; this can happen, in principle, also for our system. For this reason, we have also calculated the columnar function reported in eq. (2.19):

$$g(r_c) = \frac{1}{[D^2/2]N} \left\langle \frac{1}{\rho} \sum_{i=1}^{N} \sum_{j \neq i}^{N} \Delta_{ij}\, \delta(r_c - \boldsymbol{r_{ij}} \cdot \boldsymbol{u_i}) \right\rangle \tag{2.19}$$

where:

$$\Delta_{ij} = \Theta\left[\frac{D}{2} - \sqrt{rij - (\boldsymbol{r_{ij}} \cdot \boldsymbol{u_i})^2}\right] \tag{2.20}$$

It gives the probability of finding a particle j in a cylinder of radius $D/2$, with an axis parallel to the orientation of the particle i at a resolved (along $\boldsymbol{u_i}$) distance r_c. Δ_{ij} assures that only the particles belonging to the column are counted (Θ represents the step function), and this situation is schematized in Figure 2.7:

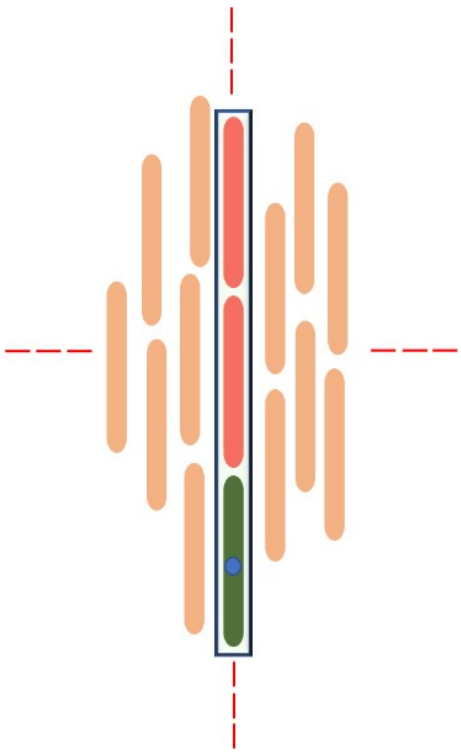

Figure 2.7: Schematization of a columnar phase. Green particle is the reference particle with orientation u_i.

In addition to the real-space correlation functions, the reciprocal-structure factor (precisely its orientational average $S(k)$) has been calculated:

$$S(k) = \left\langle \frac{1}{N} \sum_{j=1}^{N} \left| \exp\left(i\boldsymbol{k} \cdot \boldsymbol{r_j} \right) \right|^2 \right\rangle \tag{2.21}$$

where $\boldsymbol{k}$ is a reciprocal-lattice vector compatible with the computational box, $k = |\boldsymbol{k}|$ and $\langle ... \rangle$ represents a suitable orientational average over the reciprocal lattice vectors sharing the same modulus.

2.5 Mean Square Displacement

One of the requirements that a phase must have to be defined as fluid is, of course, that the particles possess a certain mobility into the phase itself. It is possible to evaluate the mobility of the particles thanks to the calculation of their mean square displacement (msd). In particular, it has been implemented the parallel and perpendicular component of the msd with respect to the principal director; the expressions are reported eq. (2.22-2.23):

$$\mathrm{msd}_{\parallel}(t) = \left\langle \left[r_{\parallel}(t) - r_{\parallel}(t=0) \right]^2 \right\rangle \tag{2.22}$$

$$\mathrm{msd}_{\perp}(t) = \left\langle \left[r_{\perp}(t) - r_{\perp}(t=0) \right]^2 \right\rangle \tag{2.23}$$

Being our MC simulations *non-dynamic*, the instantaneous value of the time t should be understood as a configuration; in other words, an 'instant' is characterized by a particular position of the centroid and orientation of the dimer; r ($\parallel$ and $\perp$) are the parallel and perpendicular component of the position of the particles with respect to the principal director (the mobility of the particles is of course calculated starting from the initial configuration). In the following Figures (2.8-2.9), two characteristic trends obtained in our simulations are reported; in particular they represent the msd for a nematic and smectic phase.
In a nematic phase (Figure 2.8) the particles prefer to move along the direction of $\boldsymbol{n}$ and the mobility is high ($\approx 10^3$ in terms of D); moreover the overall behaviour of the both component of msd is linear (the y-scale in the graphs is logarithmic). On the contrary, in a smectic phase the mobility along and perpendicularly with respect to the director is very different (Figure 2.9); this is because the intra-layer mobility of the particles is favourite with respect to the inter-layer one. What has just been said can be even more so appreciated, by looking at the behaviour of the msd vs t(configurations) shown in Figure 2.9. In fact, whereas the behaviour

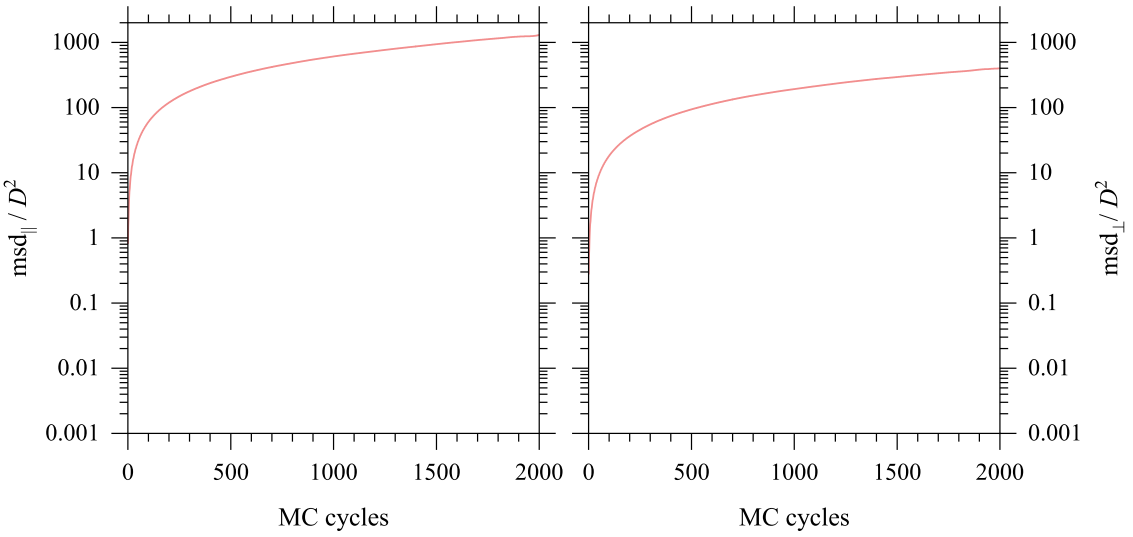

Figure 2.8: msd for a nematic phase in wich the particles forming the dimer are shifted by 1D, note that the y-scale is logarithmic;

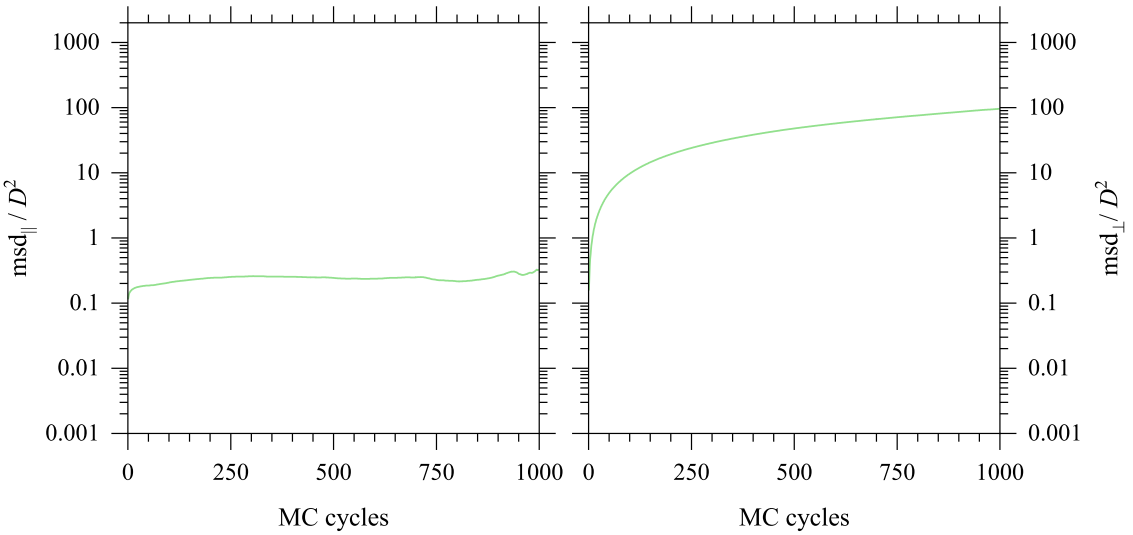

Figure 2.9: msd for a smectic phase in wich the particles forming the dimer are unshifted; note that the y-scale is logarithmic.

of the perpendicular component of $msd_\perp$ is still linear, the parallel trend is more peculiar. At the beginning, it grows steeply until it reaches a plateau: this is due to the fact that, when a particle leaves a smectic layer and then moves on to the next one, it slows down (roughly speaking). This happens because: (a) the *trapping cage effect* [24, 25] exercised by the other particles and (b) the *barrier effect* [24, 25], due to the formation of the smectic layers. All the numerical results of the calculated order parameters, some of the most representative phase diagrams and, finally, some snapshots of the investigated systems can be consulted in Appendix A and Appendix B.

2.6 Results and comments of the systematic investigation of a single-component system made up of C_{2h} hard particles

We investigated several values of shift (s), $s \in [0, 3]$: in this section, the results will be shown; anyway, as mentioned above, rather than presenting and discussing every single shift, we have chosen to discuss the whole *final* phase diagram, shown in Figure 2.10, where all the findings emerged are included (for the interested reader, some individual phase diagrams are reported in Appendix A).

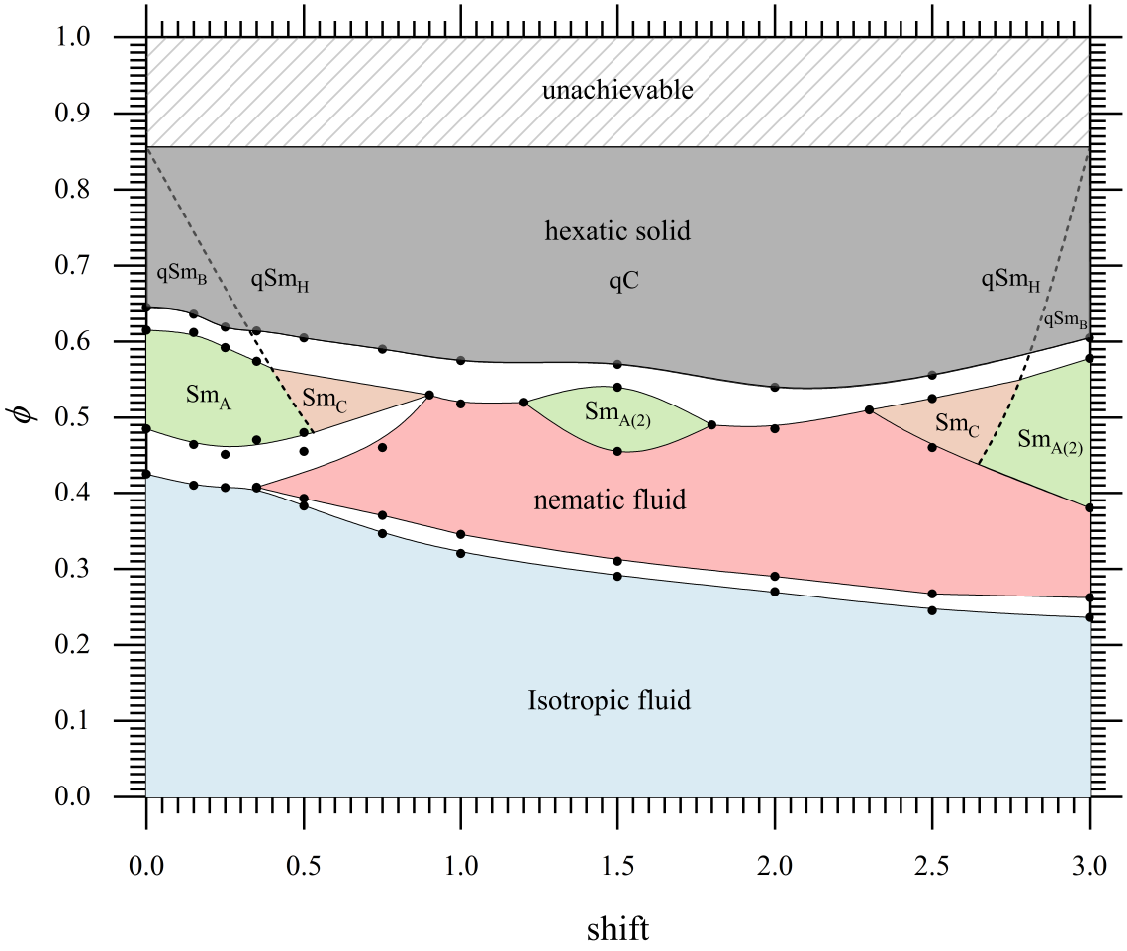

Figure 2.10: Phase diagram (ϕ vs s) of the single-component system made up of hard spherocylinder dimers. Each colour corresponds to a particular mesophase and the white regions define the co-existence zones.

The liquid-crystalline phases are enclosed between the Isotropic phase, at low values of ϕ, and the various solid phases at high values of ϕ. In general, the latter presents a monomeric hexatic order, in function of s it can be: *quasi* Sm_B (qSm_B) at $s \to 0$ and $s \to 3$; *quasi* Sm_H (qSm_H) [27] for values slightly bigger than 0 and slightly smaller than 3; *quasi* columnar (qC) for intermediate values of ϕ. The adjective *quasi*

has been chosen because the mesophases just mentioned are referable to the single hard spherocylinders composing our dimers. As regards the dense packing of hard dimers of spherocylinders the upper limit has been fixed at a 0.856, corresponding to a packing of hard spherocylinder monomers hexagonally arranged on a plane with them exactly on top of one other. Occasionally the densest packing fraction has been fixed at 0.883, the value of ϕ of the densest Bravais lattice packing, or at least the densest-known [28, 29]). The region up to $\phi = 1$ is not accessible due to the fact the the hard spherocylinders are not space-fillers. It is intriguing to note how the graph is almost symmetrical around $s = 1.5$, in particular, it can be observed how the Sm_A phase is present both at the ends of the graph and at the centre, where it forms a sort of 'eye-shaped pocket'. It should be noticed that, for values of $s < 1.5$, the layer spacing has a value comparable to that of the length of the dimer particles, whereas for $s \geq 1.5$, the distance between the layers is smaller than L of the dimer (the regions where this occurs are indicated as Sm_{A2}). Going from the ends toward the centre of the phase diagram, the Sm_A phase gradually gives rise to the Sm_C phase. The lack of a 'perfect' symmetry of the diagram is mainly due to two reasons: (1) In the surroundings of $s = 0$ there is not a nematic phase; on the contrary, a direct transition from I to Sm_A occurs. This was quite surprising because, by 'glueling' two spherocylinders (so forming the biaxial version of the single spherocylinder) potentially suitable for the formation of the biaxial nematic mesophase, no nematic phases emerge. At the other extreme, $s = 3$, the uniaxial nematic phase is present in a wide interval of ϕ. (2) As s increases, the co-existence region gently declines as effect of the enhancing of the lenght-to-width ratio. From the extensive investigation performed we can assert that for values $s \simeq 1$ and $s \simeq 2$ the only stable mesophase is the uniaxial nematic one; unfortunately, no evidence of the appearance of the biaxial nematic has been detected. Nonetheless, the destabilization of the smectic mesophase using this (realistic) model has been demonstrated: we think that is a good result, because it can be considered a new starting point for both theoretical and experimental studies. In fact, from the theoretical point of view, one can investigate a system made up, for example, of trimers, using the optimal values of shift, in order to observe, hopefully, the biaxial nematic phase. On the other hand, the experimentalists should try to test molecules having shapes similar to that of dimers exhibiting the optimal shift observed in the simulations.

Bibliography

[1] R. Berardi, L. Muccioli, S. Orlandi, M. Ricci, C. Zannoni, Computer simulations of biaxial nematics, *J. Phys. Condens. Matter*, **20**, 463101 (2008).

[2] M.J. Freiser, Ordered phases of a nematic liquid, *Phys. Rev. Lett.*, **24**, 1041-1043 (1970).

[3] J.P. Straley, Ordered phases of a liquid of biaxial particles, *Phys. Rev. A*, **10**, 1881-1887 (1974).

[4] B.R. Acharya, A. Primak, T.J. Dingemans, E. T. Samulski, S. Kumar, The elusive thermotropic biaxial nematic phase in rigid bent-core molecules, *Pramana*, **61**, 231-238 (2003).

[5] L.A. Madsen, T.J. Dingemans, M. Nakata, E.T. Samulski, Thermotropic biaxial nematic, *Phys. Rev. Lett.*, **92**, 145505 (2004)

[6] B.R. Acharya, A. Primak, S. Kumar, Biaxial nematic phase in rigid-bent-core thermotropic mesogens, *Phys. Rev. Lett.*, **92**, 145506 (2004).

[7] Y. Galerne, Characterization of biaxial nematic phases in the thermotropic liquid crystals, *Mol. Cryst. Liq. Cryst.*, **323**, 211-229 (1998).

[8] G.R. Luckhurst, Biaxial nematic liquid crystals: fact or finction?, *Thin Solid Films*, **393**, 40-52 (2001).

[9] H.C. Andersen, D. Chandler, J.D. Weeks, Roles of repulsive and attractive forces in liquids: The equilibrium theory of classical fluids (in H. Prigogine, S.A. Rice, *Adv. Chem. Phys.*, **34**), 105-156 (1976).

[10] A.V. Petukhov, J.M. Meijer, G. Jan Vroege, Particle shape effects in colloidal crystals and colloidal liquid crystals: Small-angle X-ray scattering studies with microradian resolution, *Curr. Opin. Colloid Interface Sci.*, **20**, 272-281 (2015).

[11] L. Verlet, Computer 'Experiments' on Classical Fluids. Thermodynamical Properties of Lennard-Jones Molecules, *Phys.Rev.*, **159**, 98-103 (1967).

[12] P. Bolhuis, D. Frenkel, Tracing the phase boundaries of hard spherocylinders, *J. Chem. Phys.*, **106**, 666-687 (1997).

[13] M.A. Miller, L. M. Amon, W. P. Reinhardt, Should one adjust the maximum step size in a Metropolis Monte Carlo simulation?, *Chem. Phys. Lett.*, **331**, 278-284 (2000).

[14] V.I. Manousiouthakis, M.W. Deem, Strict detailed balance is unnecessary in Monte Carlo simulation, *J. Chem. Phys.*, **110**, 2753-2756 (1999)

[15] W.Krauth, Algorithms and Computations, (Oxford University Press, 2006).

[16] A.T. Gabriel, T. Meyer, G. Germano, Molecular Graphics of Convex Body Fluids, *J. Chem. Theory Comput*, **4**, 468-476 (2008).

[17] J. Viellard-Baron, The equation of state of a system of hard spherocylinders, *Molec. Phys.*, **28**, 809-818 (1974).

[18] R. Hashim, G.R. Luckhurst, H. Nguan, arXiv:1403.0798v1 (2014).

[19] G.R. Luckhurst, S. Naemura, T.J. Sluckin, T.B.T. To, S. Turzi, Molecular field theory for biaxial nematic liquid crystals composed of molecules with C_{2h} point group symmetry, *Phys. Rev. E*, **84**, 011704 (2011).

[20] M. Cifelli, G. Cinacchi, L. De Gaetani, Smectic order parameters from diffusion data, *J.Chem. Phys.*, **125**, 164912 (2006).

[21] I.A. Zaluzhnyy, R.P. Kurta, O.Yu. Gorobtsov, A.G. Shabalin, A.V. Zozulya, A.P. Menushenkov, M. Sprung, A. Krówczyński, E. Górecka, B.I. Ostrovski, I.A. Vartanyants, Structural studies of the bond-orientational order and hexatic–smectic transition in liquid crystals of various compositions, *Soft Matter*, **13**, 3240 (2017).

[22] D.R. Nelson, B.I. Halperin, Dislocation-mediated melting in two dimensions, *Phys. Rev. B*, **19**, 2457-2484 (1979).

[23] B.I. Halperin, D.R. Nelson, Theory of two-dimensional melting, *Phys. Rev. Lett.*, **41**, 121-124 (1978).

[24] A. Patti, A. Cuetos, Brownian dynamics and dynamic Monte Carlo simulations of isotropic and liquid crystal phases of anisotropic colloidal particles: A comparative study, *Phys. Rev. E*, **86**, 011403 (2012).

[25] A. Patti, D. El Masri, R. van Roij, M. Dijkstra, Collective diffusion of colloidal hard rods in smectic liquid crystals: Effect of particle anisotropy, *J. Chem. Phys.*, **132**, 224907 (2010).

[26] K.W. Wojciechowski, D. Frenkel, A.C. Branka, Nonperiodic solid phase in a two-dimensional hard-dimer system, *Phys. Rev. Lett.*, **60**, 3168-3171 (1991).

[27] A. de Vries, On the structure of the smectic H phase, *J. Chem. Phys.*, **61**, 2367-2371 (1974).

[28] A. Bezdek, W. Kuperberg, Maximum density space packing with congruent circular cylinders of infinite length, *Mathematika*, **37**, 74-80 (1990).

[29] S. Torquato, Y. Jiao, Organizing principles for dense packings of nonspherical hard particles: Not all shapes are created equal, *Phys. Rev. E*, **86**, 011102 (2012).

CHAPTER 3

Molecular Field study of the orientational behaviour of a system made up of board-like particles in the 'partially repulsive' region of interaction

3.1 Introduction

Designing a material with specific properties necessarily requires to link molecular and macroscopic properties, in some way. This step, very often, is quite 'deceptive', because it is not ever possible to make this connection unambiguously by suitable experiments. In these cases, it is useful to have additional tools and/or techniques (as CS for example) able to achieve the aim just said; in this chapter, a work [1] is discussed where a system composed of board-like particles with D_{2h} symmetry [2] has been investigated by using a Molecular Field approach in the partially repulsive regime of orientational interactions. The orientational potential can be written (as already said in Chapter 2) as follows:

$$U = -u_0\{\mathbf{q}\cdot\mathbf{Q} + \gamma(\mathbf{q}\cdot\mathbf{B} + \mathbf{b}\cdot\mathbf{Q}) + \lambda(\mathbf{b}\cdot\mathbf{B})\} \tag{3.1}$$

where the parameters that weight, in some way, the orientational biaxiality are γ and λ. Since, as said above, the partially repulsive regime of orientational interactions is considered, γ and λ can be given by the expressions of eqs. (3.2-3.3), obtained by assuming excluded volume interactions only [3, 4]:

$$\lambda = \frac{L[(B-W)^2]}{[2(B(W^2+L^2)+W(B^2+L^2)) - (L(W^2+B^2)+6LBW)]} \tag{3.2}$$

$$\gamma = \frac{(L^2-WB)(B-W)}{[2(B(W^2+L^2)+W(B^2+L^2)) - (L(W^2+B^2)+6LBW)]} \tag{3.3}$$

Eqs. (3.2-3.3) establish a clear physical (molecular) meaning for the λ and γ, because they fix a direct relation between the biaxial parameters and the geometrical parameters characterizing the shape of a board-like particle (see Figure 3.1):

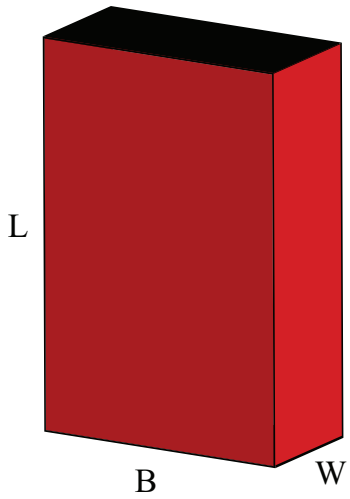

Figure 3.1: Model of board-like particles with D_{2h} symmetry (L=lenght ; B=breadth and W=width).

As a matter of fact, when the fully attractive interactions are considered ($\lambda \geq \gamma^2$), the biaxial parameters cannot be linked unambiguously and explicitly with any particle property; on the contrary, considering the partially repulsive interactions ($\lambda > 0 \ \wedge \ \lambda < \gamma^2 \ \wedge \ \lambda - |2\gamma| + 1 > 0$ [5]) it is possible to make this link in order to hopefully relate micro and macro properties of the system under examination. In order to avoid redundancy, we limited the studied cases to the region of the so-called *essential triangle* [5] reported in Figure (3.2):

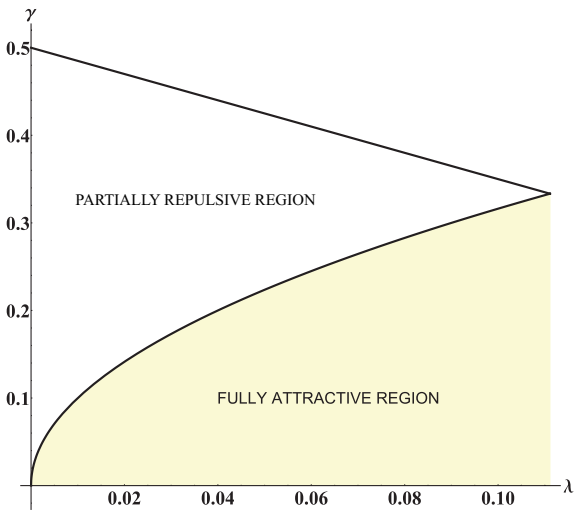

Figure 3.2: Investigated region of the essential triangle corresponding to the partially repulsive interactions, with $0 \leq \lambda \leq 0.11$ and $0 \leq \gamma \leq \frac{1}{2}$.

Having defined the boundary conditions for our problem, we can move to the cal-

culation of the possible different phase diagrams (depending on the choice of λ and γ couples). This requires to found the stable states of the studied systems (phases composed of particles sketched in Figure 3.1). When the fully attractive interactions are considered, the minimization of the Helmholtz free energy F (eq. 3.4) leads to the stable thermodynamic states of the studied fluid [6]:

$$F = \frac{u_0}{3}\left\{S^2 + \frac{1}{3}P^2 + 2\gamma\left(SD + \frac{1}{3}PC\right) + \lambda\left(D^2 + \frac{1}{3}C^2\right) - \frac{3}{\beta}ln\left(\frac{Z}{8\pi^2}\right)\right\} \tag{3.4}$$

where:

$$Z = \int_{\psi}^{2\pi}\int_{\varphi}^{2\pi}\int_{\vartheta}^{\pi} e^{-\beta(U/u_0)} sin\vartheta \, d\vartheta d\varphi d\psi \tag{3.5}$$

On the contrary, this is not true when the partially repulsive interactions are taken into account: in fact, in this case it is necessary to adopt the Minimax [5, 7–9] algorithm, because the stable states of the system are saddle points of the free energy surface. To solve the problem, we have implemented the Minimax method, following the flow chart shown in Figure 3.3, by using Mathematica® 11 software [10] for the calculations:

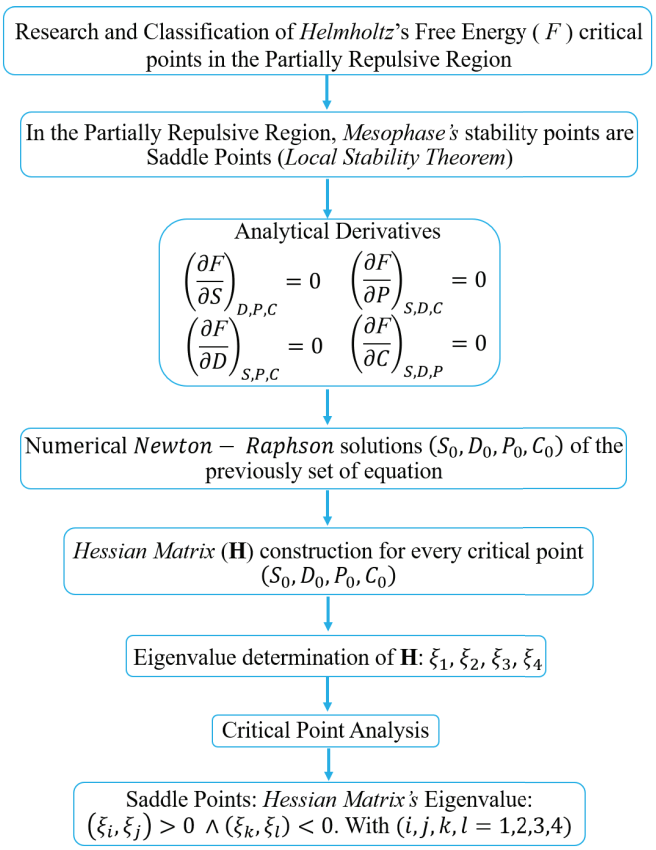

Figure 3.3: Flow diagram of the Minimax algorithm (S, D, P, C represent the order parameters).

The possibility to have the partition function available in an analytical form, allows us the analytical calculation of the derivatives mentioned in Figure 3.3, instead of using a numerical approach. The subsequent step after the implementation of the algorithm, has been to test the reliability of the obtained results. This has been done by comparing our obtained results with 4 cases, treated in literature: in the following sections this comparison will be discussed.

3.2 Comparison with the pioneering Mean Field study carried out by Straley

As said above, we tested our results (obtained for the studied cases represented by the black points in Figure 3.4) with respect to those presented by Straley [2]. In ref. [2], a molecular field approach (based on the Onsager's theory) has been taken into account, involving the excluded volumes between board-like particles with different orientations. We have calculated the phase diagram (B vs. $\beta^{-1} = (k_B T/u_0)$, reported in Figure 3.5) obtained for the investigated black points of Figure 3.4.

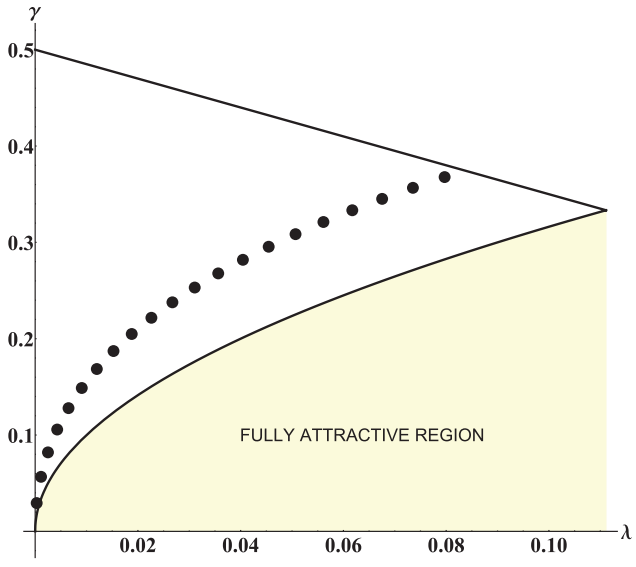

Figure 3.4: Studied cases in the partially repulsive region of the essential triangle: each point corresponds to precise values of γ and λ that are related to the shape of D_{2h} particles by means of L, B, W.

The comparison, by inspection, of our Figure 3.4 with Figure 2 of [2], allowed us to state that our results are in excellent agreement (basically, the same) with the Straley ones.

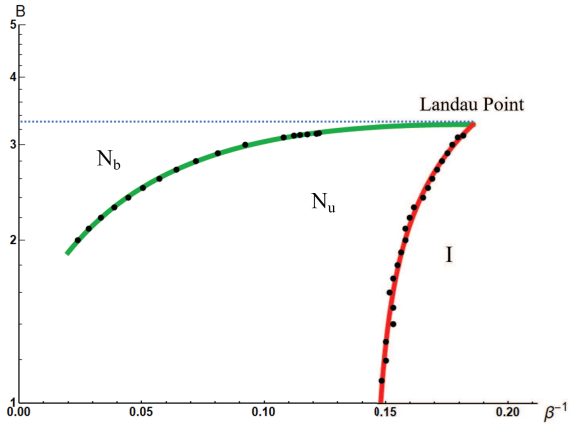

Figure 3.5: Phase diagram B vs. $\beta^{-1} = (k_B T/u_0)$ obtained (fixing W=1 and L=10) from the black point of Figure 3.4. Note that the B scale is logarithmic.

3.3 Comparison of our procedure solutions with numerical solutions obtained by Molecular Field approaches

The analytical approach used by us is alternative to the numerical one [8]; then, we tested if our approach lead to the same suggestions. To answer to this question, we compared our results with those obtained by Bisi, Romano and Virga [8]. In their work, they investigated, in particular, two points in the partially repulsive region of the essential triangle, called G ($\lambda = 1/18$ and $\gamma = 1/3$, virtually corresponding to L=12.2, B=3 and W=1) and R ($\lambda = 7/6 - 2\sqrt{3}/3$ and $\gamma = \sqrt{3}/3 - 5/12$, virtually corresponding to L=8.6, B=1.6 and W=1) points, see Figure 3.6. We calculated the trends of the orientational order parameters, reported in Figures (3.7-3.8), with respect to the reduced temperature T_{red}=$T/T_{N_{U-I}}$.

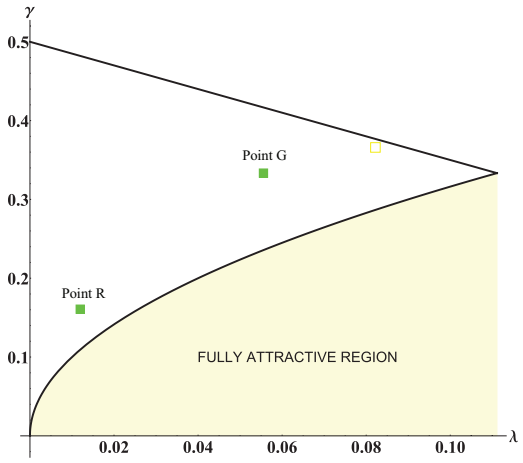

Figure 3.6: Point G and R in the partially repulsive region of the essential triangle: each point corresponds to precise values of the couple (γ, λ) of eqs. (3.2-3.3) that are related to the molecular shape by means of L, B, W.

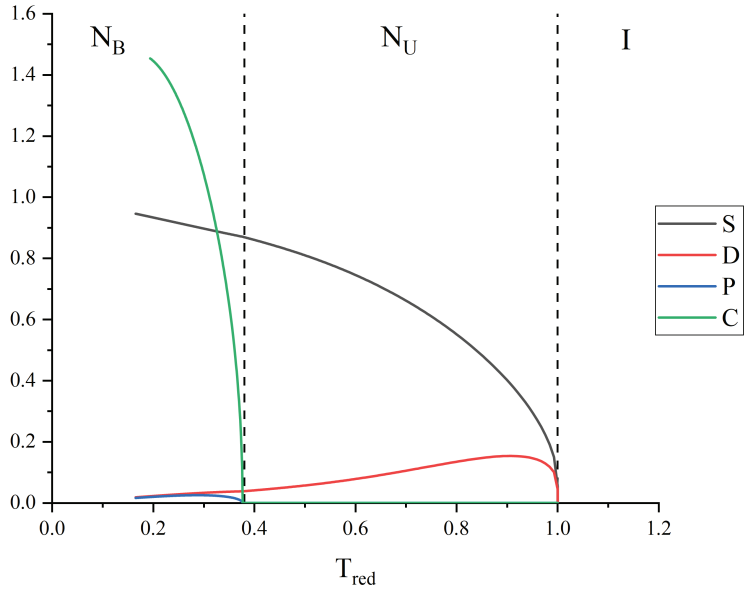

Figure 3.7: Behaviours of (S, D, P, C) orientational order parameters vs T_{red} for G point of ref. [8];

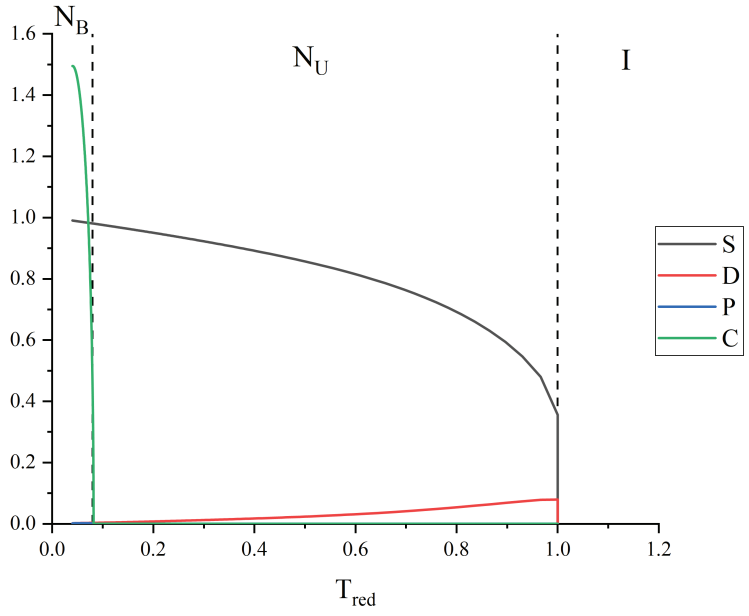

Figure 3.8: Behaviours of (S, D, P, C) orientational order parameters vs T_{red} for R point of ref. [8].

The results obtained for the G point, Figure 3.7, are in agreement with the 'reference' cases of [8]. In particular, the transition temperature between N_u and N_b phases (T_{red}=0.38) is quite well reproduced; on the contrary, our C order parameter is underestimated: this is probably due to the approximations used to obtain a closed form of the partition function.

For the R point, Figure 3.8, the trends of the order parameters are similar to those reported in [8] and the values of the transition temperature between N_u and N_b phases is well reproduced ($T_{red} = 0.08$ in our work instead of $T_{red} = 0.089$).

3.4 Comparison with Monte Carlo simulations: studying the *aspect ratio* contribution

It is well-known that the thermotropic biaxial nematic phase (for a system made up of D_{2h} particles) has never been found (unambiguously) experimentally; then, the only way to compare our results with self-consistent and reliable data is to use the CS, since in practice they produce *virtual* experimental data. The shape anisotropy [12,13] of the particles plays a decisive role in the formation of the desired phase: this is true both in the MF and CS approaches. In the latter, this parameter is quantified by the so-called aspect ratio difference ν [12, 14], whose expression is reported in eq. (3.6):

$$\nu = \frac{L}{B} - \frac{B}{W} \tag{3.6}$$

In this comparison, our aim is to investigate how this parameters affects the (possible) formation of the N_b and, at the same time, if we reproduce, in some way, by our method the data obtained by the MC simulations. We consider several different cases (Figure 3.9):

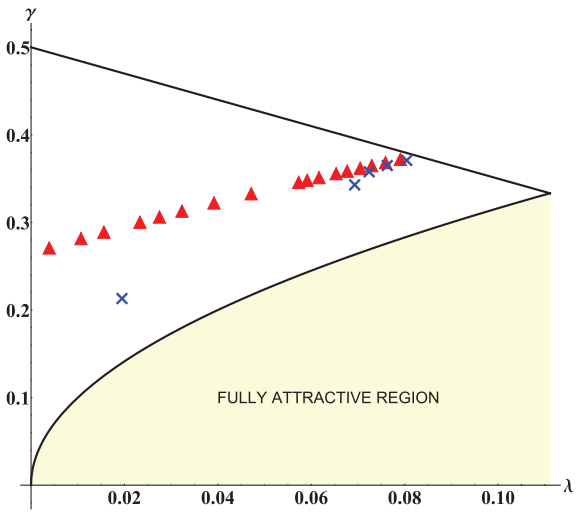

Figure 3.9: The red triangles sample the region between $\frac{L}{W} > 9$ and $2.6 < \frac{B}{W} < 3.73$. The choice fallen within these values due to the fact that in this region the simulations [12,13] predict the highest possibility of finding the biaxial nematic phase; the blue crosses sample the region investigated in [12].

Also in this case we have calculated the phase diagram showed in Figure 3.10 :

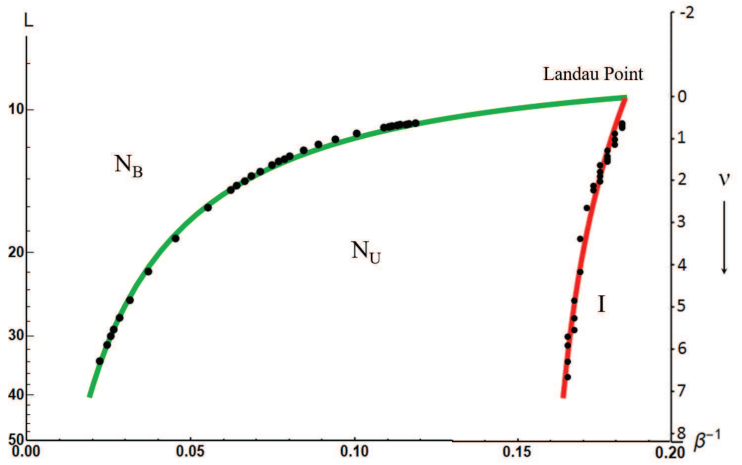

Figure 3.10: Phase diagram, L vs. $\beta^{-1} = (k_B T/u_0)$ obtained from our results (red triangles) of Figure 3.9 where W=1 and B=3.25 have been fixed; note that L scale is logarithmic.

Comparing our results with respect to what obtained in [12] and [13], we can assert that:

I. The range of stability of the N_u increases with the ν (as expected); indeed, when this value increases the particles become more elongated and tapered;

II. The N_b emerges, as can be seen in Figure 3.10, in the regions predicted by MC simulations of [13].

III. Contrary to what predicted by MC simulations in [12] we obtained the biaxial phase also for the blue cross at $\lambda = 0.07$ and $\gamma = 0.34$;

3.5 Virtual mesophase composed of goethite-shaped particles

As previously said many times in this Thesis, the existence of the thermotropic N_b is a debate that involved scientists for about 45 years and even today we are asking us about its possible existence. Anyway, it seems that for lyotropic systems the existence is out of any doubt, and in this context there is a field of research, regarding the so called *Mineral Liquid Crystals* [16], that reflects in a perfect way the close connection between the theories (MF and CS) and the real experiments. This topic is very interesting because different kind of particles of various shapes can be synthesized, and it has been reported several times in this thesis that the morphology of the particles plays a decisive role in the formation (or not) of a particular mesophase. From the MF and CS studies it is known very well that, in order to observe a N_b phase, a possible choice is that the dimensions of the particles should be chosen to have about $L/W \simeq B/W$. Goethite particles demonstrated unambiguously

that a phase composed of these particles (we should define it as colloidal suspensions [17, 18] in water) give rise to a lyotropic nematic biaxial phase. Then, our last comparison was to compare our results with those observed experimentally [15]; in fact, we used the same geometrical parameters characterizing the particles that compose the mesophase under examination. The treated case is represented by the yellow square in the Figure 3.11:

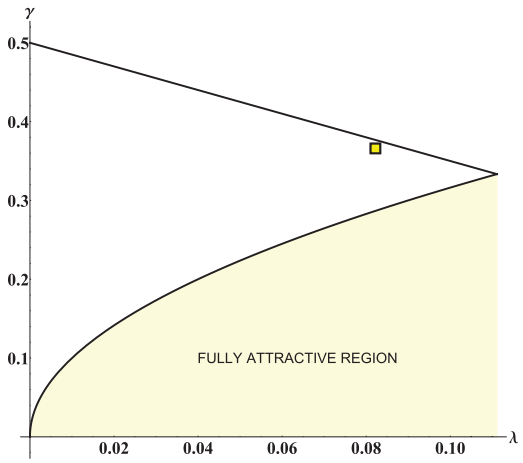

Figure 3.11: The case treated for the goethite-shaped particles is represented by the yellow square in the graph. The parallelism with the experimental work [15] has been made using: L=254 nm, B=83 nm, W=28 nm that correspond to $\lambda = 0.082$ and $\gamma = 0.366$;

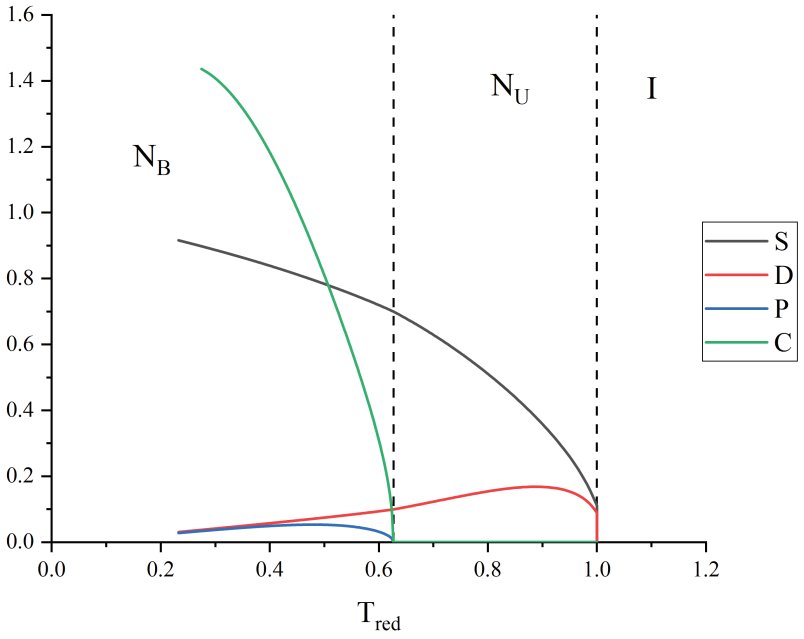

Figure 3.12: Trends of (S, D, P, C) orientational order parameters for goethite-shaped particles.

It is interesting to note that the existence of the uniaxial and biaxial nematic regions, using our procedure, has been observed when the ratios L/B and B/W are not so

far from the so-called dual shape [12] $\nu = 0$ (that corresponds to the Landau point). The tests and comparisons carried out assured us about the reliability of the method, so that we decided to extend our study to 14 new cases (all in the partially repulsive region) never investigated before.

3.6 Investigation of the dependence of the transition temperature $T_{Nb\text{-}Nu}$ on the biaxial parameters γ and λ

We decided to carry out a systematic investigation of our system made up of board-like particles, changing the morphology of them thanks to the parameters γ and λ (eqs. 3.2-3.3). In this way we are able to 'map' in which way a microscopic property of the particles (the shape) affects the macroscopic behaviour of the phase (the mesophases obtained). The map (and its sliced version) of the 14 cases studied are shown in Figure (3.13-3.14):

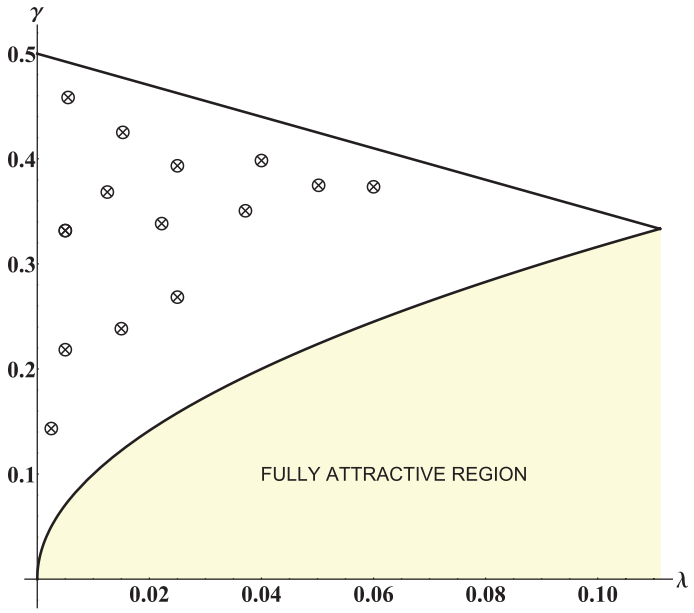

Figure 3.13: The black crosses represent the studied points, never investigated before, in the partially repulsive region.

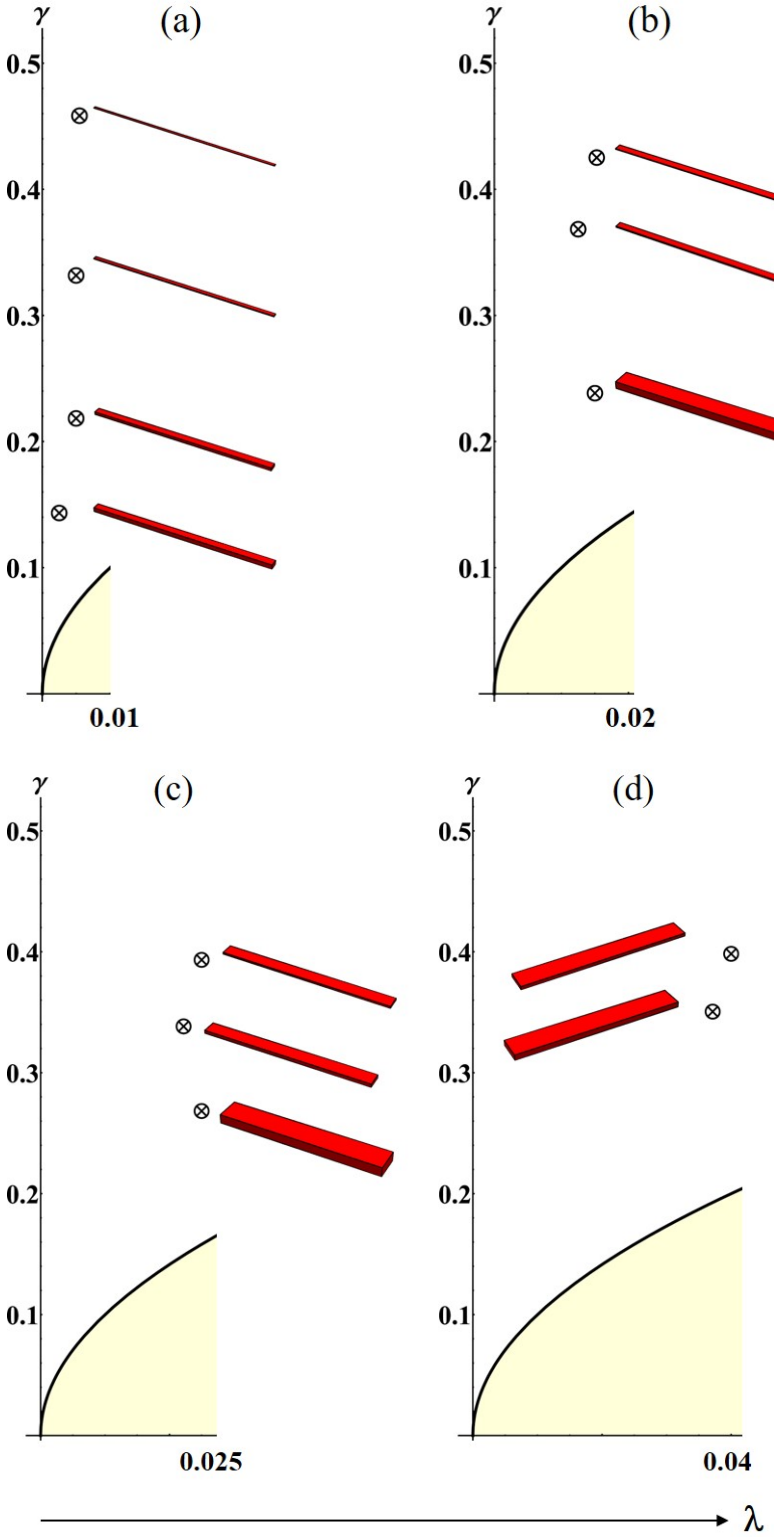

Figure 3.14: Sliced version of the graph shown in Figure 3.13: (a) $\lambda \sim 0.005$ and γ going from ~ 0.145 to ~ 0.46; (b) $\lambda \sim 0.015$ and γ going from ~ 0.24 to ~ 0.43; (c) $\lambda \sim 0.025$ and γ going from ~ 0.27 to ~ 0.40; (d) $\lambda \sim 0.04$ and γ going from ~ 0.35 to ~ 0.40. The particle shape is related to the chosen couple of λ and γ via eqs. (3.2-3.3).

Analysing the single panels of Figure 3.14 we can say that:

(a) As shown in the panel (a), our calculations suggest that fixing a small value of λ and increasing γ means increasing the length of the particle (L) with respect to its relative flatness (B) and thickness (W). It is intuitive to think that (roughly speaking) the biaxiality of the molecule decreases as γ increases; indeed, a phase made up of this tapered particles does not give rise to the N_b;

(b) Moving to the panel (b), the breadth (B) of the particles has been enhanced by increasing the value of λ , as clearly visible in Figure 3.14; here, at $T_{Nb\text{-}Nu} \approx$ 0.1, for the first time the N_b phase emerges;

(c) From the panel (c) we can observe that, for $\lambda \sim 0.025$, the relative breadth B/L become not negligible and here the transition N_b-N_u occurs at $T_{Nb\text{-}Nu} \approx$ 0.16-0.18;

(d) the same consideration made for the previous point can also be extended of panel (d) where the transition occurs at $T_{Nb\text{-}Nu} \approx$ 0.26-0.29.

Moreover, we investigated other two situations (not reported in the Figure 3.14) corresponding to $\lambda \sim 0.05$; $\gamma \sim 0.38$ and $\lambda \sim 0.06$; $\gamma \sim 0.37$ where the transition occurs respectively, at about $T_{Nb\text{-}Nu}$=0.36 and $T_{Nb\text{-}Nu}$=0.43.
The information acquired allows us to maintain that, at values of $\lambda \geq 0.01$, the flatness of the particles is enough to predict, in the regime of partially repulsive interactions, the existence of the elusive thermotropic biaxial nematic phase. The flatness of the particles plays a decisive role (at least, most important of L and W) in the formation of the biaxial mesophase, which means that is λ the dominant biaxial parameter, as already observed in [11]. Interestingly, we observed a linear correlation between the reduced temperature and the λ parameter, as shown in Figure 3.15. The correlation found for the λ parameter confirms *quantitatively* what had been (only qualitatively) predicted in [11]. On the contrary, plotting the reduced transition temperatures vs γ not revealed any correlations and, therefore, any physical relationship between this two quantities, as clearly visible in Figure 3.16:

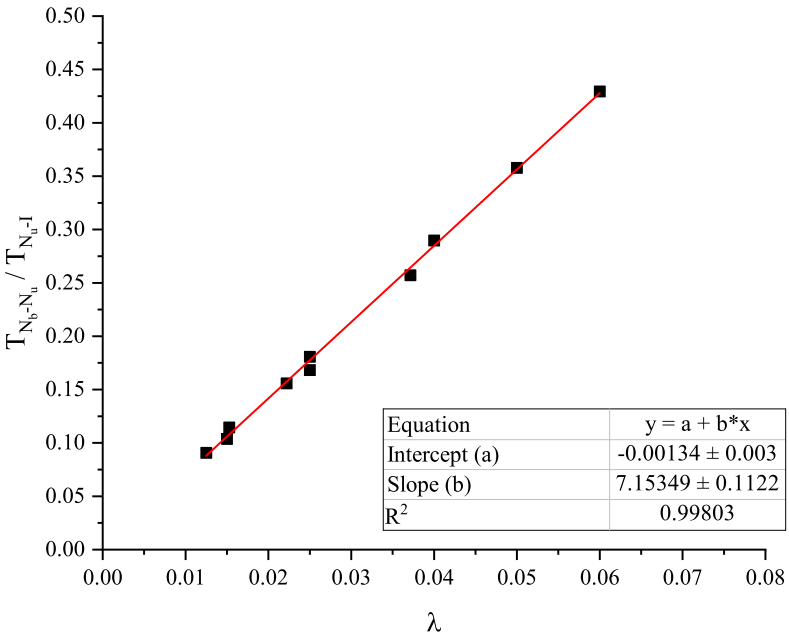

Figure 3.15: Linear dependence of the transition temperatures $\frac{T_{N_b-N_u}}{T_{N_u-N_I}}$ as a function of λ.

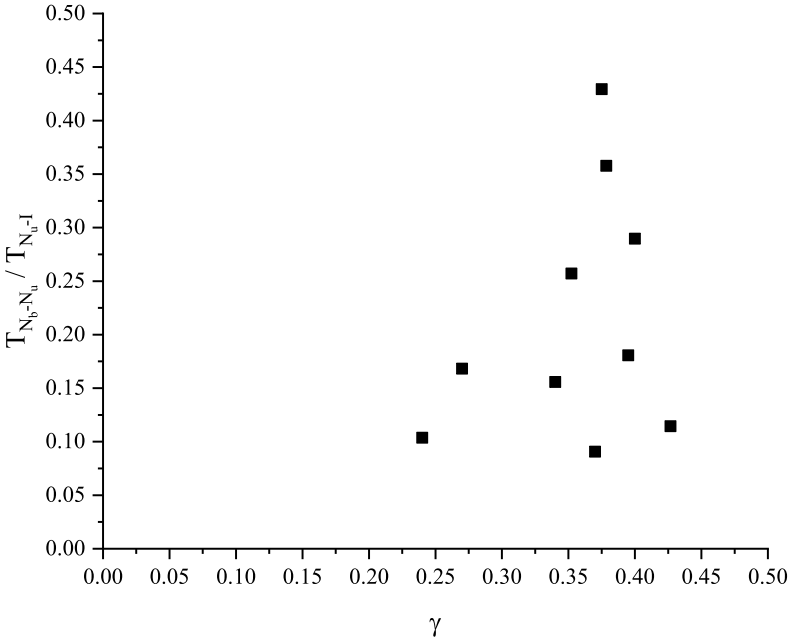

Figure 3.16: Random 'scattering' of the transition temperatures $\frac{T_{N_b-N_u}}{T_{N_u-N_I}}$ vs γ.

Bibliography

[1] G. Celebre, C. D'Urso, M. Porto, Extensive molecular field theoretical investigation of thermotropic biaxial nematics composed of board-like (D_{2h}) molecules in the partially repulsive regime of orientational interactions, *J. Mol. Liq.*, **248**, 847-853 (2017).

[2] J.P. Straley, Ordered phases of a liquid of biaxial particles, *Phys. Rev. A*, **10**, 1881-1887 (1974).

[3] R. Rosso, E.G. Virga, Quadrupolar projection of excluded-volume interactions in biaxial nematic liquid crystals, *Phys. Rev. E*, **74**, 021712 (2006).

[4] B.M.Mulder, The excluded volume of hard sphero-zonotopes, *Mol. Phys.*, **103**, 1411–1424 (2005).

[5] F. Bisi, E.G. Virga, E.C. Gartland Jr., G. DeMatteis, A.M. Sonnet, G.E. Durand, Universal mean-field phase diagram for biaxial nematics obtained from a minimax principle, *Phys. Rev. E*, **73**, 051709 (2006).

[6] G. Celebre, Statistical thermodynamics of thermotropic biaxial nematic liquid crystals: an effective, molecular-field based theoretical description by means of a closed approximate form of the orientational partition function, *J. Mol. Liq.*, **209**, 104-114 (2015).

[7] G. De Matteis, F. Bisi, E.G. Virga, Constrained stability for biaxial nematic phases, *Contin. Mech. Thermodyn.*, **19**, 1–23 (2007).

[8] F. Bisi, S. Romano, E.G. Virga, Uniaxial rebound at the nematic biaxial transition, *Phys. Rev. E*, **75**, 041705 (2007).

[9] E.C. Gartland, E.G. Virga, Minimum principle for indefinite mean-field energies, *Arch. Ration. Mech. Anal.*, **196**, 143–189 (2010).

[10] Mathematica® is a trademark of Wolfram Research Inc.

[11] F. Bisi, G.R. Luckhurst, E.G. Virga, Dominant biaxial quadrupolar contribution to the nematic potential of mean torque, *Phys. Rev. E*, **78**, 021710 (2008).

[12] S.D. Peroukidis, A.G. Vanakaras, D.J. Photinos, Supramolecular nature of the nematic-nematic phase transition of hard boardlike molecules, *Phys. Rev. E*, **88**, 062508 (2013).

[13] S.D. Peroukidis, A.G. Vanakaras, Phase diagram of hard board-like colloids from computer simulations, *Soft Matter*, **9**, 7419–7423 (2013).

[14] B. Mulder, Isotropic-symmetry-breaking bifurcations in a class of liquid-crystal models, *Phys. Rev. A*, **39**, 360–370 (1989).

[15] E. Van den Pol, A.V. Petukhov, D.M.E. Thies-Weesie, D.V. Byelov, G.J. Vroege, Experimental realization of biaxial liquid crystal phases in colloidal dispersions of boardlike particles, *Phys. Rev. Lett.*, **103**, 258301 (2009).

[16] H.N.W. Lekkerkerker, G.J. Vroege, Liquid crystal phase transitions in suspensions of mineral colloids: new life from old roots, *Phil. Trans. R. Soc. A*, **371**, 20120263 (2013).

[17] B.J. Lemaire, et al., Physical properties of aqueous suspensions of goethite (α-FeOOH) nanorods (part I), *Eur. Phys. J. E*, **13**, 291–308 (2004).

[18] B.J. Lemaire, et al., Physical properties of aqueous suspensions of goethite (α-FeOOH) nanorods (part II), *Eur. Phys. J. E*, **13**, 309–319 (2004).

CHAPTER 4

Chirality dependence of the orientational order of small helical solutes dispersed in helical nematic solvents: a Monte Carlo study

4.1 Introduction

The idea at the basis of the work [1] presented in this chapter was to address a problem about chirality [2], a topic of primary interest in chemistry in all its facets (materials, drug design, etc...). More in detail, the aim was to understand if it was possible, in some way, to discriminate unambiguously between two enantiomers. Different techniques exist (UV-Vis [3], mass spectrometry [4], vibrational circular dichroism [5], etc...) able to give information about chiral recognition; anyway, another potentially very effective technique is represented by LX-NMR (Liquid Crystal NMR) [6, 7]. In general, when two enantiomers of a chiral molecule (assumed rigid for semplicity) are dissolved in a Chiral Non-Racemic Aligning Solvent (CNRAS), as for example the PBLG (poly-γ-benzyl-L-glutamate [8–10]), it is possible to observe that they give different NMR spectra: this is due to the fact that they experience a different statistical orientational order in the medium. From the spectra, some experimental parameters W^{obs} (as for example chemical shift, dipolar couplings, quadrupolar splitting [11]) can be obtained:

$$W^{obs} \equiv \langle W_{zz} \rangle = W^{iso} + W^{aniso} = \frac{1}{3} \sum_{a}^{x,y,z} W_{aa} + \frac{2}{3} \sum_{a,b}^{x,y,z} S_{ab}^{\alpha,\omega} W_{ab} \tag{4.1}$$

$$S_{ab}^{\alpha,\omega} = \left\langle \frac{1}{2} \left(3\, cos\theta_{Z,a}^{\alpha,\omega}\, cos\theta_{Z,b}^{\alpha,\omega} - \delta_{ab}^{\alpha,\omega} \right) \right\rangle \tag{4.2}$$

where θ_{aZ} is the angle between the Z-lab axis and the molecular axis a, δ_{ab} is the Kronecker delta, the average $\langle ... \rangle$ is taken over the reorientational motions of the

molecule and α and ω represent the two different enantiomers. It is obvious that the orientational order of the particles affects the anisotropic term of the macroscopic observable(as shown in eq. 4.2): this could lead, in principle, to discriminate between the two enantiomers. On the other hand, the only chirality descriptors that take into account a real, morphological property of the particles are P (Plus, clockwise) and M (Minus, counter-clockwise), representing the handedness of a helical particle. For this kind of systems experimental data are not available; therefore we decided to turn our attention to the CS technique as generator of virtual experimental data. Our idea is to investigate, via MC simulations, different phases made up of helicoidal solutes and solvent particles then to study if the morphology of the particles can acts as a discriminating factor for the enantiorecognition.

4.2 Computational Details

To carry out our MC simulations, the helicoidal particles have been 'built' using the model of fused sphere where each helix is composed by a number, n_s, of hard spheres of diameter D, equidistantly arranged along a chord of lenght L, radius r and pitch p, both in D units (see Figure 4.1a and Figure 4.1b).

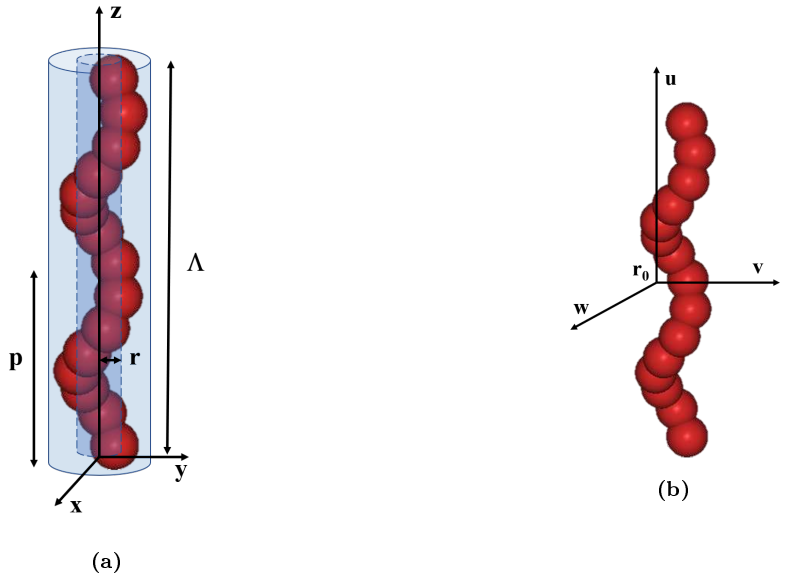

Figure 4.1: (a): Geometrical parameters of a helical particles made up of hard-fused spheres; (b) r_0 is the centroid of the helical particle, (**w,v,u**) is the triad of mutually perpendicularly unit vectors that could be right- or left handed; **u** is along the long molecular axis and **w** is along the C_2 symmetry axis.

Changing r and p values makes possible to modify the morphology of the helical particles; in particular, it is possible to obtain slender or curly particles: in some way, this allow us to *mimic* different virtual mesophases and different possible solutes. In our simulations, we considered two types of solvents: one, made up of slendered molecules ($r_\Sigma = 0.2; p_\Sigma = 9.92$) and one composed of curly particles ($r_\Sigma = 0.4; p_\Sigma = 4$); in both cases, the helices are assumed to be right-handed with L=10D and composed of 15 partially overlapping fused spheres. The schematization of this two types of helix particle is shown in Figure 4.2:

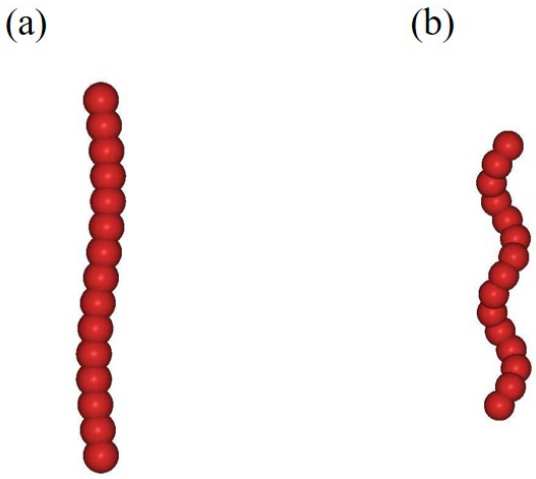

Figure 4.2: (a) the slender solvent particle ($r_\Sigma = 0.2; p_\Sigma = 9.92$) (b) the curly solvent particle with ($r_\Sigma = 0.4; p_\Sigma = 4$).

In these solvents we virtually disperse right- or left- handed (one kind at a time) solute particles, that differ for the values of r and p couples: ($r_\sigma = 0.2; p_\sigma = 9.92$); ($r_\sigma = 0.2; p_\sigma = 4$); ($r_\sigma = 0.4; p_\sigma = 4$); ($r_\sigma = 0.2; p_\sigma = 4$) and by $n_s = 3, 5, 7, 9, 11, 13, 15$ partially overlapping hard spheres of diameter D with $L = (5/7)(n_s - 1)D$. The simulation has been carried out in the NPT ensemble [12–14] and using orthorhombic boundary conditions. We considered 500 particles of solvent (assumed, as said before, right-handed in all the simulations) whose configurations have been obtained by previous numerical simulation performed in [15]. In particular:

- The configuration of the slender solvent has been obtained at P*=0.5 (being $P^* = PD^3/kT$) and ρD^3=0.044;
- The configuration of the curly solvent has been obtained at P*=0.8 (being $P^* = PD^3/kT$) and ρD^3=0.051;

In order to simulate our solute-solvent systems, 10 solvent particles have been replaced by 10 solute particles, paying particular attention to avoiding overlaps between the particles, the configuration so obtained was the starting point of the new

simulations. Being interested in monitoring the orientational order, we calculated the Saupe order matrix [6, 7] of both solute (σ) and solvent (Σ), whose elements are given by eq. (4.3):

$$S^l_{\alpha\beta} = \left\langle \frac{3}{2}(\boldsymbol{\alpha}\cdot\mathbf{n})(\boldsymbol{\beta}\cdot\mathbf{n}) - \frac{1}{2}\delta_{\alpha\beta} \right\rangle \tag{4.3}$$

where $l = \sigma, \Sigma$; $\boldsymbol{\alpha}, \boldsymbol{\beta} = \boldsymbol{w}, \boldsymbol{v}, \boldsymbol{u}$; δ is the Kronecker delta and $\langle ... \rangle$ means an average over the particles and configurations.
To study the (micro-) structure of the system, the positional (eq. 4.4) and orientational (eq. 4.5) correlation functions have been also calculated:

$$g^{l,k}(r) = \frac{1}{N_l}\left\langle \frac{1}{\rho_k}\sum_{i=1}^{N_l}\sum_{j=1\,;\,j\neq i}^{N_k}\delta(r - r_{ij}) \right\rangle \tag{4.4}$$

$$g^{l,k}_{1,\boldsymbol{w}}(r_\parallel) = \left\langle \frac{\sum_{i=1}^{N_l}\sum_{j=1\,;\,j\neq i}^{N_k}(\boldsymbol{w_i}\cdot\boldsymbol{w_j})\delta(r_\parallel - \boldsymbol{r_{ij}}\cdot\boldsymbol{n})}{\sum_{i=1}^{N_l}\sum_{j=1\,;\,j\neq i}^{N_k}\delta(r_\parallel - \boldsymbol{r_{ij}}\cdot\boldsymbol{n})} \right\rangle \tag{4.5}$$

where N_l is the number of particles of the species l, ρ_k is the number density of species k, the specification $j \neq i$ occurs when $l = k$ and δ is the δ-function, r_{ij} is the modulus of the distance $\boldsymbol{r_{ij}}$ between the centroids i and j, and, finally, $\langle ... \rangle$ represents an arithmetic average over the configurations. The positional correlation function (eq. 4.4) is useful to assess the nematic character of the phase under examination. Furthermore, to monitor the degree of correlation of the unit vectors $\boldsymbol{w}$ as a function of the projection of the distance between the centroids of the particles along $\boldsymbol{n}$, the calculation of the orientational correlation function (eq. 4.5) turn particularly useful; indeed, in this way, we can observe if a certain degree of 'resonance' between solute and solvent particles exists.

4.3 Comments on the obtained results

In the following Figures (4.3 and 4.4) the behaviour of the uniaxial order parameters (Figure 4.3), and the behaviour of the orientational correlation functions (Figure 4.4) for the examined cases, are shown:

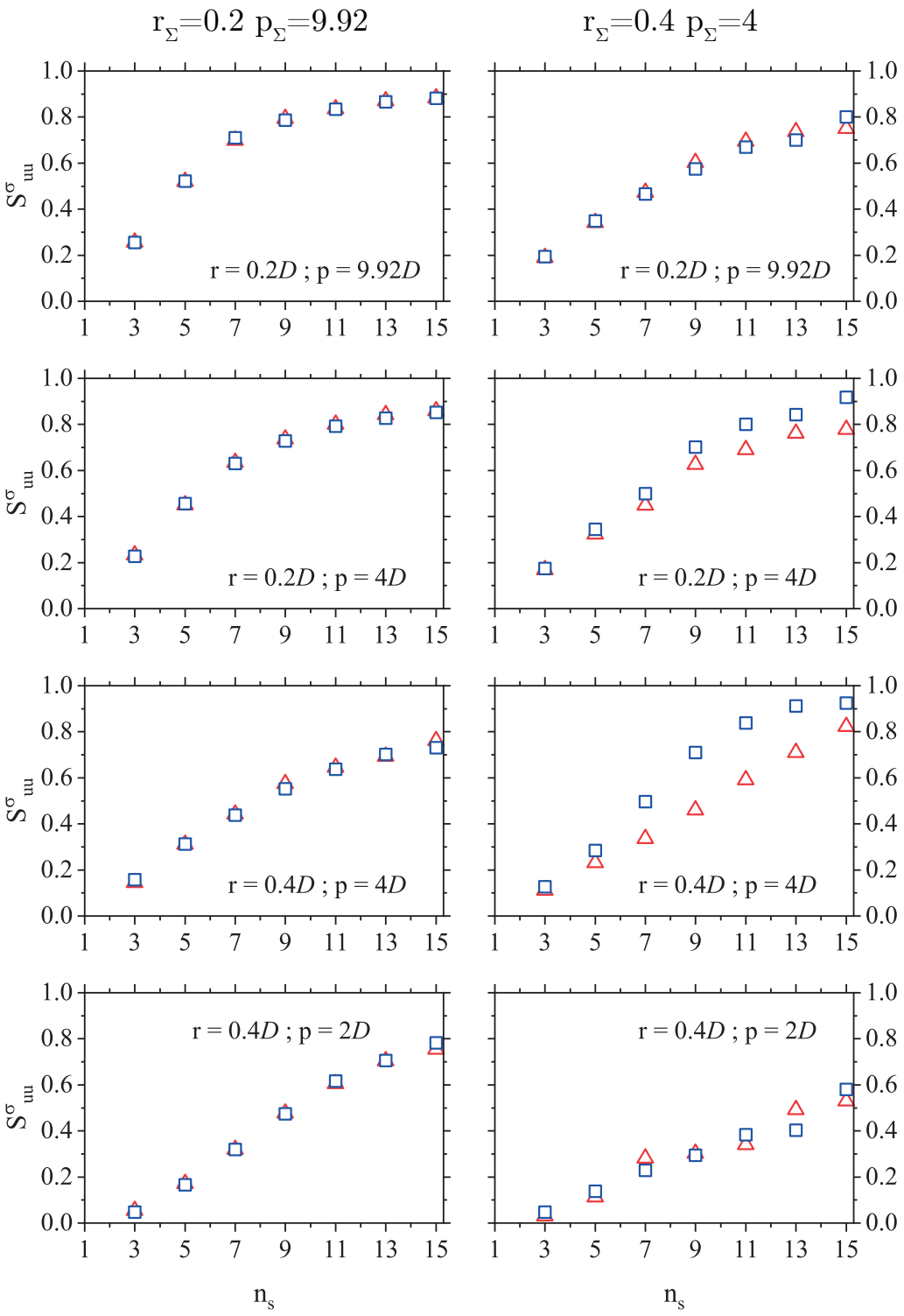

Figure 4.3: Behaviours of the uniaxial order parameter S_{uu} for the right-(blue square) and left-(red triangle) handed helical solute particles. In the left panels the solvent is the slender one ($r_\Sigma = 0.2; p_\Sigma = 9.92$) and in the right panels the solvent is the curly one ($r_\Sigma = 0.4; p_\Sigma = 4$). n_s is the number of hard fused spheres forming the solute particles.

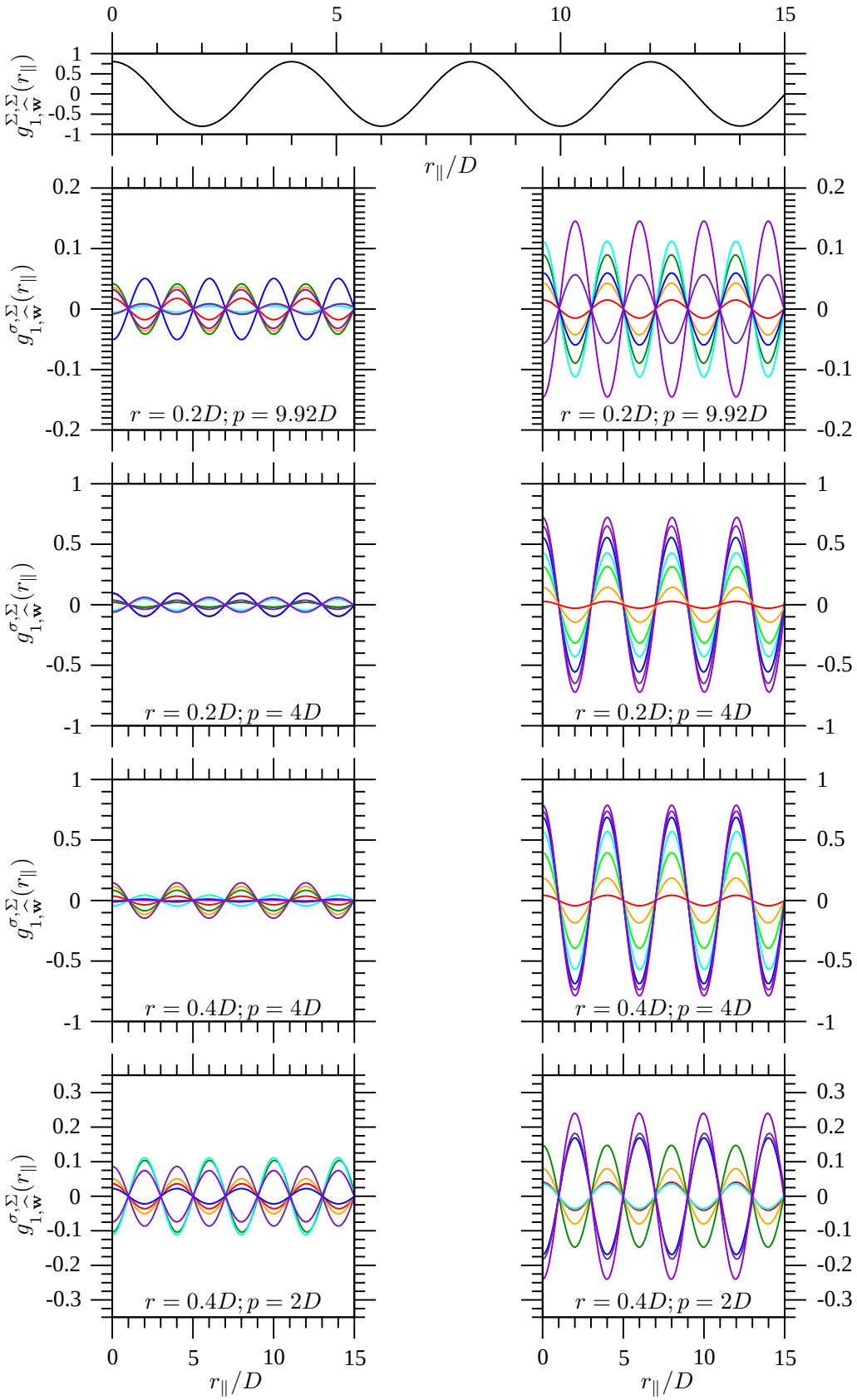

Figure 4.4: The topmost panel represents the $g^{\Sigma,\Sigma}_{1,\boldsymbol{w}}(r_\parallel)$ of the solvent with $r_\Sigma = 0.4; p_\Sigma = 4$, furthermore in each panel the corresponding trend of the $g^{l,k}_{1,\boldsymbol{w}}(r_\parallel)$ is reported: n_s=3(red); 5(orange); 7(green; 9(cyan); 11(blue); 13(indigo); 15(violet).

From the data just reported we can assert that:

I. As it could be expected, the morphology of the solvent is a parameter that has a decisive role (in this context) in enantiomeric discrimination;

II. When the solute and solvent particles are in *tune* (i.e they possess similar and comparable geometrical parameters; in particular, the value of the pitch p plays a decisive role) the behaviours of the order parameters for the two different enantiomers are very different, so that is possible to discriminate unambiguously between the enantiomers P and M;

III. The solute particles of the right- and left- handed enantiomers need to be sufficiently elongated ($n_s \geq 7$) in order to experience an appreciable different orientational order.

The three conditions reported above are respected in the middle panels on the right of Figure 4.3, ($r_\sigma = 0.4; p_\sigma = 4$) and ($r_\sigma = 0.2; p_\sigma = 4$), where it is possible to observe that the orientational order experienced by the two enantiomers is different; in particular the solute particles having the same handedness of the right-handed solvent particles exhibit a larger degree of order, reflected in the value of the uniaxial order parameter. It is interesting to note also (always considering the middle panels on the right) that, when the solute and solvent particles are in *tune*, the orientational correlation function is in 'resonance' with respect to the function (the topmost panel of Figure 4.4) calculated only for the solvent particles. At the same time, it is possible to observe that, as the n_s increases, the degree of correlation between the solute and solvent particles is enhanced: this is justified by the high value reached by the $g^{\sigma,\Sigma}_{1,\boldsymbol{w}}(r_\parallel)$. Finally, there is also a situation where it is not possible to distinguish between the two enantiomers, due to the fact that the behaviour of the uniaxial order parameter, Figure 4.3 ($r_\sigma = 0.4; p_\sigma = 2$), is more or less scattered.
The results obtained are encouraging, especially regarding the possibility of using suitable helical nematic phase (as for example the screw-like nematic phase [16, 17]) as nematic solvent in the LX-NMR experiments, in order to possibly discriminate between the two chiral species.

Bibliography

[1] J. Gutierrez Bojart, C. D'Urso, G. Celebre, G. Cinacchi, Probing the sensitivity of orientational ordering as a way towards absolute enantiorecognition: helical-particle solutes in helical-particle nematic solvents, *Phys. Rev. E*, **98**, 042704 (2018).

[2] G.H. Wagnière, Chirality and the Universal Asymmetry: Reflections on Image and Mirror Image (Wiley-VCH, Weinheim, 2007).

[3] X. Lu, J. Tang, X. Dang, X. Jing, K. Xu, H. Lia, B. Liang, Chiral recognition and determination of enantiomeric excess of chiral compounds by UVvisible-shortwave near infrared diffuse reflectance spectroscopy with chemometrics, *RSC Adv.*, **7**, 13552 (2017).

[4] X. Yu, Z-P Yao, Chiral recognition and determination of enantiomeric excess by mass spectrometry: A review, *Anal. Chim. Acta*, **968**, 1-20 (2017).

[5] R.K. Dukor, L.A. Nafie, in Encyclopedia of Analytical Chemistry: Instrumentation and Applications, Ed. R.A. Meyers (Wiley & Sons, Chichester, 2000)

[6] J.W. Emsley, J.C. Lindon, NMR Spectroscopy Using Liquid Crystals Solvents (Pergamon, New York, 1975).

[7] E.E. Burnell, C.A. de Lange, NMR of Ordered Liquids (Kluwer, Dordrecht, 2003).

[8] A. Elliot, E.J. Ambrose, Evidence of chain folding in polypeptides and proteins, *Discuss. Faraday Soc.*, **9**, 246-251 (1950).

[9] C. Robinson, Liquid-crystalline structures in solutions of a polypeptide, *Trans. Faraday Soc.*,**52**, 571-592 (1956).

[10] C. Robinson, J.C. Ward, R.B. Beevers, Liquid crystalline structure in polypeptide solutions. Part. 2, *Discuss. Faraday Soc.*, **25**, 29-42 (1958).

[11] P. Diehl, Nuclear Magnetic Resonance of Liquid Crystals (J.W. Emsley, Ed.: Reidel, Dordrecht, 1985, Chapter 7).

[12] N. Metropolis, A.W. Rosenbluth, M.N. Rosenbluth, A.H. Teller, E. Teller, Equation of State Calculations by Fast Computing Machines, *J. Chem. Phys.*, **21**, 1087-1092 (1953).

[13] W.W. Wood, NpT-Ensemble Monte Carlo Calculations for the Hard-Disk Fluid, *J. Chem. Phys.*, **52**, 729-741 (1970).

[14] M.P. Allen, J.D. Tildsley, Computer Simulation of Liquids (Clarendon, Oxford, 1987).

[15] G. Cinacchi, A. Ferrarini, A. Giacometti, H.B. Kolli, Cholesteric and screw-like nematic phases in systems of helical particles, *J. Chem. Phys.*, **147**, 224903 (2017)

[16] E. Barry, Z. Hensel, Z. Dogic, M. Shribak, R. Oldenbourg, Entropy-Driven Formation of a Chiral Liquid-Crystalline Phase of Helical Filaments, *Phys. Rev. Lett.*, **96**, 018305 (2006).

[17] H.B. Kolli, E. Frezza, G. Cinacchi, A. Ferrarini, A. Giacometti, T.S. Hudson, Communication: from rods to helices: evidence of a screw-like nematic phase, *J. Chem. Phys.*, **140**, 081101 (2014).

CHAPTER 5

The assignment of the absolute configuration of enantiomers: formulation of a mean torque potential sensitive to P and M chirality

5.1 Introduction

In the light of what observed in chapter 4, the following inference was proposed: based simply on the handedness of the particles that made up the phase, one could hypothesize that, if the helical solute and solvent particles have the same handedness, the order experienced by the solute should be higher with respect to the case in which the solute and solvent particles possess opposite handednesses. In the first case there would be a stabilizing contribution of the solute-solvent orientational interaction energy because there should be a certain degree of 'affinity' between the particles; on the contrary, if the solute and solvent particles have an opposite handedness, the orientational interaction energy would bring a destabilizing contribution. Due to the lack of experimental data, for this kind of systems the results obtained from CS technique have been used as test-bench for the formulation of a MF model based on the attempting to build a *chiral* mean-torque potential sensitive to (able to distinguish unambiguously) the P/M form of the solutes. The model chosen for the description of the helical particles (whose morphology and geometrical parameters have been shown in Figure 5.1 and Figure 5.2 respectively) is the bond-representation, proposed originally by D.J. Photinos, E.T. Samulski and coworkers [2–5]. In practice, our idea is to consider segmental additive interactions to build a 'chiral' energy term to be added to the achiral part of the potential that describe the solute-solvent interactions.

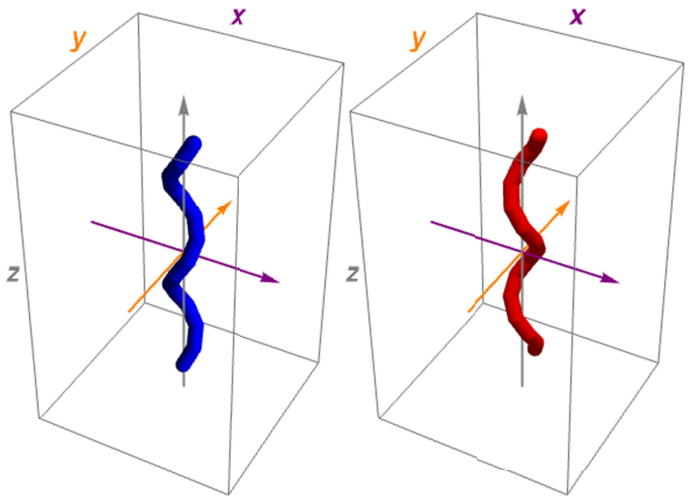

Figure 5.1: the blue helix is the P enantiomer (right-handed) and the red one is the M enantiomer (left-handed) [1].

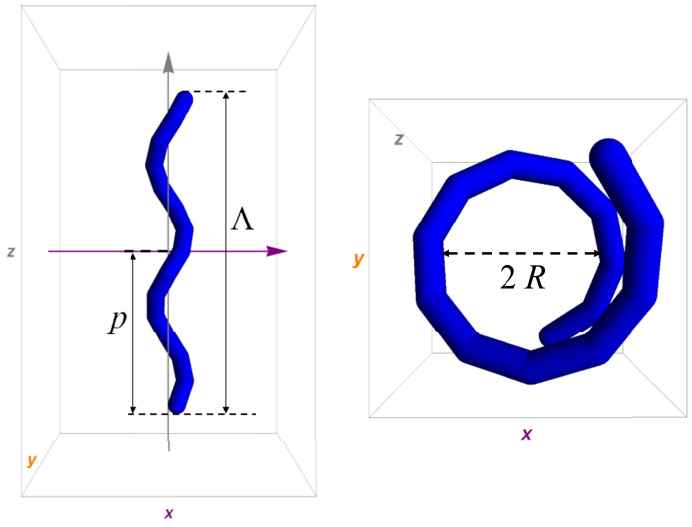

Figure 5.2: Euclidean lenght (Λ); pitch (p) and radius (R) of a helix particle [1].

5.2 Molecular Field model and calculations

Starting from the suggestions reported in refs [6–8], two orientational contributions to the potential (one achiral and one chiral) were taken into account as reported in eq 5.1:

$$U_{total} = U_{achiral} + U_{chiral} \tag{5.1}$$

with

$$U_{achiral} = -w_{\Sigma}^{0} \cdot \Lambda_{\sigma} \cdot P_2(\boldsymbol{a}_{\sigma} \cdot \boldsymbol{n}) \tag{5.2}$$

where Σ and σ stay for solvent and solute particle respectively, $P_2(...)$ is the second-order Legendre polynomial, $\boldsymbol{a}_\sigma$ represents the unit apolar vector of the helical axis of the solute's particle and w_Σ^0 gives the strength of the orientational interaction between the long molecular axis and the director; furthermore the expression of the Euclidean length Λ_σ is reported in eq. 5.3

$$\Lambda_\sigma = L_\sigma \sqrt{\frac{1}{1 + 4\pi^2 \left(\frac{R_\sigma}{p_\sigma}\right)^2}} \tag{5.3}$$

For the chiral contribution U_{chiral} of eq. 5.1, we suggest the following form as an assumption which seems reasonable from the data available:

$$U_{chiral} = (\mp)_\Sigma \, w_\Sigma^c \, L_\sigma \left(\frac{R_\Sigma}{p_\Sigma}\right)^m \left(\frac{R_\sigma}{p_\sigma}\right)^n \Psi_\sigma \, P_2(\boldsymbol{a}_\sigma \cdot \boldsymbol{n}) \tag{5.4}$$

with

$$\Psi_\sigma = (\boldsymbol{U}_\chi \cdot \boldsymbol{\rho}_{1,N})_\sigma \tag{5.5}$$

where

$$\boldsymbol{U}_\chi = \sum_{i=1}^{N-1} (\boldsymbol{b}^i \cdot \boldsymbol{b}^{i+1})(\boldsymbol{b}^i \times \boldsymbol{b}^{i+1}) \tag{5.6}$$

with $\boldsymbol{b}^i$ the segmental bond/group unit vectors and

$$\boldsymbol{\sigma}_{1,N} = \frac{\sum_{i=1}^{N-1} \boldsymbol{r}_{(i,i+1)}}{\left|\sum_{i=1}^{N-1} \boldsymbol{r}_{(i,i+1)}\right|} \tag{5.7}$$

$\boldsymbol{\sigma}_{1,N}$ represents the unit vector giving the direction of the line that joins the first and last segments constituting the solute molecule. Substituing the eq. (5.2) and eq. (5.4) in eq. (5.1) we obtained the following expression:

$$U_{total} = -w_\Sigma^0 \cdot \Lambda_\sigma \cdot P_2(\boldsymbol{a}_\sigma \cdot \boldsymbol{n}) \left[\sqrt{\frac{1}{1 + 4\pi^2 \left(\frac{R_\sigma}{p_\sigma}\right)^2}} \pm w_\chi \Psi_\sigma\right] \tag{5.8}$$

where

$$w_\chi = \frac{w_\Sigma^c}{w_\Sigma^0} \left(\frac{R_\Sigma}{p_\Sigma}\right)^m \left(\frac{R_\sigma}{p_\sigma}\right)^n \tag{5.9}$$

The handedness of the helicoidal particles has been taken into account thanks to the eq. (5.5); indeed Ψ_σ, a pseudoscalar [6–8], has the following properties:

I. $\Psi_\sigma = 0 \rightarrow U_{total} = U_{achiral}$: it means that the system is achiral (or a racemic mixture, 50:50, is present), only the achiral term survives;

II. $\Psi_\sigma \neq 0$: the system is chiral and, due to the mathematical form of the pseudoscalar term, it can be $\Psi_\sigma > 0$ if the particles are right-handed (P) and $\Psi_\sigma < 0$ if left-handed (M).

Based on the hypothesis discussed in the introduction to this chapter, it should occur that when the solute and the enantiopure solvent (whose handedness is known) share the same handedness, the orientational order experienced by the solute should be larger than the order experienced by a solute that has a handedness opposite to that of the solvent. Obviously, to test our model experimental data are needed but, unfortunately, for this kind of systems experimental data are not available. Once again, it is possible to use CS reliable data in order to test the results obtained by MF calculations. In ref. [9] the authors observed that it possible to distinguish the two enantiomers when they are dispersed in a curly solvent, $R_\Sigma = 0.4D$; $p_\Sigma = 4D$ (Figure 4.2b of Chapter 4), and when the solute and solvent particles are in *tune*; it happens for two particular solute cases called A$\rightarrow$ ($R_\sigma = 0.2D$; $p_\sigma = 4D$) and B$\rightarrow$ ($R_\sigma = 0.4D$; $p_\sigma = 4D$). From the simulated data the S_{zz}^{ach} have been calculated simply averaging S_{zz}^{P} and S_{zz}^{M} (the uniaxial order parameter for the right- and left- handed solute particles), and the values of the pseudoscalar Ψ_σ (varying L_σ and Λ_σ to investigate all the solutes considered) have been obtained. Being the system uniaxial, an analytical form of S_{zz} can be obtained, that is function of L_σ, Ψ_σ, $\left(\frac{R_\Sigma}{p_\Sigma}\right)$, $\left(\frac{R_\sigma}{p_\sigma}\right)$, w_Σ^0 and w_Σ^c. At the end of this procedure, the *best couple* of the 'w' parameters have been adjusted in order to obtain the best fit (simultaneous fit of S_{zz}^{ach}, S_{zz}^{P} and S_{zz}^{M}) between MF and CS data in order to minimize the sum of the squares between the data sets. In practice, a non linear least-squares fit by means of the tool **FindFit** of Mathematica® [10], using the Levenberg-Marquardt optimization [11–13] method, has been used.

5.3 Analysis and comments on the results obtained

The CS and MF results are shown in Figure 5.3. From the fitting procedure, described in the previous section, the best values of w_Σ^0, w_Σ^c and for the adimensional parameter w_χ result to be: $w_\Sigma^0 = 0.60\ kT/D$; $w_\Sigma^c = 11.96\ kT/D$; $w_\chi(A) = 0.10$; $w_\chi(A) = 0.20$.

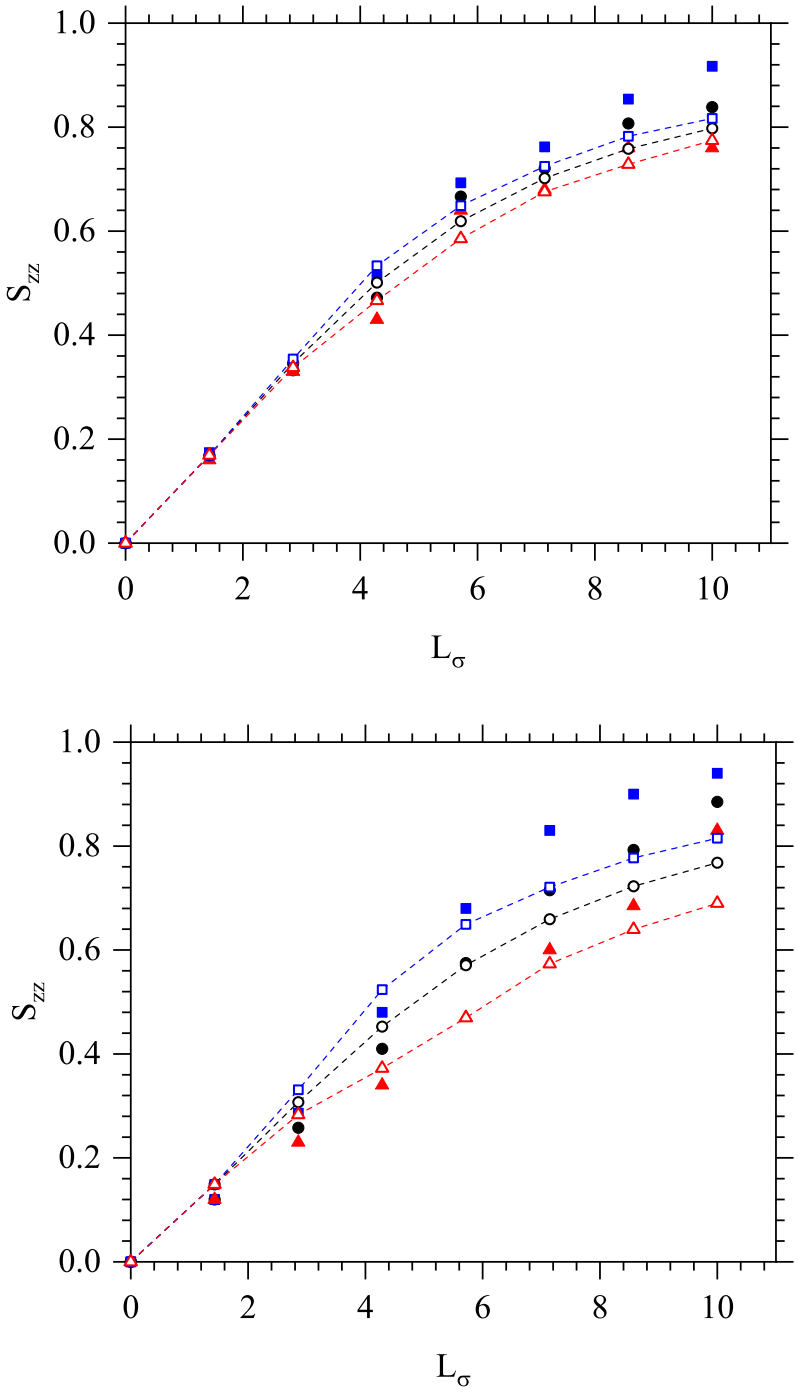

Figure 5.3: The full-filled symbols represents the CS data and the empty symbols the MF one. The behaviour of the uniaxial order parameter for the achiral (raceme mixture) (S_{zz}^{ach}) and enantiopure chiral compounds (P: S_{zz}^{P}) and (M: S_{zz}^{M}) for (top) the A system ($R_\sigma = 0.2D$; $p_\sigma = 4D$) and for the B system (bottom) ($R_\sigma = 0.4D$; $p_\sigma = 4D$) have been shown.

It is interesting to note that our inference was confirmed both by 'virtual' experimental data and by our MF model. Being the solvent right-handed the P solute particles have the higher orientational stabilization (higher order parameter). It is also important to analyse, in some way, the physical meaning of w_χ; indeed, it reflects the sensitivity of the system to the chiral interactions, as mathematically

shown in eq. (5.9). In the investigated case we have observed that $w_\chi(B) > w_\chi(A)$: according to us, it makes sense because in the B case the solute particles are more in *tune* with respect to the solvent particles and than feel better the 'tortuosity' of the solvent (promoting the diastereoisomeric-like interactions). The results obtained also suggest that in a hypothetical real experiment it would be possible, in principle, discriminate unambiguously between the two enantiomers on the basis of the orientational order experienced by helical solute particles dissolved/dispersed in a (enantiopure) helical solvent. In our opinion, to us the formulation of this chiral sensitive mean torque potential seems promising as a tool for the absolute assignment of helical solutes molecules.

Bibliography

[1] G. Celebre, G. De Luca, C. D'Urso, M.E. Di Pietro, Helical Solutes Orientationally Ordered in Anisotropic Media Composed of Helical Particles: Formulation of a Mean Torque Potential Sensitive to P and M Chirality as a Tool for the Assignment of the Absolute Configuration of Enantiomers, *J. Mol. Liq.*, xxx, xxx, submitted.

[2] D.J. Photinos, E.T. Samulski, H. Toriumi, Alkyl Chains in a Nematic Field. 1. A Treatment of Conformer Shape,*J. Phys. Chem.*, **94**, 4688-4694 (1990).

[3] D.J. Photinos, E.T. Samulski, H. Toriumi, Temperature and Chain Length Dependence of Orientational Ordering,*J. Phys. Chem.*, **94**, 4694-4700 (1990).

[4] D.J. Photinos in NMR of Orderd Liquids, E.E. Burnell and C.A. de Lange, (Kluwer Academic Publishers, Dordrecht, 2003, Chap 12).

[5] E.T. Samulski in NMR of Orderd Liquids, E.E. Burnell and C.A. de Lange, (Kluwer Academic Publishers, Dordrecht, 2003, Chap 13).

[6] W.J.A. Goossens, A molecular theory of the cholesteric phase and of the twisting power of optically active molecules in a nematic liquid crystal, *Mol. Cryst. Liq. Cryst.*, **12**, 237-244 (1970).

[7] B.W. van der Meer, G. Vertogen, A.J. Dekker, J.G.J Ypma, A molecular-statistical theory of the temperature-dependent pitch in cholesteric liquid crystals,*J. Chem. Phys.*, **65**, 10-15 (1976).

[8] R. Memmer, Computer simulation of chiral liquid crystal phases VIII. Blue phases of the chiral Gay-Berne fluid, *Liq. Cryst.*, **27**, 533-546 (2000).

[9] J. Gutierrez Bojart, C. D'Urso, G. Celebre, G. Cinacchi, Probing the sensitivity of orientational ordering as a way towards absolute enantiorecognition: helical-particle solutes in helical-particle nematic solvents, *Phys. Rev. E*, **98**, 042704 (2018).

[10] Mathematica® is a trademark of Wolfram Research, Inc.

[11] K. Levenberg, A Method for the Solution of Certain Problems in Least Squares, *Quart. Appl. Math.*, **2**, 164-168 (1944).

[12] D. Marquardt, An Algorithm for Least-Squares Estimation of Nonlinear Parameters, *SIAM J. Appl. Math.*, **11**, 431-441 (1963).

[13] D.M. Bates, D.G. Watts, Nonlinear Regression and Its Applications (Wiley, New York, 1988)

APPENDIX A

Numerical results for the extensive investigation of single-component system made up of C_{2h} hard-particles

- $L = 5D$; $D = 1 \rightarrow$ geometrical parameters of the spherocylinder;
- $L_{sf} = L + D$; $L_{dimer} = L_{sf} + (2shift)$;
- Phase = phase of the system;
- vb= simulation carried out using a triclinic box (variable box);
- vbo= simulation carried out using a triclinic box and starting from an ordered configuration (i.e. all the particles aligned along the same direction);
- $P^* = PD^3/kT$;
- $\phi = \rho V_{dim} \rightarrow V_{dim} = 8,901D^3$ and ρ the number density;
- S = uniaxial order parameter;
- $S_w = D_{2h}$ biaxial order parameter (calculated using $\boldsymbol{w}$);
- $S_{w_\perp} = D_{2h}$ biaxial order parameter (calculated using $\boldsymbol{w}_\perp$);
- $P_{C2h} = C_{2h}$ biaxial order parameter;
- τ = positional order parameter (k=1);
- τ_2 = positional order parameter (k=2);
- τ_C = positional order parameter peculiar for the Sm_C phase;
- θ = tilt angle (degree) between the normal layer and the principal director.

shift=0

Phase	P^*	ϕ	S	S_w	$S_{w_\perp}$	P_{C2h}	τ	τ_2
I	0.10	0.198	0.023	0.020	0.022	0.008	0.049	0.055
I	0.20	0.259	0.027	0.021	0.022	0.008	0.048	0.055
I	0.30	0.300	0.030	0.021	0.023	0.009	0.047	0.054
I	0.40	0.331	0.036	0.024	0.025	0.009	0.050	0.059
I	0.50	0.357	0.043	0.025	0.027	0.010	0.050	0.056
I	0.60	0.378	0.048	0.025	0.025	0.009	0.047	0.054
I	0.70	0.400	0.064	0.030	0.029	0.009	0.046	0.053
$\mathrm{Sm_A}$	0.80	0.483	0.951	0.256	0.027	0.015	0.879	0.621
$\mathrm{Sm_A}$	0.90	0.507	0.969	0.257	0.021	0.012	0.913	0.698
$\mathrm{Sm_A}$	1.00	0.527	0.976	0.262	0.026	0.015	0.927	0.740
$\mathrm{Sm_A}$	1.10	0.543	0.981	0.264	0.026	0.014	0.940	0.782
$\mathrm{Sm_A}$	1.20	0.558	0.984	0.261	0.021	0.011	0.949	0.810
$\mathrm{Sm_A}$	1.30	0.571	0.987	0.262	0.021	0.012	0.954	0.830
$\mathrm{Sm_A}$	1.40	0.584	0.989	0.264	0.022	0.011	0.961	0.852
$\mathrm{Sm_A}$	1.50	0.596	0.991	0.264	0.022	0.011	0.966	0.870
$\mathrm{Sm_A}$	1.60	0.607	0.992	0.264	0.022	0.011	0.969	0.883
$\mathrm{qSm_B}$	1.70	0.647	0.996	0.264	0.020	0.012	0.979	0.919
$\mathrm{qSm_B}$	1.80	0.657	0.996	0.277	0.037	0.012	0.978	0.916
$\mathrm{qSm_B}$	1.90	0.665	0.997	0.310	0.081	0.012	0.942	0.785
$\mathrm{qSm_B}$	2.00	0.669	0.997	0.329	0.106	0.012	0.980	0.921

shift=0.15

Phase	P^*	ϕ	S	S_w	$S_{w_\perp}$	P_{C2h}	τ	τ_2
I	0.10	0.197	0.033	0.029	0.031	0.012	0.066	0.075
I	0.20	0.258	0.038	0.029	0.031	0.012	0.064	0.074
I	0.30	0.299	0.042	0.029	0.031	0.012	0.063	0.073
I	0.40	0.330	0.048	0.031	0.033	0.012	0.063	0.072
I	0.50	0.355	0.056	0.032	0.033	0.012	0.062	0.073
I	0.60	0.378	0.068	0.035	0.036	0.012	0.063	0.072
I	0.70	0.400	0.091	0.042	0.039	0.013	0.063	0.072
$\mathrm{Sm_A}$	0.80	0.477	0.949	0.263	0.037	0.021	0.839	0.514
$\mathrm{Sm_A}$	0.90	0.500	0.964	0.267	0.036	0.021	0.881	0.608
$\mathrm{Sm_A}$	1.00	0.518	0.971	0.270	0.038	0.020	0.899	0.657
$\mathrm{Sm_A}$	1.10	0.534	0.977	0.271	0.036	0.021	0.917	0.708
$\mathrm{Sm_A}$	1.20	0.549	0.981	0.272	0.037	0.022	0.925	0.733
$\mathrm{Sm_A}$	1.30	0.562	0.984	0.272	0.035	0.021	0.933	0.759
$\mathrm{Sm_A}$	1.40	0.575	0.987	0.275	0.038	0.020	0.938	0.775
$\mathrm{Sm_A}$	1.50	0.586	0.989	0.272	0.034	0.021	0.943	0.792
$\mathrm{Sm_A}$	1.60	0.596	0.990	0.275	0.037	0.022	0.947	0.805
$\mathrm{Sm_A}$	1.70	0.607	0.991	0.274	0.036	0.021	0.951	0.817
$\mathrm{qSm_B}$	1.80	0.639	0.994	0.293	0.060	0.023	0.954	0.828
$\mathrm{qSm_B}$	1.90	0.649	0.994	0.285	0.050	0.022	0.958	0.841
$\mathrm{qSm_B}$	2.00	0.653	0.994	0.291	0.057	0.021	0.959	0.846

shift=0.25

Phase	P^*	ϕ	S	S_w	$S_{w_\perp}$	P_{C2h}	τ	τ_2
I	0.10	0.196	0.034	0.028	0.031	0.012	0.066	0.075
I	0.20	0.257	0.038	0.029	0.031	0.012	0.064	0.074
I	0.30	0.298	0.044	0.030	0.032	0.012	0.063	0.073
I	0.40	0.329	0.050	0.031	0.032	0.012	0.063	0.073
I	0.50	0.354	0.060	0.033	0.034	0.013	0.063	0.073
I	0.60	0.377	0.077	0.037	0.035	0.013	0.063	0.072
I	0.70	0.398	0.105	0.044	0.040	0.013	0.063	0.072
$\mathrm{Sm_A}$	0.80	0.467	0.937	0.259	0.037	0.021	0.778	0.403
$\mathrm{Sm_A}$	0.90	0.490	0.958	0.265	0.036	0.021	0.840	0.508
$\mathrm{Sm_A}$	1.00	0.510	0.969	0.268	0.036	0.021	0.867	0.568
$\mathrm{Sm_A}$	1.10	0.526	0.976	0.271	0.037	0.021	0.884	0.613
$\mathrm{Sm_A}$	1.20	0.540	0.979	0.272	0.038	0.022	0.898	0.651
$\mathrm{Sm_A}$	1.30	0.553	0.982	0.274	0.038	0.021	0.903	0.667
$\mathrm{Sm_A}$	1.40	0.565	0.984	0.275	0.039	0.021	0.912	0.692
$\mathrm{Sm_A}$	1.50	0.577	0.987	0.274	0.036	0.021	0.920	0.717
$\mathrm{Sm_A}$	1.60	0.587	0.989	0.274	0.036	0.021	0.921	0.719
$\mathrm{qSm_B}$	1.70	0.623	0.993	0.326	0.104	0.024	0.899	0.653
$\mathrm{qSm_B}$	1.80	0.633	0.994	0.290	0.056	0.021	0.918	0.710
$\mathrm{qSm_B}$	1.90	0.638	0.993	0.274	0.034	0.020	0.928	0.742
$\mathrm{qSm_B}$	2.00	0.649	0.995	0.278	0.040	0.022	0.921	0.720

shift=0.35

Phase	P^*	ϕ	S	S_w	$S_{w_\perp}$	P_{C2h}	τ	τ_2
I	0.1	0.195	0.034	0.029	0.031	0.012	0.066	0.075
I	0.2	0.256	0.039	0.029	0.031	0.012	0.065	0.074
I	0.3	0.296	0.045	0.03	0.031	0.012	0.063	0.073
I	0.4	0.327	0.053	0.031	0.032	0.012	0.063	0.073
I	0.5	0.352	0.069	0.035	0.034	0.012	0.062	0.072
I	0.6	0.375	0.095	0.041	0.037	0.013	0.063	0.072
I	0.7	0.396	0.171	0.058	0.04	0.013	0.064	0.072
Nu	0.8	0.422	0.6	0.157	0.037	0.019	0.078	0.074
Sm_A	0.9	0.481	0.951	0.262	0.036	0.021	0.785	0.397
Sm_A	1	0.501	0.967	0.268	0.037	0.021	0.826	0.471
Sm_A	1.1	0.518	0.975	0.27	0.037	0.021	0.844	0.517
Sm_A	1.2	0.532	0.979	0.271	0.036	0.02	0.85	0.525
Sm_A	1.3	0.545	0.982	0.272	0.037	0.023	0.861	0.552
Sm_A	1.4	0.557	0.984	0.274	0.039	0.02	0.863	0.556
Sm_A	1.5	0.569	0.987	0.027	0.037	0.021	0.861	0.548
Sm_A	1.6	0.624	0.995	0.293	0.059	0.022	0.846	0.513
qSm_B,qSm_H	1.7	0.63	0.997	0.287	0.051	0.179	0.147	0.107
qSm_B,qSm_H	1.8	0.636	0.996	0.31	0.081	0.017	0.842	0.503
qSm_B,qSm_H	1.9	0.654	0.998	0.618	0.491	0.394	0.347	0.132
qSm_B,qSm_H	2	0.665	0.998	0.732	0.644	0.645	0.213	0.113

shift=0.35-vb

Phase	P^*	ϕ	S	S_w	$S_{w_\perp}$	P_{C2h}	τ	τ_2
Sm_A	1.50	0.570	0.987	0.277	0.042	0.023	0.874	0.584
Sm_A	1.60	0.581	0.989	0.275	0.038	0.034	0.842	0.504
qSm_B,qSm_H	1.70	0.626	0.995	0.292	0.058	0.028	0.797	0.406
qSm_B,qSm_H	1.80	0.635	0.996	0.271	0.030	0.017	0.807	0.425
qSm_B,qSm_H	1.90	0.640	0.996	0.260	0.015	0.021	0.909	0.685
qSm_B,qSm_H	2.00	0.651	0.997	0.345	0.128	0.257	0.103	0.076

shift=0.50

Phase	P^*	ϕ	S	S_w	$S_{w_\perp}$	P_{C2h}	τ	τ_2	τ_C	ϑ
I	0.10	0.192	0.040	0.033	0.036	0.014	0.077	0.088		
I	0.20	0.253	0.047	0.034	0.036	0.015	0.075	0.086		
I	0.30	0.293	0.057	0.036	0.037	0.015	0.075	0.085		
I	0.40	0.324	0.072	0.039	0.040	0.015	0.073	0.085		
I	0.50	0.349	0.097	0.044	0.042	0.015	0.074	0.085		
I	0.60	0.372	0.173	0.061	0.045	0.016	0.074	0.085		
N_u	0.70	0.400	0.620	0.017	0.043	0.022	0.080	0.084		
N_u	0.80	0.422	0.738	0.020	0.044	0.025	0.091	0.086		
N_u	0.90	0.442	0.813	0.225	0.046	0.026	0.107	0.085		
Sm_A	1.00	0.488	0.959	0.271	0.044	0.026	0.728	0.313	0.726	1.300
Sm_A	1.10	0.506	0.972	0.276	0.046	0.026	0.753	0.341	0.747	0.888
Sm_C	1.20	0.520	0.978	0.279	0.047	0.114	0.205	0.125	0.760	14.501
Sm_C	1.30	0.534	0.980	0.278	0.044	0.152	0.188	0.117	0.757	17.045
Sm_C	1.40	0.549	0.985	0.296	0.067	0.386	0.124	0.094	0.811	29.702
Sm_C	1.50	0.563	0.990	0.315	0.090	0.440	0.120	0.092	0.821	30.435
Hex	1.60	0.609	0.994	0.373	0.166	0.581	0.064	0.082	0.876	39.293
Hex	1.70	0.620	0.996	0.330	0.107	0.513	0.101	0.082	0.591	36.807
Hex	1.80	0.623	0.997	0.322	0.097	0.530	0.100	0.085	0.883	38.927
Hex	1.90	0.629	0.993	0.297	0.064	0.534	0.080	0.083	0.867	38.113
Hex	2.00	0.636	0.992	0.329	0.106	0.587	0.077	0.084	0.376	36.526

shift=0.75

Phase	P^*	ϕ	S	S_w	$S_{w_\perp}$	P_{C2h}	τ	τ_2
I	0.10	0.189	0.028	0.020	0.021	0.008	0.044	0.051
I	0.20	0.249	0.028	0.020	0.021	0.081	0.045	0.051
I	0.30	0.289	0.035	0.021	0.021	0.079	0.043	0.050
I	0.40	0.318	0.045	0.023	0.023	0.083	0.043	0.050
I	0.50	0.346	0.117	0.039	0.027	0.083	0.043	0.050
N_u	0.60	0.378	0.670	0.168	0.023	0.013	0.046	0.050
N_u	0.70	0.401	0.763	0.195	0.024	0.013	0.061	0.051
N_u	0.80	0.419	0.817	0.211	0.024	0.014	0.048	0.050
N_u	0.90	0.437	0.854	0.223	0.025	0.015	0.048	0.050
N_u	1.00	0.454	0.888	0.234	0.025	0.016	0.054	0.050
Sm_C	1.10	0.483	0.959	0.257	0.027	0.018	0.147	0.067
Sm_C	1.20	0.505	0.978	0.263	0.026	0.028	0.138	0.073
Sm_C	1.30	0.522	0.985	0.269	0.031	0.019	0.193	0.076
Hex	1.40	0.605	0.997	0.815	0.755	0.833	0.099	0.062
Hex	1.50	0.617	0.998	0.738	0.652	0.809	0.098	0.062
Hex	1.60	0.630	0.998	0.832	0.778	0.896	0.103	0.064
Hex	1.70	0.640	0.998	0.880	0.842	0.911	0.094	0.066
Hex	1.80	0.649	0.998	0.890	0.855	0.922	0.093	0.066
Hex	1.90	0.655	0.998	0.873	0.832	0.912	0.098	0.068
Hex	2.00	0.660	0.998	0.849	0.800	0.917	0.097	0.068

shift=1.0

Phase	P^*	ϕ	S	S_w	$S_{w_\perp}$	P_{C2h}	τ	τ_2
I	0.10	0.185	0.042	0.034	0.038	0.014	0.077	0.088
I	0.20	0.244	0.051	0.035	0.037	0.015	0.075	0.086
I	0.30	0.283	0.063	0.038	0.038	0.015	0.075	0.086
I	0.40	0.313	0.088	0.045	0.042	0.015	0.074	0.085
N_u	0.50	0.352	0.665	0.179	0.040	0.022	0.079	0.087
N_u	0.60	0.379	0.784	0.214	0.041	0.023	0.083	0.087
N_u	0.70	0.400	0.837	0.230	0.041	0.025	0.086	0.086
N_u	0.80	0.419	0.876	0.242	0.042	0.025	0.078	0.086
N_u	0.90	0.436	0.901	0.252	0.045	0.029	0.081	0.088
N_u	1.00	0.452	0.921	0.581	0.045	0.029	0.084	0.090
N_u	1.10	0.468	0.942	0.313	0.048	0.031	0.087	0.093
N_u	1.20	0.493	0.970	0.352	0.050	0.056	0.145	0.128
N_u	1.30	0.509	0.979	0.294	0.068	0.140	0.150	0.145
Hex	1.40	0.590	0.997	0.479	0.306	0.633	0.120	0.116
Hex	1.50	0.592	0.997	0.415	0.221	0.544	0.168	0.168
Hex	1.60	0.604	0.997	0.421	0.229	0.588	0.119	0.122
Hex	1.70	0.606	0.996	0.402	0.204	0.607	0.135	0.131
Hex	1.80	0.618	0.997	0.451	0.269	0.646	0.151	0.149
Hex	1.90	0.619	0.996	0.470	0.295	0.640	0.209	0.209
Hex	2.00	0.629	0.996	0.429	0.241	0.621	0.114	0.110

shift=1.0-vbo

Phase	P^*	ϕ	S	S_w	$S_{w_\perp}$	P_{C2h}	τ	τ_2
Hex	1.50	0.067	0.998	0.412	0.216	0.526	0.149	0.148
Hex	1.60	0.068	0.997	0.450	0.268	0.589	0.157	0.155
Hex	1.70	0.069	0.997	0.391	0.190	0.587	0.128	0.130
Hex	1.80	0.071	0.998	0.440	0.254	0.598	0.133	0.128
Hex	1.90	0.071	0.997	0.465	0.289	0.617	0.203	0.205
Hex	2.00	0.071	0.996	0.437	0.252	0.595	0.137	0.132

shift=1.5

Phase	P^*	ϕ	S	S_w	$S_{w_\perp}$	P_{C2h}	τ	τ_2
I	0.10	0.178	0.043	0.034	0.036	0.014	0.077	0.088
I	0.20	0.236	0.053	0.036	0.037	0.014	0.075	0.086
I	0.30	0.274	0.074	0.041	0.039	0.015	0.074	0.085
N_u	0.40	0.325	0.683	0.187	0.039	0.021	0.077	0.085
N_u	0.50	0.354	0.826	0.228	0.040	0.025	0.077	0.085
N_u	0.60	0.378	0.871	0.241	0.039	0.026	0.081	0.088
N_u	0.70	0.400	0.906	0.252	0.040	0.026	0.087	0.093
N_u	0.80	0.422	0.932	0.261	0.043	0.024	0.109	0.112
N_u	0.90	0.445	0.958	0.272	0.047	0.029	0.210	0.209
Sm_A	1.00	0.472	0.974	0.276	0.046	0.027	0.505	0.505
Sm_A	1.10	0.492	0.982	0.283	0.051	0.032	0.669	0.669
Sm_A	1.20	0.521	0.991	0.289	0.055	0.041	0.768	0.768
Hex	1.30	0.578	0.997	0.277	0.037	0.272	0.201	0.206
Hex	1.40	0.589	0.998	0.445	0.261	0.454	0.203	0.200
Hex	1.50	0.600	0.998	0.367	0.157	0.457	0.230	0.228
Hex	1.60	0.611	0.998	0.392	0.189	0.513	0.236	0.237
Hex	1.70	0.618	0.998	0.495	0.327	0.604	0.207	0.214
Hex	1.80	0.623	0.998	0.488	0.318	0.599	0.142	0.128
Hex	1.90	0.624	0.997	0.606	0.476	0.671	0.206	0.207
Hex	2.00	0.641	0.999	0.539	0.385	0.686	0.110	0.105

shift=2.00

Phase	P^*	ϕ	S	S_w	$S_{w_\perp}$	P_{C2h}	τ	τ_2
I	0.10	0.172	0.047	0.037	0.040	0.015	0.081	0.093
I	0.20	0.229	0.058	0.039	0.040	0.016	0.081	0.092
I	0.30	0.268	0.089	0.048	0.044	0.016	0.079	0.090
N_u	0.40	0.322	0.821	0.229	0.040	0.024	0.084	0.092
N_u	0.50	0.352	0.877	0.245	0.041	0.025	0.089	0.093
N_u	0.60	0.377	0.912	0.256	0.042	0.027	0.108	0.097
N_u	0.70	0.398	0.935	0.264	0.044	0.028	0.087	0.094
N_u	0.80	0.420	0.952	0.269	0.044	0.030	0.100	0.099
N_u	0.90	0.448	0.969	0.337	0.128	0.161	0.115	0.111
Hex	1.00	0.549	0.996	0.875	0.834	0.955	0.160	0.167
Hex	1.10	0.573	0.998	0.933	0.911	0.976	0.131	0.133
Hex	1.20	0.588	0.998	0.933	0.911	0.976	0.110	0.123
Hex	1.30	0.602	0.998	0.945	0.928	0.981	0.141	0.153
Hex	1.40	0.612	0.998	0.910	0.881	0.967	0.133	0.151
Hex	1.50	0.625	0.999	0.783	0.712	0.922	0.148	0.163
Hex	1.60	0.635	0.999	0.920	0.893	0.970	0.159	0.174
Hex	1.70	0.648	0.999	0.884	0.846	0.956	0.140	0.157
Hex	1.80	0.657	0.999	0.721	0.628	0.901	0.172	0.197
Hex	1.90	0.664	0.999	0.731	0.642	0.904	0.144	0.256
Hex	2.00	0.670	0.999	0.750	0.667	0.909	0.205	0.227

shift=2.0-vbo

Phase	P^*	ϕ	S	S_w	$S_{w_\perp}$	P_{C2h}	τ	τ_2
N_u	1.00	0.458	0.976	0.278	0.046	0.038	0.104	0.106
N_u	1.10	0.479	0.984	0.052	0.052	0.035	0.109	0.111
Hex	1.20	0.551	0.997	0.298	0.064	0.092	0.100	0.099
Hex	1.30	0.563	0.997	0.275	0.034	0.054	0.117	0.116
Hex	1.40	0.573	0.997	0.318	0.091	0.041	0.085	0.099
Hex	1.50	0.571	0.996	0.286	0.050	0.034	0.092	0.102
Hex	1.60	0.587	0.997	0.380	0.017	0.060	0.094	0.105
Hex	1.70	0.595	0.998	0.288	0.051	0.054	0.108	0.099
Hex	1.80	0.596	0.998	0.264	0.020	0.052	0.117	0.123
Hex	1.90	0.591	0.996	0.288	0.052	0.055	0.104	0.112
Hex	2.00	0.602	0.997	0.286	0.049	0.011	0.105	0.107

shift=2.0-vb-point to point compression

Phase	P^*	ϕ	S	S_w	$S_{w_\perp}$	P_{C2h}	τ	τ_2
Hex	1.50	0.585	0.998	0.329	0.106	0.030	0.096	0.101
Hex	1.60	0.595	0.998	0.327	0.103	0.035	0.097	0.102
Hex	1.70	0.603	0.999	0.341	0.121	0.041	0.095	0.101
Hex	1.80	0.612	0.999	0.335	0.113	0.036	0.087	0.096
Hex	1.90	0.620	0.999	0.344	0.125	0.040	0.080	0.090
Hex	2.00	0.626	0.999	0.339	0.119	0.040	0.084	0.090

shift=2.5

Phase	P^*	ϕ	S	S_w	$S_{w_\perp}$	P_{C2h}	τ	τ_2
I	0.10	0.166	0.031	0.025	0.026	0.010	0.055	0.062
I	0.20	0.222	0.040	0.027	0.027	0.099	0.054	0.061
I	0.25	0.243	0.054	0.031	0.029	0.010	0.054	0.061
N_u	0.28	0.269	0.691	0.186	0.026	0.015	0.054	0.061
N_u	0.30	0.283	0.769	0.205	0.026	0.015	0.055	0.060
N_u	0.35	0.303	0.831	0.223	0.027	0.016	0.054	0.060
N_u	0.40	0.320	0.865	0.232	0.027	0.016	0.054	0.060
N_u	0.50	0.351	0.909	0.245	0.027	0.017	0.054	0.060
N_u	0.60	0.376	0.935	0.252	0.027	0.017	0.056	0.060
N_u	0.70	0.400	0.955	0.258	0.027	0.019	0.058	0.061
N_u	0.80	0.423	0.969	0.263	0.029	0.020	0.061	0.060
N_u	0.90	0.449	0.981	0.267	0.030	0.032	0.069	0.066
Sm_C	1.00	0.476	0.988	0.275	0.038	0.089	0.089	0.067
Sm_C	1.10	0.495	0.991	0.274	0.036	0.034	0.095	0.088
Sm_C	1.20	0.517	0.994	0.288	0.053	0.050	0.128	0.076
Hex	1.30	0.568	0.998	0.287	0.050	0.125	0.058	0.068
Hex	1.40	0.579	0.998	0.287	0.500	0.019	0.634	0.073
Hex	1.50	0.589	0.998	0.284	0.046	0.018	0.088	0.089
Hex	1.60	0.597	0.998	0.279	0.039	0.010	0.065	0.074
Hex	1.70	0.605	0.998	0.284	0.046	0.094	0.072	0.075
Hex	1.80	0.615	0.999	0.029	0.049	0.013	0.072	0.079
Hex	1.90	0.620	0.999	0.288	0.051	0.057	0.079	0.084
Hex	2.00	0.627	0.999	0.288	0.051	0.013	0.076	0.081

shift=3.0

Phase	P^*	ϕ	S	S_w	$S_{w_\perp}$	P_{C2h}	τ	τ_2
I	0.10							
I	0.20	0.216	0.054	0.035	0.034	0.012	0.068	0.075
N_u	0.30	0.283	0.834	0.230	0.033	0.019	0.073	0.074
N_u	0.40	0.321	0.904	0.248	0.032	0.022	0.074	0.076
N_u	0.50	0.361	0.949	0.261	0.033	0.022	0.179	0.094
Sm_A	0.60	0.416	0.981	0.272	0.036	0.025	0.802	0.447
Sm_A	0.70	0.447	0.987	0.273	0.035	0.023	0.876	0.598
Sm_A	0.80	0.473	0.990	0.274	0.035	0.029	0.909	0.685
Sm_A	0.90	0.494	0.992	0.274	0.036	0.027	0.929	0.747
Sm_A	1.00	0.513	0.994	0.275	0.035	0.026	0.945	0.796
Sm_A	1.10	0.529	0.995	0.275	0.035	0.028	0.952	0.822
Sm_A	1.20	0.545	0.996	0.276	0.036	0.034	0.937	0.772
Sm_A	1.30	0.558	0.997	0.278	0.038	0.029	0.960	0.851
Sm_A	1.40	0.572	0.997	0.278	0.038	0.037	0.958	0.842
Hex	1.50	0.610	0.999	0.274	0.033	0.061	0.752	0.279
Hex	1.60	0.613	0.998	0.271	0.029	0.013	0.866	0.547
Hex	1.70	0.619	0.999	0.283	0.044	0.041	0.828	0.442
Hex	1.80	0.622	0.998	0.271	0.029	0.080	0.845	0.477
Hex	1.90	0.634	0.998	0.273	0.031	0.092	0.871	0.557
Hex	2.00	0.645	0.999	0.265	0.020	0.084	0.868	0.556

APPENDIX B

Phase diagrams and phase sequences of the system made up of hard dimer of shifted spherocylinders

In this appendix the most representative phase diagrams (PD^3/kT vs ϕ) and the snapshots of the systems (made up of dimer of shifted spherocylinders) have been reported. The phases have been identified using the following notation and colour code:

- ◇ I= Isotropic
- ◇ Nu= Uniaxial Nematic
- ◇ SmA= smectic A
- ◇ SmC= smectic C
- ◇ qSmB= *quasi* smectic B
- ◇ qSmH= *quasi* smectic H
- ◇ Hex= hexagonal

In the phase diagrams the co-existence and the unachievable regions are represented by the shaded and dashed area respectively. In the snapshots we did not used the subscripts for the identification of the mesophases for graphic reasons. The colour code used for the snapshot is sensible to the orientation of the long molecular axis with respect to the principal director (i.e shades of blue $\vartheta \simeq 0°$; shades of red $\vartheta \simeq 90°$).

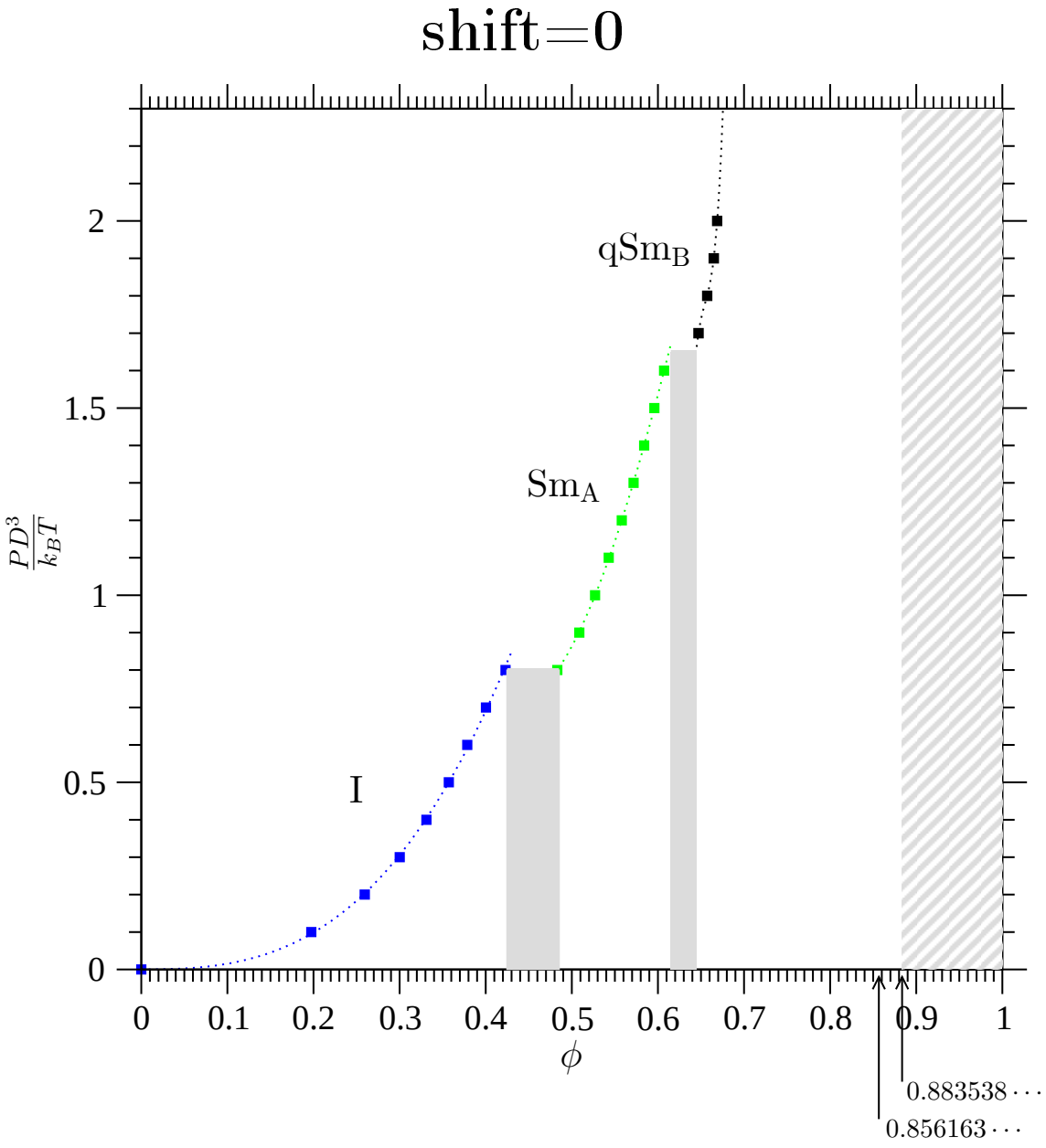

Figure B.1: Phase diagram of the D_{2h} system made up of dimer where the spherocylinders are shifted by 0D.

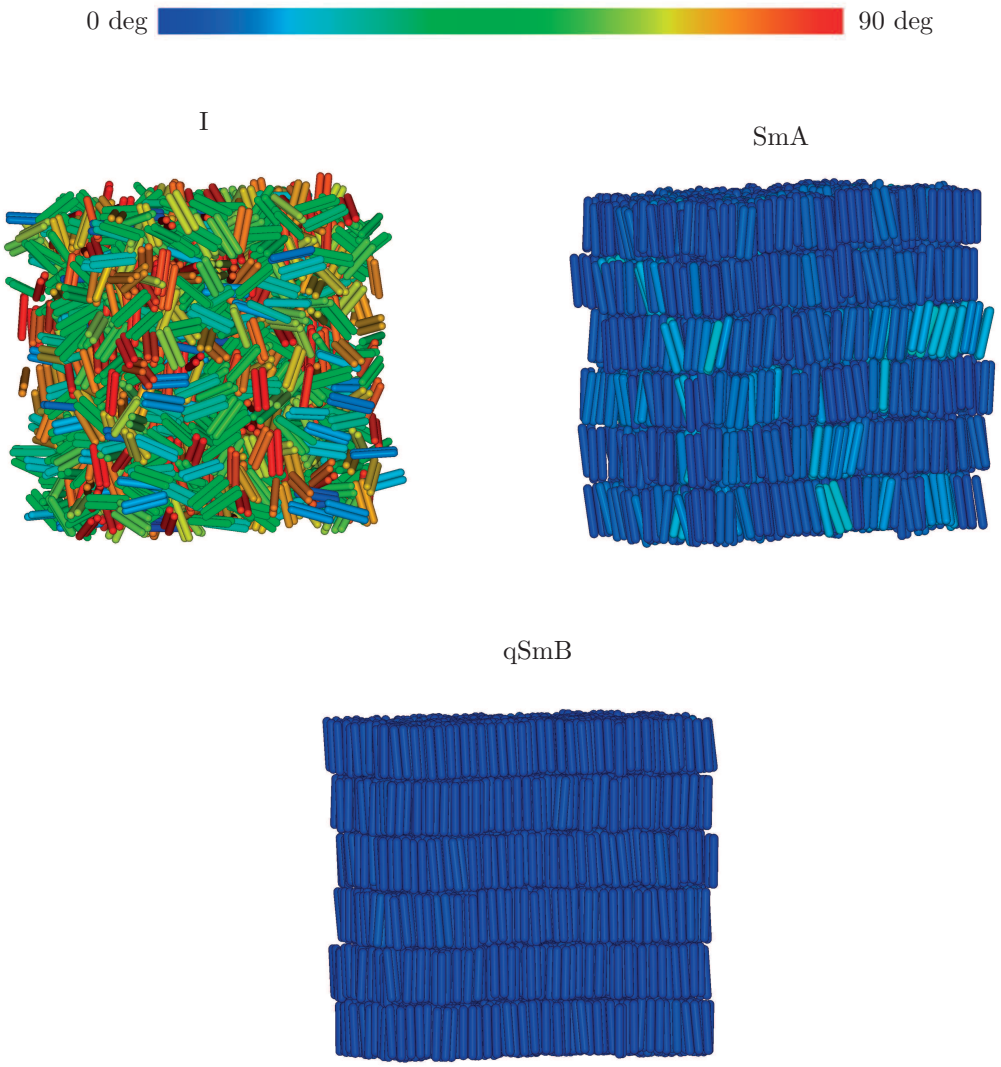

Figure B.2: Snaphosts of the D_{2h} system, with shift=0, at $\frac{PD^3}{kT} = 0.30$; 0.80 and 1.70.

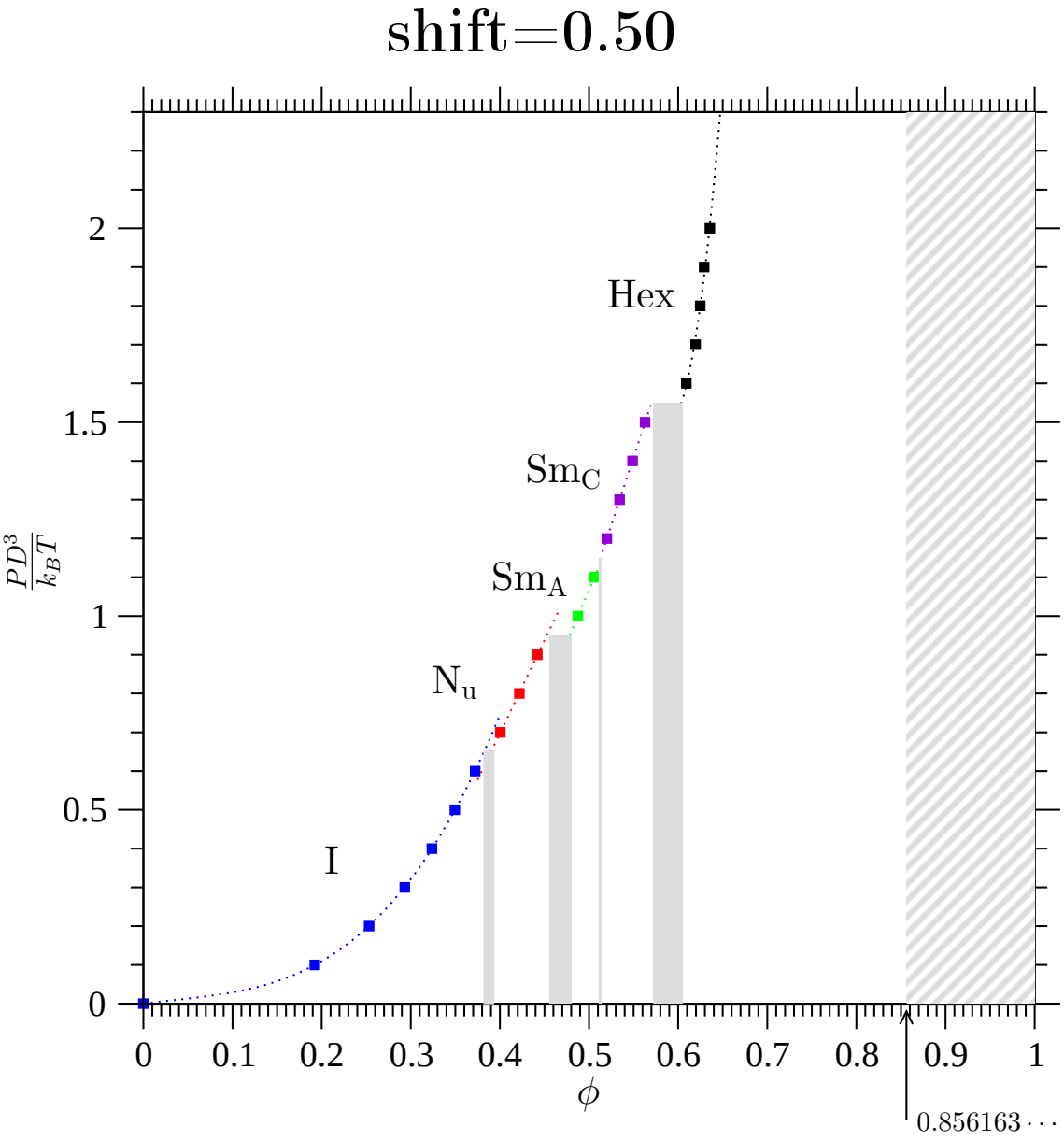

Figure B.3: Phase diagram of the C_{2h} system made up of dimer where the spherocylinders are shifted by 0.5D.

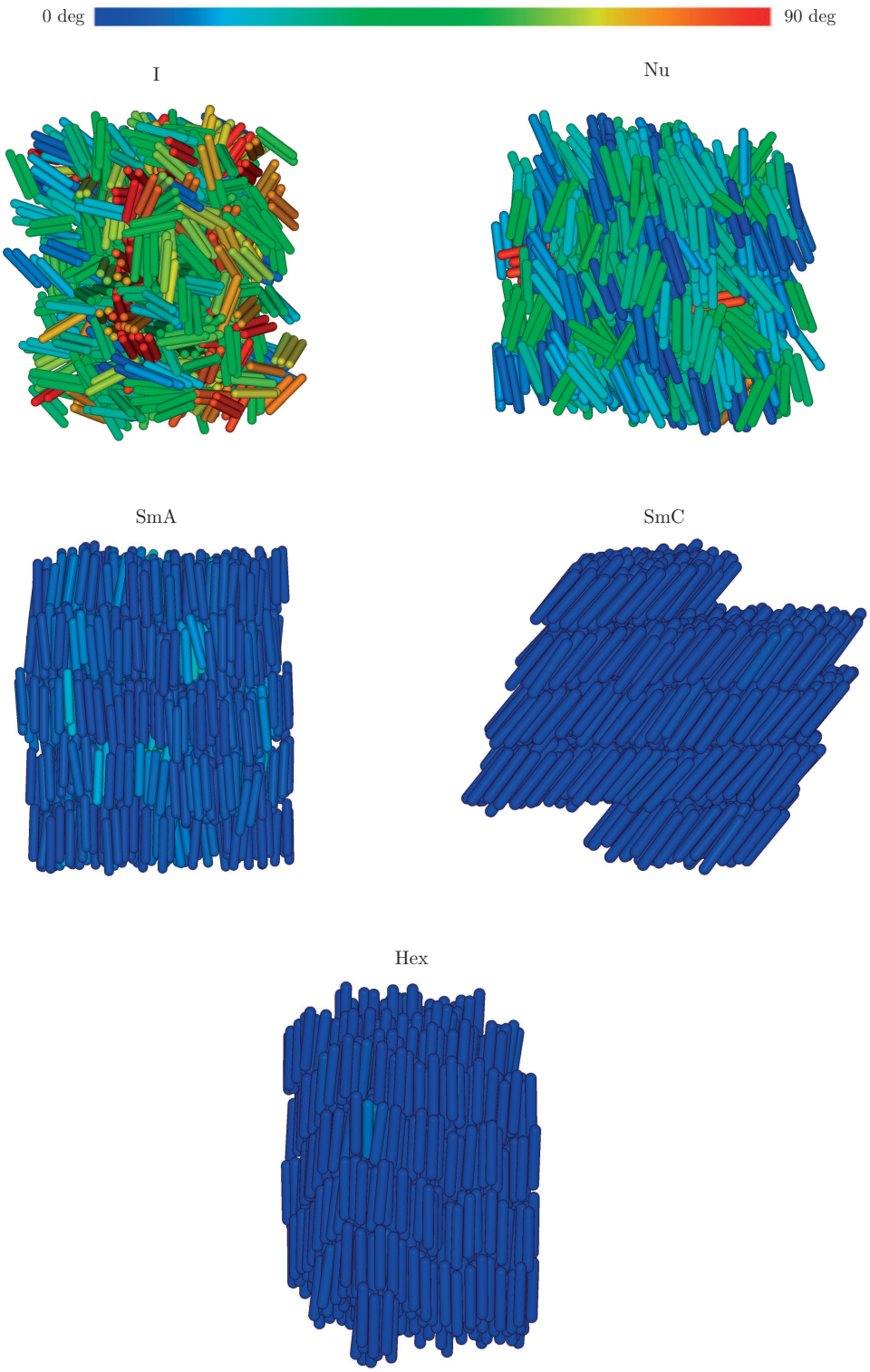

Figure B.4: Snaphosts of the C_{2h} system, with shift=0.50, at $\frac{PD^3}{kT}$ = 0.60; 0.70; 1.00; 1.60 and 2.00.

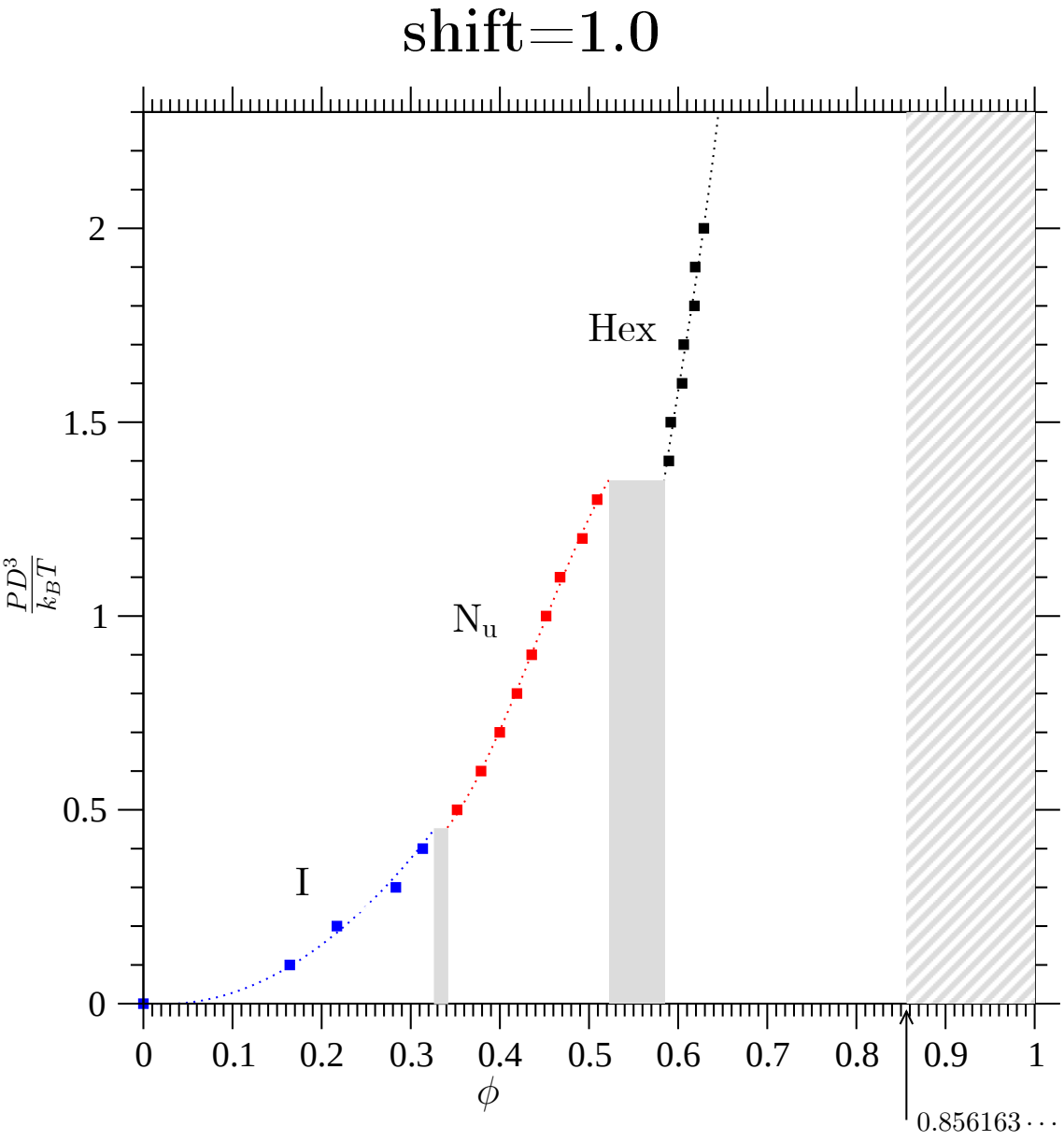

Figure B.5: Phase diagram of the C_{2h} system made up of dimer where the spherocylinders are shifted by 1.0D.

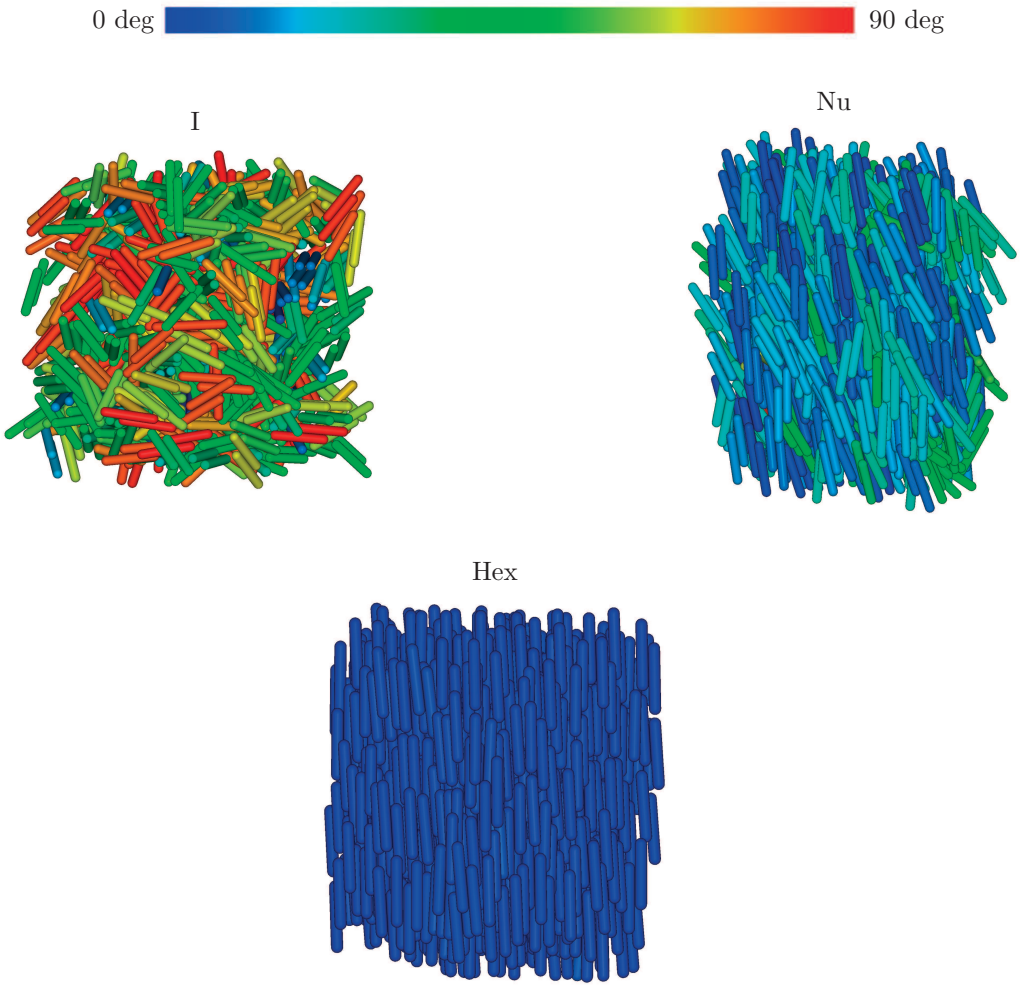

Figure B.6: Snaphosts of the C_{2h} system, with shift=1.0, at $\frac{PD^3}{kT} = 0.40; 0.60; 1.70$.

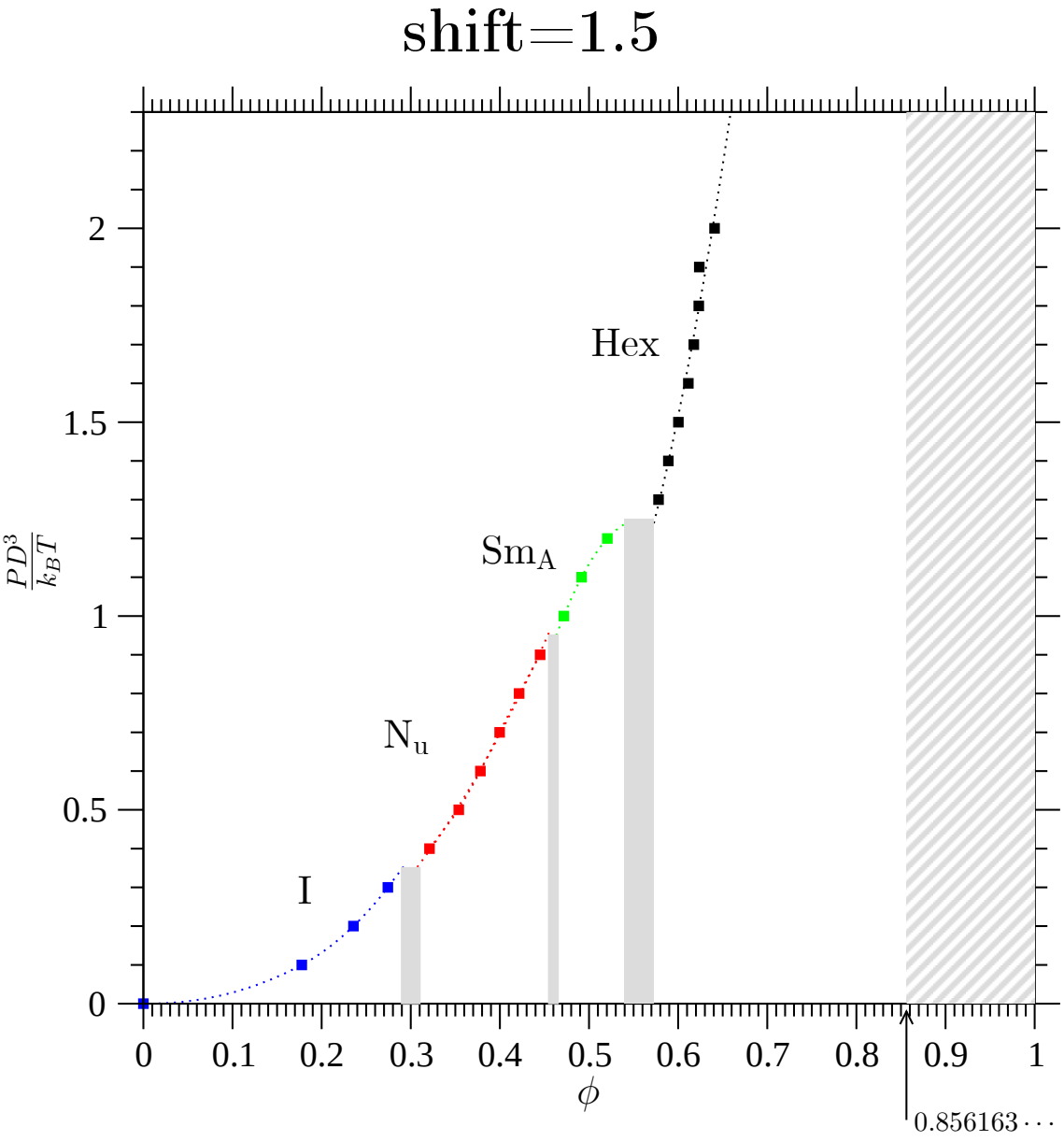

Figure B.7: Phase diagram of the C_{2h} system made up of dimer where the spherocylinders are shifted by 1.5D.

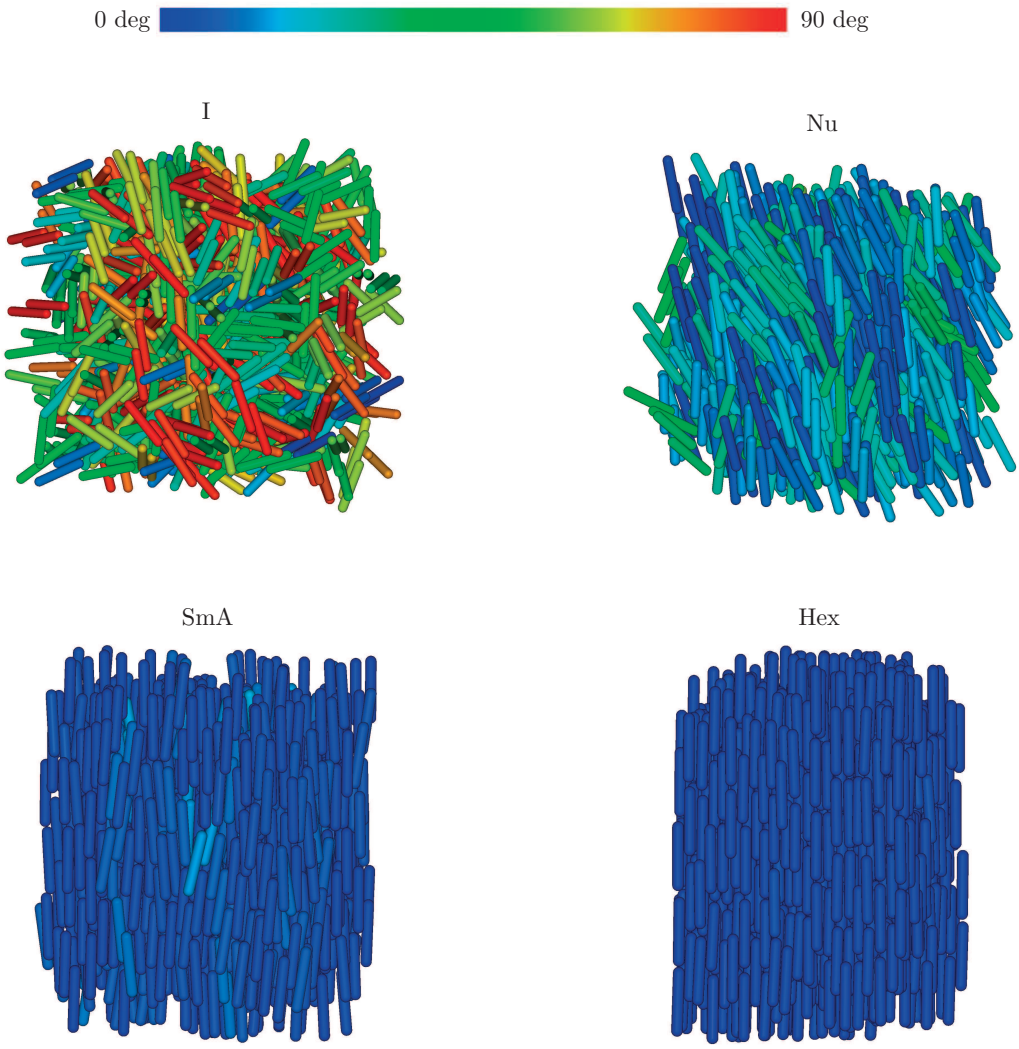

Figure B.8: Snaphosts of the C_{2h} system, with shift=1.50, at $\frac{PD^3}{kT}$ = 0.20; 0.50; 1.10 and 1.60.

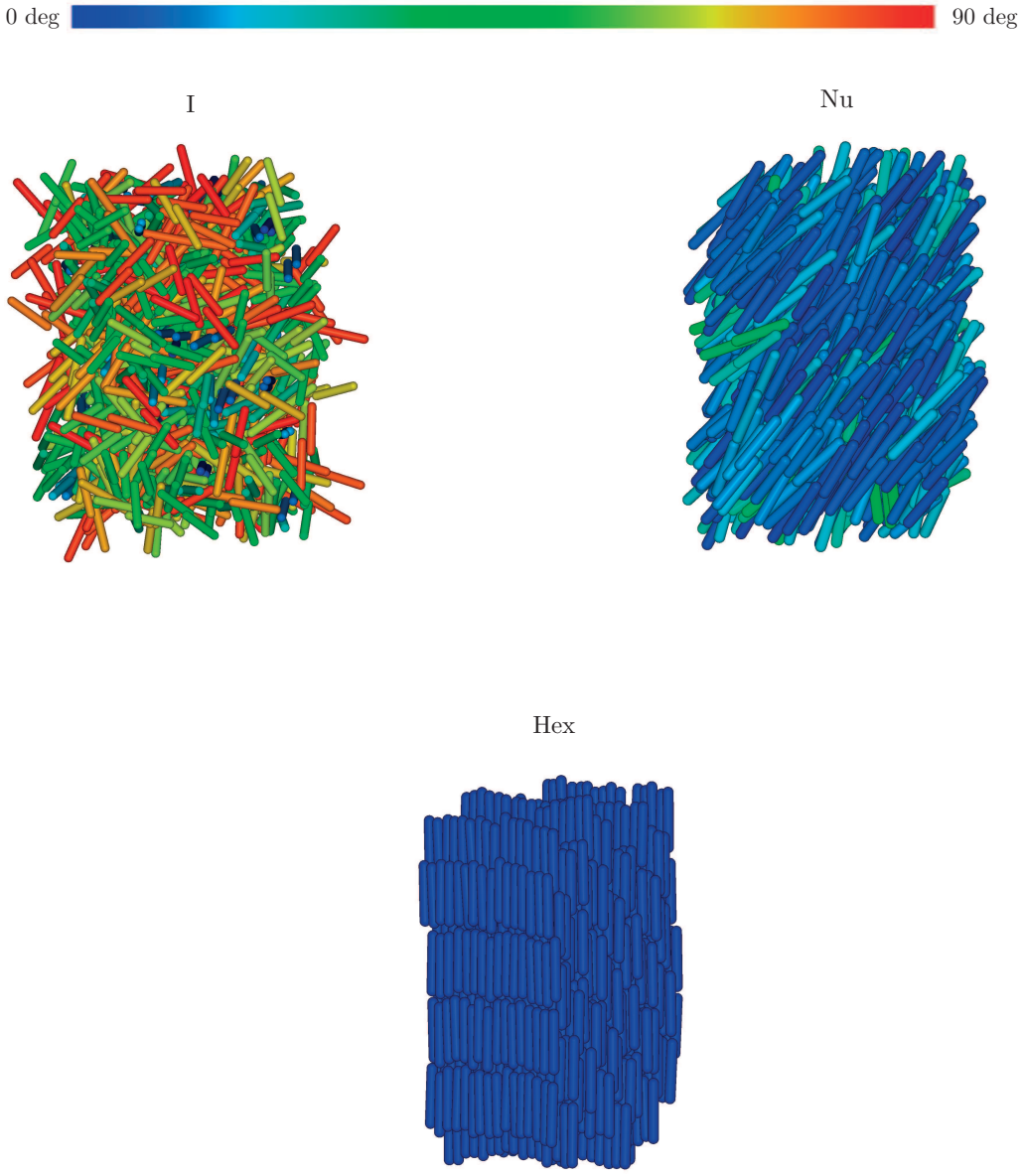

Figure B.9: Snaphosts of the C_{2h} system, with shift=2.0, at $\frac{PD^3}{kT} = 0.20$; 0.50 and 1.60.

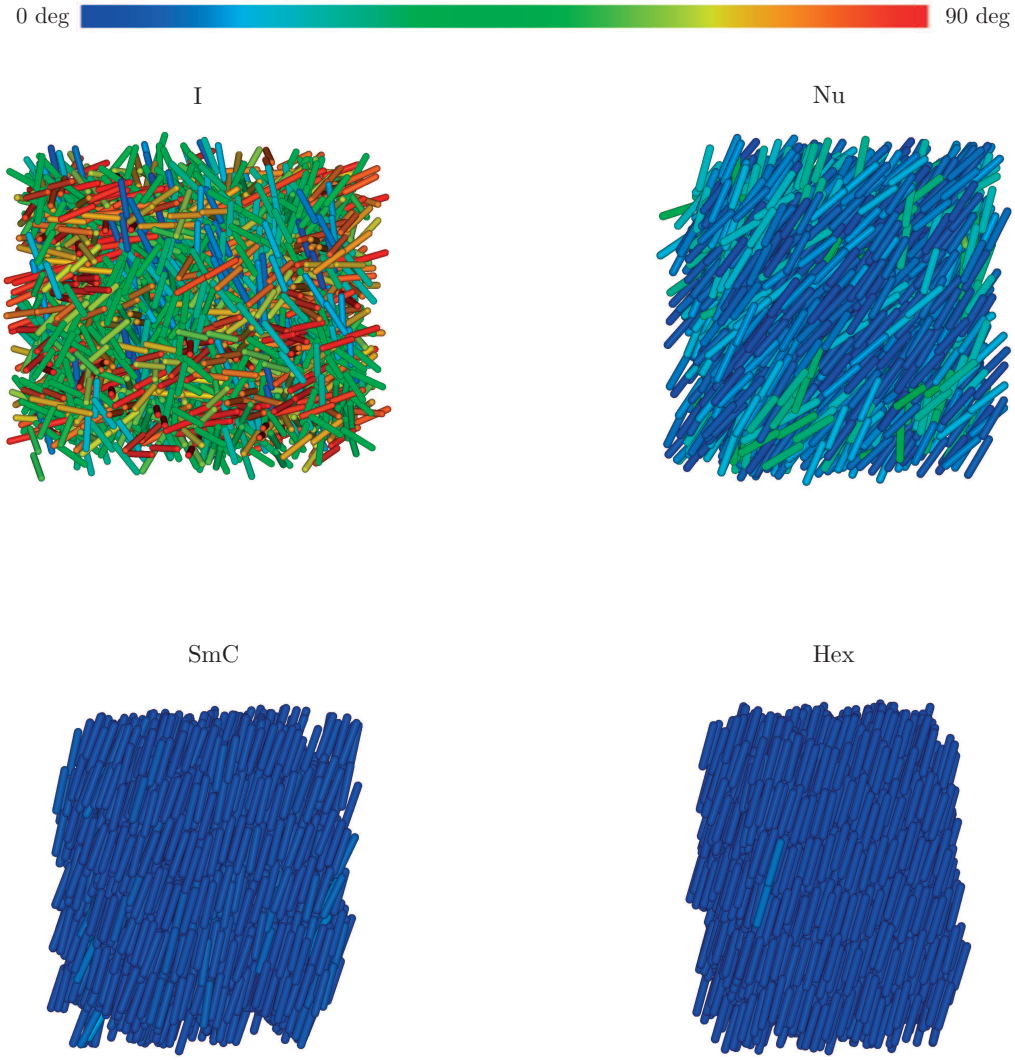

Figure B.10: Snaphosts of the C_{2h} system, with shift=2.5, at $\frac{PD^3}{kT} = 0.10$; 0.40; 1.10 and 1.60.

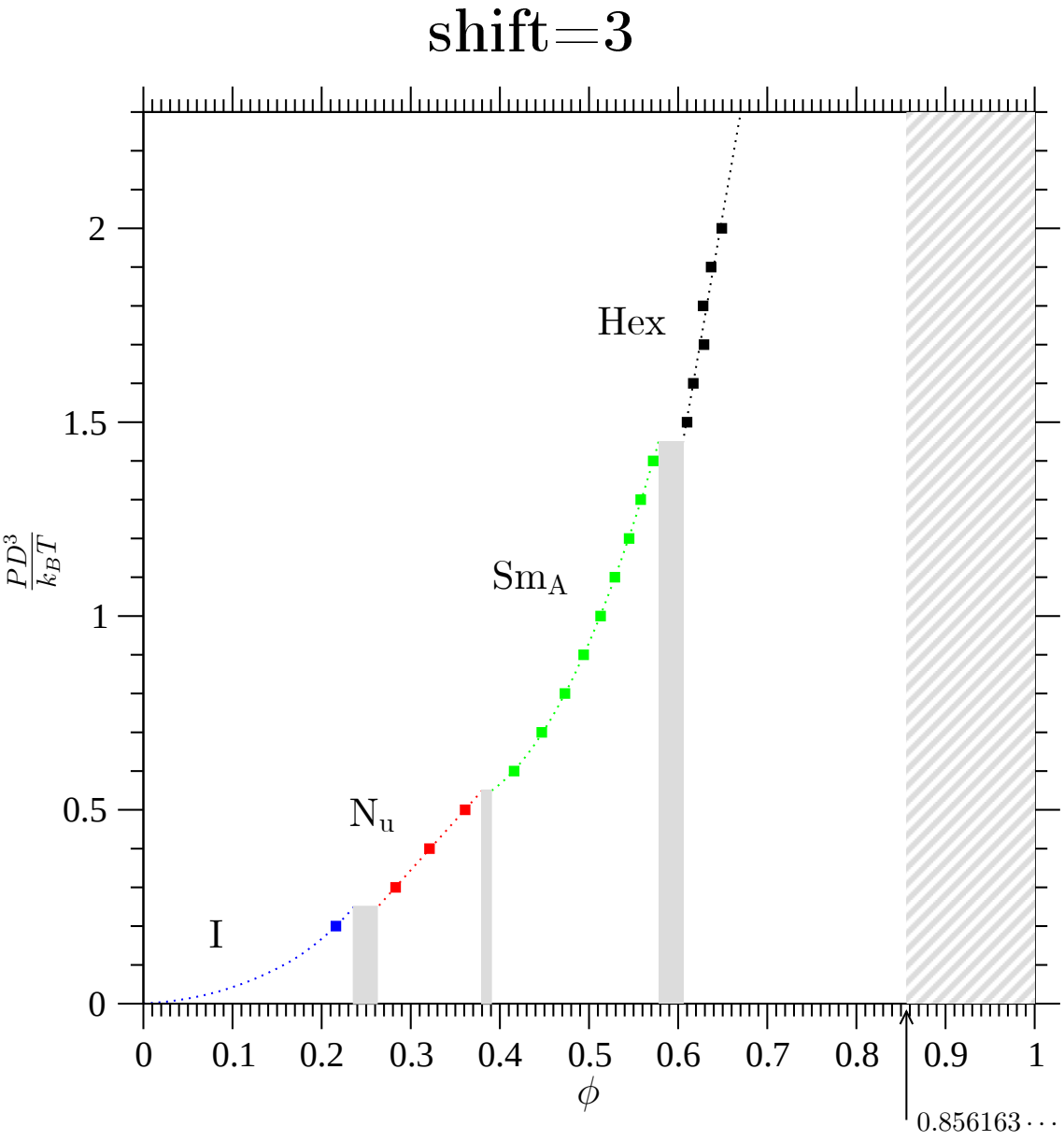

Figure B.11: Phase diagram of the C_{2h} system made up of dimer where the spherocylinders are shifted by 3.0D.

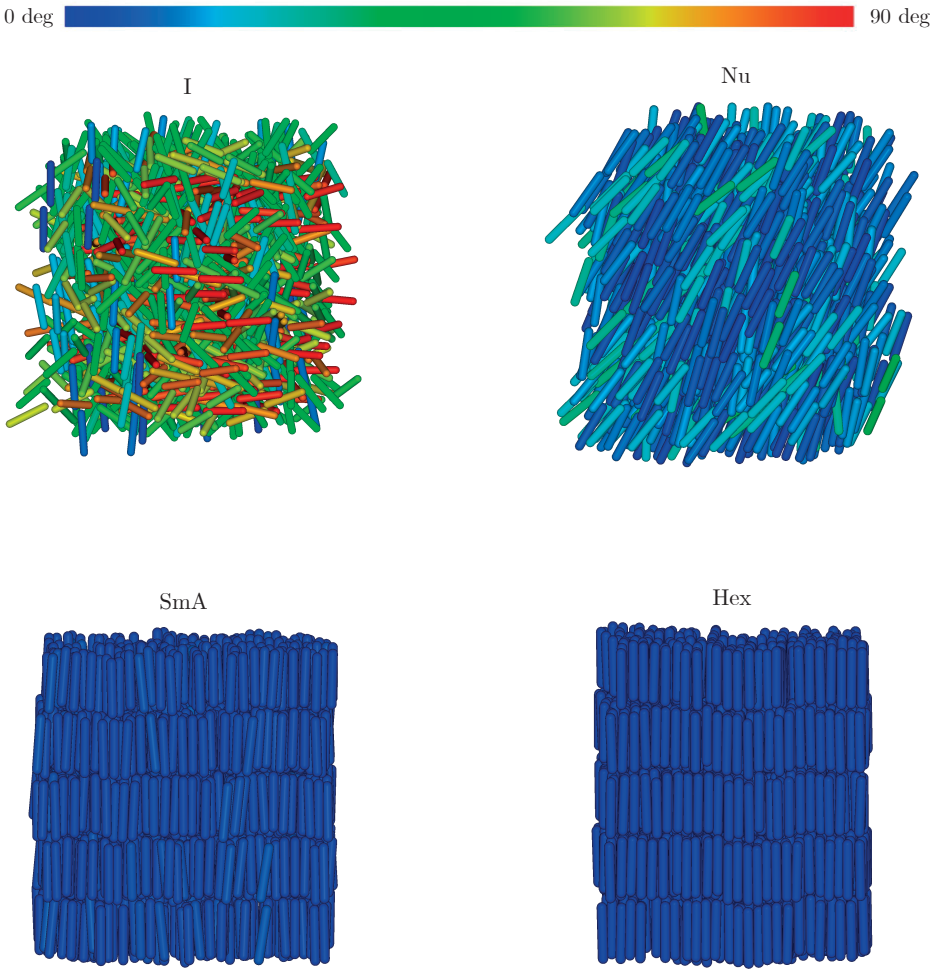

Figure B.12: Snaphosts of the C_{2h} system, with shift=3.0, at $\frac{PD^3}{kT} = 0.20$; 0.40; 1.00 and 1.70.

List of Publications

- G. Celebre, C. D'Urso, M. Porto, Extensive molecular field theoretical investigation of thermotropic biaxial nematics composed of board-like (D_{2h}) molecules in the partially repulsive regime of orientational interactions, *J. Mol. Liq.*, **248**, 847-853 (2017).

- J. Gutierrez Bojart, C. D'Urso, G. Celebre, G. Cinacchi, Probing the sensitivity of orientational ordering as a way towards absolute enantiorecognition: helical-particle solutes in helical-particle nematic solvents, *Phys. Rev. E*, **98**, 042704 (2018).

- G. Celebre, G. De Luca, C. D'Urso, M.E. Di Pietro, Helical Solutes Orientationally Ordered in Anisotropic Media Composed of Helical Particles: Formulation of a Mean Torque Potential Sensitive to *P* and *M* Chirality as a Tool for the Assignment of the Absolute Configuration of Enantiomers, *J. Mol. Liq.*, xxx, xxx, 2018, submitted.

- C. D'Urso, G. Celebre, G. Cinacchi, Phase behaviour of hard-C_{2h} symmetric-particle systems, xxx, xxx, xxx, in preparation.

Oral presentations

- Alla ricerca 'virtuale' di Smart Materials vantaggiosi energeticamente e più performanti: NMR e Computer Simulations, Università della Calabria, 2018.
- Partially Ordered Condensed Fluids Investigated by Monte Carlo Simulation: two studies, 9^{th} Italian-Japanese Workshop on Liquid Crystals and 13^{th} National SICL Meeting held in Pavia (Italy) from September 17^{th} to September 20^{th}, 2018.

PhD School

- Liquid Crystal Modelling and Simulation: A Comprehensive Introduction held in Erice (TP) from July 14^{th} to July 18^{th}, 2017.

Acknowledgements

La sezione dei ringraziamenti risulta essere sempre molto difficile da redigere, a maggior ragione nel momento in cui si conclude un percorso lungo come questo. Molte persone hanno contribuito al raggiungimento di questo traguardo che mi ha fatto crescere sia dal punto di vista professionale sia dal punto di vista umano. Chi mi conosce bene sa che purtroppo la redazione di testi non è il mio forte, tuttavia proverò ad esprimere quello che sento in queste poche righe. Nel pieno spirito di questo lavoro di Tesi l'ordine in cui i ringraziamenti sono stati redatti è puramente casuale :)

Ringrazio la mia ragazza Raffaella che nonostante la distanza, le difficoltà ed il mio essere testardo ha sempre creduto in me spronandomi a dare il meglio ed a non mollare mai, un pezzo di questo finale è anche tuo!

Ringrazio la mia famiglia che mi ha supportato in tutto il percorso Universitario facendo sacrifici e rendendo possibili i miei studi.

Ringrazio quelli che posso considerare i miei fratelli acquisiti: Mario e Piero. Con voi ho condiviso la maggior parte di questo lungo cammino durato 8 anni; la nostra amicizia è una di quelle cose che porterò per sempre nel mio cuore, ovunque noi saremo.

Infine un ringraziamento speciale va a tutti i componenti del Gruppo di Ricerca presso il quale ho svolto non solo il Dottorato, ma anche Tesi Triennale e Magistrale. Parto, ovviamente, dal mio supervisore prof. Celebre, nel mio processo di crescita ha avuto un ruolo predominante. I miei mille difetti non sono stati facili da gestire (tanto da meritare l'appellativo di fattore entropico), tuttavia, grazie ancora per la dedizione e la correttezza con la quale mi ha seguito durante gli studi.

Ringrazio il prof. Giorgio Cinacchi, è stato per me e per la mia formazione una figura fondamentale, professionalità, dedizione e disponibilità sono 3 aggettivi che raramente in tempi moderni si possono riscontrare in una sola persona.

Ringrazio la prof. Giuseppina De Luca, sempre pronta a supportarmi e a consigliarmi nei momenti di bisogno. Nonostante non abbia avuto un ruolo di protagonista all'interno del mio lavoro, posso tranquillamente affermare che ha lasciato un segno indelebile nel raggiungimento della meta. Tengo anche a menzionare una persona alla quale tengo molto: la dott.ssa Maria Enrica Di Pietro, nonostante la sua

'assenza' anche lei è stata una persona che ha avuto un ruolo importante in questa formativa esperienza. Infine, ho da dire un grande grazie alla schiera di *supporters* che giornalmente hanno dovuto subire le mie lamentele e battute (freddure), senza di loro sicuramente le giornate lavorative sarebbero state molto più cupe e prive di quel 'brio' che ha contribuito ad esprimermi al meglio. Pertanto, grazie a: Rosachiara (rosmarino), la pazienza è la virtù dei forti si dice, sopportarmi non è stato facile lo ammetto; Maria Francesca Colella (piccola chirale) grazie per i tui buongiorno udibili solo a pochi centimetri di distanza e per i rumori molesti emessi dai tuoi devices, infine, grazie anche a te Emanuela Lombardo tesista e designer del ***Gruppo***!